The Role of Iron in the Arctic Carbon Cycle

by

Adrianna Trusiak

A dissertation submitted in partial fulfillment
of the requirements for the degree of
Doctor of Philosophy
(Earth and Environmental Sciences)
in the University of Michigan
2020

Doctoral Committee:

Associate Professor Rose M. Cory, Chair
Professor Joel D. Blum
Associate Professor Gregory J. Dick
Professor George W. Kling
Professor Nathan D. Sheldon

Adrianna Trusiak

atrusiak@umich.edu

ORCID iD: 0000-0002-7793-9329

Dedication

To Chrumcia and Jason- thank you for always being a constant.

Acknowledgements

Thank you to my advisor Rose Cory to her guidance, patience, and encouragement over the years. This project has been as much satisfaction and fun as it has been frustrating and challenging, but thank you for supporting me and pushing me not to give up, but also to do the right thing and accept when things do not work out. Also, for styling my hair into unicorn horn for a solstice party at Toolik Field Station. Thank you to George Kling for being my unofficial second advisor and always having time to meet and discuss data, field plans, my progress, and career development. Thanks both to Rose and George for teaching me how to stay organized, write well, and be critical of my and others work. Thank you to my committee- Joel Blum, Greg Dick, and Nathan Sheldon for asking big picture questions, making me think of how my research impact other work, and for their feedback on my presentations, progress, and career plans.

Thank you for all current and former Cory and Kling lab students and technicians who guided me and were there for me during this long process. Especially Lija Treibergs who was as committed to this project as I was. Thank you staying late with me to "iron out" the arctic iron cycle (at least we saw some auroras and polar bears!) and for being a wonderful friend and co-worker. Thank you to Vincent Noël and John Bargar for introducing me to the synchrotron work and patiently explaining this new technique to me. Thank you for everyone at Toolik Field Station- your support in terms of logistics and everyday life at the station is incredible and I could not have done all this work without you (and all of the cookies, bread, and lemon bars!). Thank you for all of the office staff at the University of Michigan, especially Nancy Kingsbury and Paula Frank for putting in last minute orders and helping ship the instruments and supplies

safely to Alaska, Washington, and California. Thanks to Karin Block for giving a young undergrad a chance to fall in love with research and for your continuous friendship and guidance throughout the years!

I am grateful to funding agencies for supporting my dissertation research. Thanks to National Science Foundation for the Graduate Research Fellowship, to University of Michigan for the Rackham Merit Fellowship, the Rackham Research Grant, Rackham Conference Travel Grant, and Scott Turner Awards that supported my research throughout the years and allowed me to establish collaborations with other researchers and pursue new methods.

Thanks to my friends, old and new! Andrea, Jamie, Kevin, and Marlin- thank you for always being there to talk about anything but research. My visits to New York when I got to see you all were the best recharge I could get while being in graduate school. Plus, you always updated me on all things hip and cool. At Michigan- thank you Jenny for always being there to vent and talk about our struggles and for your extensive and honest feedback on my writing. Thanks to Katy for our every-so-often lunches to catch up and eat sweet potato fries. And huge thank you to everyone else (Lija, Chris, Annie, Derek, Alex K., Ruby, Alex T., Jade, Aislinn, Dhurba, and so many more) for their smiles, hellos, outings, and support. Thank you to the Creature Conservancy, both all of the wonderful staff and all of the great furry (and not so furry) animals, for letting me feel like I am making a difference.

Many thanks to my parents! I know that I have made many changes throughout my career and said "I am quitting" thousands of times, but thank you for being there to support my decisions. Thanks to my sister, my niece and nephew for providing a different perspective on life and reminding me that a failed lab experiment does not mean the end of the world. Also, for keeping me updated on all things GenZ. Thanks to Christine Asidao- I am so happy I got paired

to work with you at CAPS and got to continue working together. Thank you for slowing me down and making me look at things from a different prospective. Thank you Chrumi for needing me and giving me a purpose on the days when I felt lost, and thank you for all of the licks. Last, thank you Jason! I honestly do not know if I would reach this point if you have not entered my life (sorry it had to be right around prelims!). Thank you for always supporting me, believing in me during the times when I could not believe in myself, for your honesty, and for your cooking. We have been having many great adventures together and I am excited for more in the future!

Table of Contents

List of Tables

List of Figures

Abstract

Interactions between iron and organic carbon (OC) in soils influence the amount of soil OC that is oxidized to carbon dioxide (CO_2), a greenhouse gas warming our planet. Although both microbial and abiotic iron redox reactions can oxidize soil OC to CO_2, the role of abiotic iron redox reactions in the oxidation of soil OC to CO_2 remains poorly understood. Oxidation of reduced ferrous iron (Fe(II)) by dissolved oxygen produces hydroxyl radical (•OH), a reactive oxidant that may oxidize dissolved OC (DOC) to CO_2. Production of •OH from Fe(II) oxidation has been well-studied in controlled laboratory experiments, but it is unknown whether this process is an important pathway for the oxidation of DOC to CO_2 in soils. To address this knowledge gap, the oxidation of Fe(II) and the subsequent •OH and CO_2 production were measured in arctic soil waters. •OH was produced in all soil waters studied in the Arctic, and the oxidation of Fe(II) by dissolved oxygen was found to be the main source of •OH. The •OH produced from this reaction oxidized DOC to CO_2 in controlled laboratory experiments and in soil waters. The production yield of CO_2 from the oxidation of DOC by •OH varied by 2- to 50-fold possibly due to differences in DOC chemical composition. On a broader, landscape scale, Fe(II) production rates, and thus •OH and CO_2 production rates, varied by landscape age and vegetation type. For example, Fe(II) production rates were higher in the upland, older mineral-rich soils with tussock vegetation than the lowland, younger organic-rich soils with wet sedge vegetation. In all soils, the magnitude of •OH and CO_2 production depended on the balance of (i) the rates of Fe(II) oxidation by dissolved oxygen and (ii) the rates of Fe(II) production. Dissolved oxygen supplied to the soils with rainfall oxidized Fe(II), resulting in higher •OH and

CO_2 production than under static, waterlogged conditions. During rainfall events, Fe(II) was continuously detected despite oxidizing conditions, suggesting that Fe(II) production exceeded its oxidation. Under static, waterlogged conditions, Fe(II) oxidation, and thus •OH and CO_2 production, was limited by the supply of dissolved oxygen to the soils. On a landscape scale in the Arctic, the rates of CO_2 production from DOC oxidation by •OH in soils were comparable to the rates of CO_2 production from microbial respiration of DOC in surface waters. Thus, this dissertation research demonstrated a novel pathway for soil OC oxidation where abiotic interactions between iron and OC can be an important source of CO_2 to the atmosphere. As the Arctic warms, permafrost soils are thawing and releasing high concentrations of iron and OC that are susceptible to oxidation. The conversion of this permafrost OC to CO_2 will result in positive and accelerating feedback to climate change. The results from this thesis improve our ability to predict this feedback by identifying the controls on the magnitude of the CO_2 produced from iron-mediated OC oxidation in soils.

Chapter 1
Introduction

1.1 The Role of Dissolved Organic Carbon in the Global Carbon Cycle

Dissolved organic carbon (DOC) is a critical intermediate in the global carbon (C) cycle [1-3]. DOC released from decaying plant material into surface or soil waters can be readily oxidized to carbon dioxide (CO_2), a greenhouse gas, and released to the atmosphere. The flux of CO_2 to the atmosphere from DOC oxidation in freshwaters is comparable to the amount of other net C fluxes on Earth, making it a critical component of the global C cycle [3]. However, there is a limited understanding of the controls on the amount of DOC that is oxidized to CO_2 because the abiotic processes that can oxidize DOC to CO_2 are poorly understood.

Oxidation of DOC to CO_2 is usually attributed to microbial respiration. However, recent studies in the Alaskan Arctic showed that abiotic processes can produce as much CO_2 from oxidation of DOC as produced from microbial respiration of DOC [4,5]. For example, Page et al. [4] estimated that CO_2 production from oxidation of DOC during abiotic iron redox reactions in arctic soils may be comparable to microbial respiration of DOC to CO_2 in arctic surface waters. This abiotic DOC oxidation is particularly important in the Arctic because there are high carbon and iron concentrations in arctic soils that are being released from thawing permafrost soils with warming [6-10].

Arctic soils store twice as much C as there is currently in the atmosphere [6-10]. This C has been stored in permanently frozen permafrost soils for thousands of years, and thus, has not been active in the modern C cycle. However, the Arctic is warming twice as fast as the rest of

the world [11,12]. Warmer air surface temperatures are warming the soils and increasing the depth of the annually thawed, active soil layer [13]. This thawing of permafrost soils releases previously frozen C that can be oxidized to CO_2 and released to the atmosphere. Along with the C, iron is released from thawing permafrost soils, likely increasing the importance of abiotic iron redox reactions in oxidizing the newly released C to CO_2 [10,14].

Oxidation of permafrost C to CO_2 in the Arctic provides a positive and accelerating feedback to global climate change [12,15]. Understanding how much DOC will be oxidized to CO_2 is crucial in estimating the effects of thawing permafrost on future global climate change. However, we are currently unable to predict the amount of permafrost DOC that will be oxidized to CO_2 as the Arctic warms in part because controls on abiotic iron redox reactions that could lead to oxidation of DOC to CO_2 are not well understood.

1.2 Hydroxyl Radical Production

Recent work showed that hydroxyl radical (•OH), one the strongest oxidants of C in the environment [15-17], can be produced from redox reactions involving reduced ferrous iron (Fe(II)) and reduced DOC as electron donors [4,18-20]. Specifically, dissolved oxygen oxidizes Fe(II) and reduced DOC to produce •OH (Equations 1-6) [21-23]. Fe(II) and reduced DOC oxidation are expected to proceed as a three step reaction where superoxide (O_2^-; Eqn. 1, Eqn. 4), hydrogen peroxide (H_2O_2; Eqn. 2, Eqn. 5), and •OH (Eqn. 3, Eqn. 6) are produced [21-23]. Out of these three reactive oxygen species, •OH is the most likely to oxidize DOC due to its highly reactive and nondiscriminatory nature [20,24].

$$\textbf{Eqn. 1}\quad Fe(II) + O_2 \rightarrow Fe(III) + O_2^{-\cdot}$$

$$\textbf{Eqn. 2}\quad Fe(II) + HO_2^{\cdot} \rightarrow Fe(III) + HO_2^- \xrightarrow{H^+} Fe(III) + H_2O_2$$

$$\textbf{Eqn. 3}\ \ Fe(II) + H_2O_2 \rightarrow Fe(III) + OH^- + \bullet OH$$

$$\textbf{Eqn. 4}\ \ DOC_{red} + O_2 \rightarrow DOC_{ox} + O_2^{-\cdot}$$

$$\textbf{Eqn. 5}\ \ DOC_{red} + HO_2^{\cdot} \rightarrow DOC_{ox} + HO_2^- \xrightarrow{H^+} DOC_{ox} + H_2O_2$$

$$\textbf{Eqn. 6}\ \ DOC_{red} + H_2O_2 \rightarrow DOC_{ox} + OH^- + \bullet OH$$

Once produced, •OH may oxidize DOC [24,25]. •OH reacts with DOC by addition (hydroxylation) or hydrogen atom abstraction, resulting in the production of organic and hydroperoxyl radicals [24-26]. These radicals might initiate additional degradation reactions with DOC to produce partially oxidized aromatic and aliphatic compounds, low molecular weight acids, and CO_2 [24-27]. The production of CO_2 from DOC oxidation by •OH was shown in a controlled laboratory setting where •OH was produced through electrochemical reactions in simulated natural waters [25]. It has been suggested that the oxidation of DOC by •OH to CO_2 could be important in Fe(II)- and DOC-rich soils in the tropical and arctic environments where •OH is produced from oxidation of Fe(II) and reduced DOC [4,28]. However, it is unknown whether the •OH produced from these redox reactions could oxidize DOC to CO_2 and, if so, how that oxidation could impact the C cycle.

1.3 Hydroxyl Radical Production Across the Arctic Landscape

Prior work showed that •OH is produced upon oxidation of arctic soil waters in proportion to the amount of Fe(II) and DOC present [4]. Fe(II) and reduced DOC are common products of anaerobic microbial respiration in waterlogged soils [29]. As a result, waterlogged arctic soils are rich in Fe(II) and reduced DOC, creating ideal conditions for •OH production upon oxidation of these soils by dissolved oxygen [4,29-31]. However, the amount of Fe(II) and

DOC in waterlogged soils varies 10- to 100- fold across the Alaskan Arctic landscape due to differences in (1) landscape surface age and (2) vegetation type [4,30,31].

The landscape in the Alaskan Arctic has been glaciated at different times resulting in a gradient of land surface ages that have otherwise been exposed to the same climate conditions [32]. These differences in surface ages lead to varying thickness of organic mats, water saturation content, and contact with mineral soils, resulting in higher Fe(II) and DOC concentrations and lower pH in soil waters from the older landscapes than from the younger landscapes [4,31,32]. As a result, it is expected that •OH production is higher on the older landscapes due to the higher Fe(II) and DOC concentrations compared to the younger landscapes [4]. However, differences in •OH production between the older and younger landscape surface ages have not been previously studied.

In addition to the landscape surface ages, Fe(II) and DOC concentrations also vary between the two dominant vegetation types in the Arctic- wet sedge and tussock. Wet sedge dominated landscapes are lowland areas, usually waterlogged with a thick organic mat [33]. In contrast, tussock dominated landscapes are upland, usually drier with a thin organic layer and iron-rich mineral layer present close to the surface [33]. Soil waters from wet sedge dominated landscapes are more reduced than soil waters from tussock dominated landscapes because of the waterlogged conditions that limit the diffusion of dissolved oxygen into the soil [4]. Thus, wet sedge dominated soil waters have low dissolved oxygen concentrations and high Fe(II) and DOC concentrations, which favor high •OH production upon oxidation [4]. In contrast, soil waters from tussock dominated landscapes are more oxidized, resulting in high dissolved oxygen and lower Fe(II) and DOC concentrations [4]. While it has been shown that Fe(II) and DOC concentrations are higher in soil waters from wet sedge than from tussock dominated landscapes

[4], we do not know if higher Fe(II) and DOC concentrations are due to the higher Fe(II) and DOC production rates on those landscapes or due to the longer time since the last glaciation and thus, longer accumulation time of Fe(II) and DOC in soil.

1.4 The Controls on the Magnitude of Hydroxyl Radical Production in Arctic Soils

The current estimates of •OH production in arctic soils from Fe(II) and reduced DOC oxidation are based on two assumptions [4]. First, it is assumed that Fe(II) and reduced DOC in the waterlogged soils are continuously exposed to dissolved oxygen and thus, are immediately oxidized to produce •OH [4]. Second, it is assumed that Fe(II) and reduced DOC production rates in soils are fast enough to re-supply reduced species that can be oxidized by dissolved oxygen to produce •OH [4]. It is unlikely that these assumptions hold in the natural soil environment because •OH production in soils depends on the balance between dissolved oxygen supply and the production rates of Fe(II) and reduced DOC. For example, if dissolved oxygen supply is lower than Fe(II) and reduced DOC production, •OH production will be limited by the dissolved oxygen supply, and thus lower than previously estimated [4]. Currently it remains unknown how much •OH is produced *in situ* when •OH production is limited by the dissolved oxygen supplied to the soils or by the Fe(II) and reduced DOC production rates in soils.

In soils the balance between dissolved oxygen supply and consumption impacts the magnitude of •OH production. Under ambient waterlogged conditions, dissolved oxygen can be supplied to soils by the introduction of oxygenated rain water during precipitation events, by diffusion from the atmosphere, through the lowering of the water table height, and from plant aerenchyma [29, 34-39]. Once supplied, dissolved oxygen is consumed by abiotic redox reactions and microbial respiration. The majority of the soil waters in the Arctic contain low dissolved oxygen concentration [4,30,31], suggesting that the consumption rate of dissolved

oxygen is close to its supply rate. However, the controls on the balance between dissolved oxygen supply and consumption in soil waters have not been studied.

Fe(II) and reduced DOC production and consumption rates will also determine the magnitude of •OH production in soil waters [4]. Understanding of controls on the rates of Fe(II) and reduced DOC production and oxidation is needed to predict the magnitude of •OH production across different landscape surface ages and vegetation types in the Arctic. Fe(II) and reduced DOC in soil waters are produced from microbial reduction, mineral dissolution, and desorption [29,40-42]. There is a strong correlation between concentrations of Fe(II) and DOC across arctic and boreal regions suggesting that both are produced through similar processes [4,43,44]. In addition, aromatic C within DOC may aid microbial reduction of Fe(III) to Fe(II), thus increasing Fe(II) production rates [29,43-45]. Once produced, Fe(II) and reduced DOC are consumed or altered through microbial oxidation or through abiotic redox reactions where Fe(II) and reduced DOC are oxidized by dissolved oxygen to produce •OH [4]. Waterlogged, low oxygen soils commonly found in the Arctic contain high Fe(II) and reduced DOC concentrations [4,29,30], suggesting that Fe(II) and reduced DOC production rates exceed their oxidation rates. Thus, field measurements of low oxygen and high Fe(II) and reduced DOC across the Alaskan Arctic [4,29,30] suggest that oxygen supply might be limiting the magnitude of •OH production in those soil waters, although this hypothesis has not been tested.

1.5 Summary

In summary, no study has determined controls on the magnitude of •OH production in arctic soils or shown whether •OH production might impact C cycling by oxidizing DOC to CO_2. Identifying controls on the magnitude of •OH and CO_2 production is needed to predict how much •OH and CO_2 are produced in arctic soils and how that might change as the Arctic warms. DOC

oxidation by •OH in soil waters is currently not included in any earth climate system or biogeochemical models as a pathway for DOC oxidation. Considering the highly reactive and nondiscriminatory nature of •OH, this abiotic process might increase estimates of CO_2 released from arctic soils [4,25]. Thus, the goal of my thesis was to develop an understanding of •OH production in arctic soils and the fate of that •OH once produced. Specifically, my objectives were to test the following hypotheses:

1. The magnitude of •OH production is dependent on the dissolved oxygen supply to soils and Fe(II) and DOC production rates.

2. •OH produced from oxidation of Fe(II) and reduced DOC oxidizes DOC to CO_2.

3. DOC chemical composition impacts the amount of CO_2 that is produced from oxidation of DOC by •OH.

To test these hypotheses on the controls and products of •OH production in arctic soil waters, I carried out experiments in the Alaskan Arctic using natural gradients in Fe(II) and DOC concentrations. These gradients in Fe(II) and DOC were driven by the differences in landscape surface age and vegetation type. My approach was to measure •OH and subsequent CO_2 production in arctic soil waters, along with other variables including changes in Fe(II), DOC, and oxygen supply. I related these changes in chemistry to the measured •OH and CO_2 production.

While this dissertation is focused on the role of •OH in the arctic C cycle, the processes studied here likely have implications for the global C cycle. •OH production from Fe(II) oxidation could happen in any Fe(II)- and DOC-rich soils on Earth. Consistent with this expectation, •OH production from abiotic Fe(II) and reduced DOC oxidation has been shown in tropical soils and temperate lakes [28,46,47]. Controls on •OH and CO_2 production identified in my work could be used to better estimate CO_2 emissions from soils on Earth.

1.6 Thesis Structure

In **Chapter 2**[1], I identified the primary controls on •OH production and showed that, once produced, •OH can oxidize DOC to CO_2. I showed that Fe(II) was the primary electron donor to produce •OH. I also measured H_2O_2 production, which is an intermediate expected to be produced if Fe(II) oxidation is the source of •OH produced [22]. I measured CO_2 production during oxidation of DOC by •OH for the first time in natural soil waters. However, the range in the amount of CO_2 produced per mol •OH in soil waters was on average higher than the expected production yield of 0.3 mol CO_2 per 1 mol •OH from controlled laboratory studies [25]. This large variability in the production yield of CO_2 per •OH might be due to the differences in the pH or DOC chemical composition of different soil waters.

In **Chapter 3**[2] I used mesocosms to understand how two landscape controls, landscape surface age and vegetation type, affect •OH production. I collected soil cores from the two dominant landscape surface ages and vegetation types, and measured Fe(II), DOC, and •OH production in those soils. I found that Fe(II) and DOC production rates were generally higher on the older rather than the younger landscapes and on the tussock landscapes rather than wet sedge landscapes. While the landscape age results in the mesocosm study agreed with the previous field measurements [4], the vegetation type results in mesocosm study were opposite to the previous field measurements. I found that the contrasting results were due to the downhill transport of Fe(II) and DOC from upland tussock dominated landscapes to wet sedge dominated landscapes in the field. The downhill transport resulted in higher Fe(II) and DOC, and thus higher •OH concentrations, measured in the wet sedge than in tussock soils in the field. In

---

[1] Trusiak A., Treibergs L.A., Kling G.W., and Cory R.M., *Geochim. Cosmochim. Acta*, 2018
[2] Trusiak A., Treibergs L.A., Kling G.W., and Cory R.M, *Soil Syst.*, 2019

controlled mesocosm experiments, there was no hydrological connectivity and no downhill transport of Fe(II), causing the production of Fe(II), DOC, and •OH to be lower in wet sedge than in the tussock soils. I found that the landscape connectivity between tussock and wet sedge dominated landscapes is important in transporting Fe(II) and DOC across the landscape, and in controlling the rates of CO_2 production from •OH.

To better estimate the magnitude of •OH, and CO_2 production in soils under changing dissolved oxygen supply, in **Chapter 3** I also measured changes in soil chemistry, including dissolved oxygen and Fe(II) concentrations, and •OH production under static waterlogged conditions and during rainfall in arctic soils. I found that under static waterlogged conditions in arctic soils, •OH production was limited by dissolved oxygen supply to the soils. The dissolved oxygen supplied to the soil by diffusion from the atmosphere, through the lowering of the water table height, and from plant aerenchyma [29,34-39] was not sufficient to oxidize all of the Fe(II) produced. Fe(II) production rates in the soils were high enough to support •OH production even under small to medium size rainfall events, when dissolved oxygen was supplied at higher rates in the oxygenated rain water than under waterlogged conditions. During rainfall events, •OH production was up to three times higher than during waterlogged conditions. While previous work measured •OH production from 24-hour oxidation of soil waters in the atmosphere [4], I measured *in situ* •OH production under natural conditions and showed that •OH production in soils is lower than previously estimated due to the limited dissolved oxygen supply. Thus, the magnitude of •OH and CO_2 production might be an order of magnitude lower than previously estimated, depending on the precipitation patterns that supply oxygen from the atmosphere.

In **Chapter 4**, I studied the controls of DOC oxidation by •OH to explain the variability in the production yield of CO_2 per •OH measured in soil waters in Chapter 1. In a controlled

study with DOC solutions amended with Fe(II), I measured how the amount of CO_2 produced during oxidation of DOC by •OH varied with pH and with DOC composition. I found that CO_2 was produced from oxidation of DOC by •OH in all of the DOC solutions amended with Fe(II), just like in the majority of arctic soil waters. The production yield of CO_2 per •OH did not vary with the pH across the pH range of soil waters, therefore pH could not explain the variability in the production yield of CO_2 per •OH measured in soil waters. However, DOC chemical composition did affect the production yield of CO_2 per •OH. Specifically, the production yield of CO_2 per •OH decreased with the increasing antioxidant content of the DOC, quantified as electron donating capacity (EDC) of DOC. DOC with a high EDC or antioxidant content reacted with •OH to produce low energy radicals instead of CO_2, resulting in the lower production yield of CO_2 per •OH. My results show that the variability in the production yield of CO_2 per •OH observed in soil waters can be explained by the differences in the antioxidant content of DOC across soil waters. To scale up CO_2 production from the oxidation of DOC by •OH across the landscape, differences in DOC composition must be taken into consideration.

1.7 References

1. Aufdenkampe, K., Mayorga, E., Raymond, P.A., Melack, J.M., Doney, S.C., Alin, S.R., Aalto, R., and Yoo, K. (2011) *Front. Ecol. Environ.* 9, 53–60.

2. Cole, J.J., Prairie, Y.T., Caraco, N.F., McDowell, W.H., Tranvik, L.J., Striegl, R.G., Duarte, C.M., Kortelainen, P., Downing, J.A., Middelburg, J.J., and Melack, J. (2007) *Ecosystems* 10, 171–184.

3. Raymond, P.A, J. Hartmann, Lauerwald, R., Sobek, S., McDonald, C., Hoover, M., Butman, D., Striegl, R., Mayorga, E., Humborg, C., Kortelainen, P., Dürr, H., Meybeck, M., Ciais, P., and Guth, P. (2013) *Nature*, 2013, 503, 355–9.

4. Page, S. E., Kling, G. W., Sander, M., Harrold, K. H., Logan, J. R., McNeill, K., and Cory, R. M. (2013). Dark formation of hydroxyl radical in arctic soil and surface waters. *Environ. Sci. Technol.* 47, 12860–12867.

5. Cory, R.M., Ward, C.P., Crump, B.C., and Kling, G.W. (2014) Sunlight controls water column processing of carbon in arctic freshwaters. *Science* 345, 925–928.

6. Elmquist, M., Semiletov, I., Guo, L., and Gustafsson, Ö. (2008) Pan-Arctic patterns in black carbon sources and fluvial discharges deduced from radiocarbon and PAH source apportionment markers in estuarine surface sediments. *Global Biogeochem. Cycles* 22.

7. Davidson E.A., and Janssens, I.A. (2006) Temperature sensitivity of soil carbon decomposition and feedbacks to climate change. *Nature* 440, 165–73.

8. Tarnocai, C., Canadell, J.G., Schuur, E.A.G., Kuhry, P., Mazhitova, G., and Zimov, S. (2009) Soil organic carbon pools in the northern circumpolar permafrost region. *Global Biogeochem. Cycles* 23, GB2023.

9. Schuur, E.A.G., Vogel, J.G., Crummer, K.G., Lee, H., Sickman, J.O., and Osterkamp, T.E. (2009) The effect of permafrost thaw on old carbon release and net carbon exchange from tundra. *Nature* 459, 556–9.

10. Ping, C. L., Michaelson, G. J., Jorgenson, M. T., Kimble, J. M., Epstein, H., Romanovsky, V. E., and Walker, D.A. (2008). High stocks of soil organic carbon in the North American Arctic region. *Nature Geoscience* 1, 615–619.

11. Mack, M.C, Schuur, E.A.G., Bret-Harte, M.S., Shaver, G.R., and Chapin, F.S. (2004) Ecosystem carbon storage in arctic tundra reduced by long-term nutrient fertilization. *Nature* 431, 440–3.

12. Schuur, E.A.G., Vogel, J.G., Crummer, K.G., Lee, H., Sickman, J.O., and Osterkamp, T.E. The effect of permafrost thaw on old carbon release and net carbon exchange from tundra. *Nature* 2009, 459, 556–9.

13. Keller, K., Blum, J. D., and Kling, G. W. (2007). Geochemistry of Soils and Streams on Surfaces of Varying Ages in Arctic Alaska. *Arctic, Antarctic, and Alpine Research* 39(1), 84–98.

14. Bowen, J.C., Ward, C.P., Kling, G.W., Cory, R.M. Arctic amplification of global warming strengthened by sunlight oxidation of permafrost carbon to CO_2. *In review.*

15. MacDougall, A. H., Avis, C.A., and Weaver, A. J. (2012). Significant contribution to climate warming from the permafrost carbon feedback. *Nature Geoscience* 5, 719–721.

16. Faust, B. C., and Hoigné, J. (1990). Photolysis of Fe(III)-hydroxy complexes as sources of •OH in clouds, fog and rain. *Atmospheric Environment Part A, General Topics* 24, 79–89.

17. Mopper, K., & Zhou, X. (1990). Hydroxyl radical photoproduction in the sea and its potential impact on marine processes. *Science* 250, 661–4.

18. Page, S. E., Logan, J. R., Cory, R. M., and McNeill, K. (2014). Evidence for dissolved organic matter as the primary source and sink of photochemically produced hydroxyl radical in arctic surface waters. *Environ. Sci. Processes & Impacts* 16, 807–822.

19. Burns, J. M., Craig, P. S., Shaw, T. J., and Ferry, J. L. (2010). Multivariate examination of Fe(II) / Fe(III) cycling and consequent hydroxyl radical generation. *Environ. Sci. Technol.* 44, 7226–7231.

20. Page, S. E., Sander, M., Arnold, W. A., and McNeill, K. (2012). Hydroxyl radical formation upon oxidation of reduced humic acids by oxygen in the dark. *Environ. Sci. Technol.* 46, 1590–1597.

21. Tong, M., Yuan, S., Ma, S., Jin, M., Liu, D., Cheng, D., and Wang, Y. (2016). Production of Abundant Hydroxyl Radicals from Oxygenation of Subsurface Sediments. *Environ. Sci. Technol.* 50, 214–221.

22. Haber, F., and Weiss, J. (1932). Uber die Katalyse des Hydroperoxydes. *Die Naturwissenschaften* 20, 948–950.

23. Stumm, W., & Lee, F. G. (1961). Oxygenation of ferrous iron. *Industrial and engineering chemistry* 53, 143–146.

24. Westerhoff, P., Aiken, G., Amy, G., and Debroux, J. (1999). Relationships between the structure of natural organic matter and its reactivity towards molecular ozone and hydroxyl radicals. *Water Research* 33, 2265–2276.

25. Goldstone, J. V., Pullin, M. J., Bertilsson, S., and Voelker, B. M. (2002). Reactions of hydroxyl radical with humic substances: Bleaching, mineralization, and production of bioavailable carbon substrates. *Environ.Sci. Technol.* 36, 364–372.

26. Sulzberger, B., and Durisch-Kaiser, E. (2009). Chemical characterization of dissolved organic matter (DOM): A prerequisite for understanding UV-induced changes of DOM absorption properties and bioavailability. *Aquatic Sciences* 71, 104–126.

27. Waggoner, D. C., Chen, H., Willoughby, A. S., and Hatcher, P. G. (2015). Formation of black carbon-like and alicyclic aliphatic compounds by hydroxyl radical initiated degradation of lignin. *Organic Geochemistry* 82, 69–76.

28. Hall, S. J., and Silver, W. L. (2013). Iron oxidation stimulates organic matter decomposition in humid tropical forest soils. *Global Change Biology 19*(9), 2804–2813.

29. Lipson, D.A., Jha, M., Raab, T. K., and Oechel, W. C. (2010). Reduction of iron (III) and humic substances plays a major role in anaerobic respiration in an Arctic peat soil. *J. Geophys. Res. Biogeosciences* 115, 1–13.

30. Herndon, E. M., Yang, Z., Bargar, J., Janot, N., Regier, T. Z., Graham, D. E., and Liang, L. (2015). Geochemical drivers of organic matter decomposition in arctic tundra soils. *Biogeochemistry* 126, 397–414.

31. Lipson, D.A., Zona, D., Raab, T.K., Bozzolo, F., Mauritz, M., and Oechel, W.C. (2012) Water-table height and microtopography control biogeochemical cycling in an Arctic coastal tundra ecosystem. *Biogeosciences* 9, 577–591.

32. Hobbie, J. E. and G. W. Kling, editors. 2014. A Changing Arctic: Ecological Consequences for Tundra, Streams, and Lakes. Oxford University Press, 331.

33. Muller, S. V., Racoviteanu, A. E., and Walker, D. A. (1999) Landsat MSS derived land-cover map of northern Alaska: Extrapolation method sand a comparison with photo-interpreted and AVHRR-derived maps. *Int. J. Remote Sens.* 20, 2921.

34. King, J.Y., Reeburgh, W.S., and Regli, S.K. (1998) Methane emission and transport by arctic sedges in Alaska: Results of a vegetation removal experiment. *J. Geophys. Res. Atmos.* 103, 29083–29092.

35. Updegraff, K., Bridgham, S.D., Pastor, J., Weishampel, P., and Harth, C. (2001) Response of CO_2 and CH_4 emissions from peatlands to warming and water table manipulation. *Ecol. Appl.* 11, 311–326

36. King, J.Y., Reeburgh, W.S., Thieler, K.K., Kling, G.W., Loya, W.M., Johnson, L.C., and Nadelhoffer, K.J. (2002) Pulse-labeling studies of carbon cycling in Arctic tundra ecosystems: The contribution of photosynthates to methane emission. *Glob. Biogeochem. Cycles* 16, 1–8.

37. Zona, D., Oechel, W.C., Kochendorfer, J., Paw, U.K.T., Salyuk, A.N., Olivas, P.C., and Lipson, D.A. (2009) Methane fluxes during the initiation of a large-scale water table manipulation experiment in the Alaskan Arctic tundra. *Glob. Biogeochem. Cycles* 23, 1–11. 12.

38. Knorr, K.H., Glaser, B., and Blodau, C. (2008) Fluxes and 13C isotopic composition of dissolved carbon and pathways of methanogenesis in a fen soil exposed to experimental drought. *Biogeosciences* 5, 1457–1473.

39. Knorr, K.H., Oosterwoud, M.R., and Blodau, C. (2008) Experimental drought alters rates of soil respiration and methanogenesis but not carbon exchange in soil of a temperate fen. *Soil Biol. Biochem*. 40, 1781–1791

40. Stumm, W., and Sulzberger, B. (1992) The cycling of iron in natural environments: Considerations based on laboratory studies of heterogeneous redox processes. *Geochim. Cosmochim. Acta* 56, 3233–3257.

41. Luther, G.W., Kostka, J.E., Church, T.M., Sulzberger, B., and Stumm,W. (1992) Seasonal iron cycling in the salt-marsh sedimentary environment: The importance of ligand complexes with Fe(II) and Fe(III) in the dissolution of Fe(III) minerals and pyrite, respectively. *Mar. Chem.* 40, 81–103.

42. Weber, K.A., Achenbach, L.A., and Coates, J.D. (2006) Microorganisms pumping iron: Anaerobic microbial iron oxidation and reduction. *Nat. Rev. Microbiol.* 4, 752–764.

43. Knorr, K.H. (2013) DOC-dynamics in a small headwater catchment as driven by redox fluctuations and hydrological flow paths—Are DOC exports mediated by iron reduction/oxidation cycles? *Biogeosciences* 10, 891–904.

44. Weyhenmeyer, G.A., Prairie, Y.T., Tranvik, L.J. (2014) Browning of boreal freshwaters coupled to carbon-iron interactions along the aquatic continuum. *PLoS ONE* 9, e88104.

45. Roden, E.E., and Wetzel, R.G. (1996) Organic carbon oxidation and suppression of methane production by microbial Fe(III) oxide reduction in vegetated and unvegetated freshwater wetland sediments. *Limnol. Oceanogr.* 41, 1733–1748.

46. Tong, M., Yuan, S., Ma, S., Jin, M., Liu, D., Cheng, D., and Wang, Y. (2016). Production of Abundant Hydroxyl Radicals from Oxygenation of Subsurface Sediments. *Environ. Sci. Technol.* 50, 214–221.

47. Minella, M., De Laurentiis, E., Maurino, V., Minero, C., Vione, D. (2015) Dark production of hydroxyl radicals by aeration of anoxic lake water. *Sci. Total Environ.* 527–528, 322–327.

Chapter 2
The Role of Iron and Reactive Oxygen Species in the Production of CO_2 in Arctic Soil Waters[1]

2.1 Abstract

Hydroxyl radical (•OH) is a highly reactive oxidant of dissolved organic carbon (DOC) in the environment. •OH production in the dark was observed through iron and DOC mediated Fenton reactions in natural environments. Specifically, when dissolved oxygen (O_2) was added to low oxygen and anoxic soil waters in arctic Alaska, •OH was produced in proportion to the concentrations of reduced iron (Fe(II)) and DOC. Here we demonstrate that Fe(II) was the main electron donor to O_2 to produce •OH. In addition to quantifying •OH production, hydrogen peroxide (H_2O_2) was detected in soil waters as a likely intermediate in •OH production from oxidation of Fe(II). For the first time in natural systems we detected carbon dioxide (CO_2) production from •OH oxidation of DOC. More than half of the arctic soil waters tested showed production of CO_2 under conditions conducive for production of •OH. Findings from this study strongly suggest that DOC is the main sink for •OH, and that •OH can oxidize DOC to yield CO_2. Thus, this iron-mediated, dark chemical oxidation of DOC may be an important component of the arctic carbon cycle.

[1] Trusiak A., Treibergs L.A., Kling G.W., and Cory R.M., *Geochim. Cosmochim. Acta*, 2018

2.2 Introduction

Hydroxyl radical (•OH) is one of the strongest oxidants in the environment and thus plays important roles in the oxidation of organic carbon in the atmosphere and in surface waters [1-4]. Most research on •OH as an oxidant of organic carbon has been done in sunlit environments, where •OH is produced by photochemical processes [e.g., 4,5-7]. Recent work has focused on the light-independent 'dark' pathway for •OH production during redox reactions likely involving reduced iron (Fe(II)) or dissolved organic carbon (DOC) as electron donors (Fig. 2.1) [8-12]. Oxidation of Fe(II) or reduced DOC by oxygen (O_2) can produce hydrogen peroxide (H_2O_2; Fig. 2.1) [9,13,14]. Once produced, H_2O_2 can react with remaining Fe(II) or reduced DOC to yield •OH (Fig. 2.1). Therefore, •OH is produced where Fe(II) and reduced DOC are present, suggesting that •OH is an important oxidant in these environments.

The predecessors to •OH production, Fe(II) and reduced DOC, are common products of anaerobic microbial respiration in waterlogged soils or lake sediments [15,16]. When waterlogged soils are flushed with oxygenated water, or at the oxic-anoxic boundary in soils or sediments, •OH may be produced [8-12]. Prior research observed •OH production from soil waters draining the dominant vegetation types of the low Arctic in proportion to concentrations of reduced soil water constituents including Fe(II) and DOC [10]. In addition, •OH production from aeration of soil waters increased along a gradient of low to high reducing conditions from dry upland soils to wet lowland habitats in the Arctic [10]. Specifically, soil waters draining from wet sedge vegetation had the highest reducing conditions (i.e., highest electron donating capacities from high concentrations of reduced constituents) [10]. Upon introduction of O_2, wet sedge soil waters produced the greatest •OH compared to soil waters from dry upland areas low in reduced constituents [10]. It was estimated that together Fe(II) and reduced DOC accounted

for ~ 90% of the electron donating capacity of those soil waters, which contain low concentrations of other potential reductants like sulfide [10]. Thus, Fe(II) and reduced DOC were inferred to be the main reductants of O_2 yielding •OH in arctic soil waters (Fig. 1) [10]. Studies in lake water and lake sediments have also concluded that Fe(II) and reduced DOC were the main electron donors upon introduction of O_2 in the production of •OH [11,12]. However, the relative importance of Fe(II) versus DOC as electron donors to yield •OH in natural systems is unknown, in part because concentrations of Fe(II) and DOC often co-vary in soils or sediments [10].

Determining the relative importance of Fe(II) versus reduced DOC as electron donors to produce •OH requires quantifying the fraction of the total electron donating capacity *in-situ* in soils or sediments from the oxidation of Fe(II) versus the oxidation of reduced DOC. Total electron donating capacity of Fe(II) (i.e., electrons released from Fe(II) oxidation) can be quantified, but the redox moieties within DOC are poorly characterized and thus difficult to isolate and quantify in natural soils [17,18]. However, comparison of electrons released from the oxidation of Fe(II) to Fe(III) alone to the total electron donating capacity (i.e., electrons released from all reduced constituents) may identify the relative importance of Fe(II) versus DOC as the electron donors to produce •OH; this method would be particularly effective in environments where other potential reductants are present at much lower concentrations.

Once •OH is produced in soils or sediments, its fate and consequences for carbon cycling are poorly understood. From studies of •OH in simulated surface waters containing high concentrations of •OH and DOC, •OH is expected to rapidly oxidize DOC [19]. However, in natural waters, soils, or sediments, DOC may compete with chloride, bromide, or carbonates as a sink for •OH [10,16,20]. Recent work showed that in high DOC surface waters low in salts or

carbonates, DOC was the main sink for •OH [4]. While DOC is expected to be the sink for •OH in surface waters or soils of the Arctic, the products of the oxidation of DOC by •OH can yield several organic or inorganic compounds [5].

•OH reacts with DOC by addition (i.e., hydroxylation) or hydrogen atom abstraction producing organic and hydroperoxyl radicals [21]. Those radicals may initiate additional degradation of DOC, ultimately forming partially-oxidized or degraded aromatic or aliphatic compounds [22,23], low molecular weight organic acids, or CO_2 [5]. Using artificially generated •OH and simulated natural waters, Goldstone et al. [5] reported a yield of 0.3 mole of CO_2 from the oxidation of DOC by 1 mole of •OH. Page et al. [10] used this laboratory yield to estimate that the amount of CO_2 produced from •OH in natural soil waters could be on the same order of magnitude as the amount of CO_2 produced by bacterial respiration of DOC in surface waters of the Alaskan Arctic. Page et al. [10] concluded that oxidation of DOC by •OH could be an important source of CO_2 in boreal and arctic regions given the vast stores of organic carbon residing in waterlogged soils conducive to redox cycling. Similarly, Hall and Silver [24] suggested oxidation of DOC by •OH to CO_2 is important in tropical soils where they observed a strong, positive correlation between Fe(II) oxidation and CO_2 production. However, the effects of •OH on the fate of DOC in natural systems remain poorly understood because no study has directly measured the CO_2 produced from oxidation of DOC by •OH in soils or soil waters.

The objectives of this study were to (1) determine the relative importance of Fe(II) versus reduced DOC in the production of •OH, and (2) determine whether oxidation of DOC by •OH produces CO_2 in natural soil and surface waters. To address these knowledge gaps on the controls of dark •OH production and its fate, we measured concentrations of •OH produced upon introduction of air to low-O_2 and anoxic soil waters and to oxic surface waters in the Alaskan

Arctic. We also quantified production of H_2O_2, an expected key reactant produced from oxidation of either Fe(II) or reduced DOC in low-O_2 and anoxic waters. To identify the relative importance of Fe(II) versus DOC as electron donors (or other reductants present in natural waters), we quantified the oxidation of Fe(II) to Fe(III) alongside changes in total electron donating capacity upon introduction of O_2. Finally, we quantified production of CO_2 from the oxidation of DOC by •OH in soil waters.

2.3 Study Sites and Sampling Strategy

Soil and surface water samples were collected May – August 2015 and July – September 2016 near Toolik Lake Field Station on the North Slope of Alaska in the arctic tundra (Fig. 2.2). The objective in sampling surface waters was to verify the conceptual model for dark •OH production, i.e., that dark •OH is produced upon introduction of O_2 to low-O_2 waters (Fig. 2.1) [10]. Thus, we would not expect to detect high •OH production in the oxic surface waters near Toolik Lake, in contrast to the low O_2 soil waters in this region. Study sites for soil water sample collection represented the dominant land surface ages and vegetation types (Table 2.S1) [25] and were expected to differ in soil water chemistry primarily due to variability in calcium carbonate [26]. Soil water samples were collected from younger glacial surfaces (Itkillik I, ~60,000 yr BP (years Before Present) and Itkillik II, ~14,000 yr BP), and from an older glacial surface (Sagavanirktok, ~250,000 yr BP) [27]. In addition, soil waters were collected on the Arctic Coastal Plain in northern Alaska and from areas adjacent to glacial-fed rivers. Soil waters on younger surfaces were expected to have higher pH and conductivity than waters on older surfaces due to weathering and depletion of calcium carbonate over geologic time [26]. Soil waters collected on the Arctic Coastal Plain or next to glacial-fed rivers (the Sagavanirktok and Saviukviayak Rivers) were also expected to have higher pH and conductivity than soil waters

sampled near Toolik in this and prior work (Fig. 2.S4; Table 2.S1) [10] due to calcareous loess deposits [28]. Soil waters sampled from the younger and older landscape ages were collected from the two dominant ecosystem types: the upland tussock tundra and the lowland wet sedge tundra [29]. The dominant vegetation above all soil waters collected on the coastal plain and near the Sagavanirktok River was wet sedge tundra. Soil waters collected near the Saviukviayak River (*also spelled as* Saviukviak) were collected beneath birch-willow vegetation.

2.4 Methods

2.4.1 Soil and surface water collection and characterization

Soil water samples were collected below the ground surface using a stainless steel needle attached to a plastic syringe with a 3-way valve. The needle and syringe were triple rinsed with soil water before collection of bubble-free water to avoid introduction of oxygen (O_2) from air into the syringe. Water was pulled from the ground through the needle slowly to minimize collection of soil particles. Once the syringe was filled, soil water was transferred from the syringe to black BOD bottles, overfilling the bottle to minimize introduction of O_2 from air, and then stoppering. Surface waters were collected by dipping the BOD bottle into the water after triple rinsing the bottle with sample. Temperature, pH, and conductivity on unfiltered soil or surface water samples were measured in the field immediately after collection. For each soil or surface water sample collected, a subset of the water was filtered in the field using pre-combusted Whatman GF/F filters for analysis of dissolved organic carbon (DOC) concentrations. Water for analysis of cation concentrations was also collected in the field by filtering a subset of the sample through sample-rinsed Whatman 0.45 μm polypropylene filters. Subsamples for DOC and cation analysis were preserved with 6 N HCl. Subsamples for DOC and cations were stored in the dark at 4 ºC until analysis. Filtered and preserved samples for DOC and cation

analysis were analyzed on a Shimadzu TOC-V analyzer (CV ~ 5% on duplicate samples or standards) [30] and a Perkin Elmer ICP (CV ~ 3% on duplicate samples or standards), respectively.

After collection in the field, BOD bottles of surface and soil waters were transferred to an anoxic glove box (97% ultrapure nitrogen, 3% ultrapure hydrogen atmosphere) at Toolik Field Station (within 30 minutes to six hours after collection for sites farthest away from the station). Dissolved oxygen (DO) concentrations were measured in the glove box using an optical DO probe (YSI; 1% standard error). Soil and surface waters were analyzed for electron donating capacity (EDC), total iron and Fe(II), •OH, H_2O_2, and CO_2 production at room temperature (Fig. 2.3, details *below*). For each analysis (EDC, iron, •OH, H_2O_2, CO_2) sample waters were split into triplicates for initial, control, and treated subsamples. All values reported for EDC, iron, •OH, H_2O_2, and CO_2 are mean ± standard error from the triplicate samples. The chemical composition of unamended surface waters might have changed slightly if the waters were under-saturated with O_2 before sampling. Unamended soil waters were likely close representations of the chemical composition of water collected in the field, given the short duration between collection and analysis and the limited exposure to the atmosphere or to light.

2.4.2 Electron donating capacity and iron oxidation

For quantification of initial electron donating capacity (EDC), total iron, and Fe(II) from soil and surface waters, subsamples were analyzed immediately after filtration (0.2 μm Sterivex filter) in the anoxic glove box (initial; Fig. 2.3). EDC, total iron, and Fe(II) were quantified again after filtered subsamples were oxidized by O_2 for 24 hours (+air; Fig. 2.3). EDC was measured colorimetrically using 2, 2-azino-bis (3-ethylbenzothiazoline-6-sulfonic acid) (ABTS+•) [10]. For the EDC measurements, soil waters were often diluted by 2 - 200 fold with

aerated MilliQ water (deionized water further purified to achieve a resistivity of 18.2 MΩ and treated by UV to reduce residual organics). Total iron and Fe(II) concentrations were quantified colorimetrically by the ferrozine method [30]. Soil waters often had to be diluted 2 - 80 fold in aerated MilliQ water due to high Fe(II) concentrations. Absorbance for both EDC and iron were measured on spectrofluorometer (Aqualog, Horiba Scientific), at 734 nm and 562 nm, respectively, using 1 cm pathlength cuvettes. Change in EDC and Fe(II) between initial and oxidized waters represent electrons released from oxidation of all reduced constituents and electrons released from oxidation of Fe(II), respectively, in surface and soil waters.

To test whether ABTS+• could detect electron donating capacity from the high concentrations of Fe(II) in these soil waters, the EDC was measured over the range of Fe(II) concentrations using ferrous iron solutions, in the form of ferrous ammonium sulfate. Ferrous ammonium sulfate solutions were prepared in 0.01 N HCl at concentrations of Fe(II) observed in these soil waters (Fig. 2.S1) [10]. At Fe(II) concentrations above 50 μM, ABTS+• did not detect all electrons that could be donated from Fe(II), leading to lower EDC than expected based on the Fe(II) concentration (Fig. 2.S1). This underestimate in EDC was likely due to complexation of Fe(II) with the high concentration of phosphate (~2.7 mM) in the ABTS+• buffer, resulting in less Fe(II) available to donate electrons to ABTS+•. This test of ABTS+• with Fe(II) standard ferrous iron solutions suggests that ABTS+• may underestimate electrons donated from Fe(II) in surface or soil waters with Fe(II) concentrations > 50 μM.

2.4.3 •OH production

Terephthalate (TPA) was used as a probe to quantify •OH production in this study, the same probe as used previously in these soil waters [10]. During summer 2015, unfiltered subsamples of soil water were analyzed for •OH production following protocols described in

Page et al. [10]. Although Page et al. [10] reported no difference in •OH production between unfiltered versus filtered soil waters, during the summer of 2016 soil waters were filtered before •OH analysis (0.2 μm Sterivex filters) to minimize potential biological •OH production. The initial •OH production was quantified upon addition of soil or surface water samples to O_2-free TPA, with TPA present in excess (initial; Fig. 2.3). O_2-free TPA was prepared by bubbling with nitrogen. The solution was then stored in the dark in the glove box. Initial •OH production was quantified after 24 hours to allow for any •OH initially present in the sample to react with TPA. Production of •OH from oxidation of reduced constituents by O_2 was quantified by adding soil or surface waters to O_2- free TPA that was then exposed to O_2 by adding air (+air; Fig. 2.3). These aerated samples were allowed to react for 24 hours (+air; Fig. 2.3) and stirred every hour for 12 hours. After 24 hours the •OH concentrations in the initial and oxidized (+air) waters were determined using standard additions to the samples of 0, 25, and 50 nM 2-hydroxyterephthalic acid (hTPA, the product of TPA reaction with •OH) [32] to account for matrix effects. hTPA was quantified on an Acquity Ultra High Performance H-Class Liquid Chromatography (uPLC; Waters, Inc.) with fluorescence detection (excitation 250 nm, emission 410 nm) on an Acquity uPLC BEH C_{18} column (2.1 x 50 mm; 1.7 μm). The yield for hTPA formation from •OH reaction with TPA was assumed to be 35% [9,10].

2.4.4 Hydrogen peroxide production

During summer 2016, a subset of soil waters was analyzed for H_2O_2 using the Amplex Red method [33,34] on the uPLC (excitation 565 nm, emission 587 nm). Undiluted, 0.2 μm-filtered soil waters were added to aerated Amplex Red reagents (+air; Fig. 2.3) to allow for oxidation of soil water. There was no control for the +air treatment for H_2O_2 production due to the inability to limit introduction of O_2 to the samples with addition of Amplex Red reagents.

However, verification of the presence of H_2O_2 was conducted by addition of catalase to soil water, which rapidly decomposes H_2O_2 to water and O_2. Thus, soil water containing 3 mg L^{-1} catalase (+catalase, +air; Fig. 2.3) should yield no H_2O_2 upon introduction of air. H_2O_2 produced during oxidation in the presence and absence of catalase was quantified one hour after addition of soil water to the Amplex Red reagent. H_2O_2 was quantified using standard additions (500 - 2500 nM of H_2O_2 added) with three replicates per concentration of added H_2O_2, after subtraction of the background signal from Amplex Red alone.

2.4.5 CO_2 production

To quantify CO_2 production from the introduction of an oxidant to soil water, nitrogen-sparged aliquots of H_2O_2 were added to soil waters to achieve a final concentration of 50 or 100 μM H_2O_2 (+ H_2O_2; Fig. 2.3). Controls were amended with the same volume of O_2-free MilliQ water to account for any change in dissolved CO_2 due to introduction of MilliQ water (control; Fig. 2.3). Both controls and amended vials had no headspace. In addition, four different soil waters were oxidized with a range of H_2O_2 concentrations (5 - 300 μM). After letting the control or +H_2O_2 soil waters react for 24 hours at room temperature in the dark, soil waters were analyzed for dissolved inorganic carbon (DIC) concentration using a DIC analyzer (Apollo, Inc.). Change in DIC between oxidized and control soil waters represents CO_2 produced by H_2O_2 during the 24-hour oxidation.

•OH production was also quantified from each soil water oxidized by H_2O_2 (Fig. 2.3) to test the hypothesis that the production of CO_2 was due to oxidation of DOC by •OH. However, absolute •OH production may have differed between the same +H_2O_2 soil water used to quantify CO_2 versus to quantify •OH due to differences in methodological constraints for detection of DIC versus •OH. The volume of soil water and thus concentration of Fe(II) exposed to the same

concentration of H_2O_2 differed between the undiluted subsample of soil water quantified for CO_2 production, versus the diluted subsample of the same soil water quantified for •OH production. This is because quantification of •OH requires soil water to be diluted (~17-fold) with added TPA, to ensure that TPA is present in excess of other constituents that may scavenge •OH (see *methods* above) [34]. These methodological constraints resulted in the same concentration of H_2O_2 added to higher concentrations of soil water constituents in the soil waters used to test CO_2 production compared to the soil waters used to quantify •OH production (Fig. 2.3, 2.S3). The ratio of H_2O_2 added per mol Fe(II) in sample waters was higher in the subsamples used to quantify •OH production compared to the subsamples used to quantify changes in CO_2. Thus, it is possible that •OH production is higher in the subsample used to quantify CO_2 production compared to the subsample used to measure •OH. However, we assume that dilution does not affect trends in •OH production between soil waters; that is, a soil water exhibiting relatively high •OH production compared to another soil water will do so independent of dilution. When relating trends in CO_2 production versus •OH production from soil waters amended with H_2O_2, •OH production is expressed as the "relative" •OH (Fig. 2.7, 2.9).

Because no study has directly measured CO_2 production from oxidation of DOC by •OH in any natural water, we first tested this reaction by exposing a reference isolate of terrestrially-derived DOC to •OH produced by the Fenton reaction (i.e., •OH was produced by reaction of Fe(II) with H_2O_2). Suwannee River Fulvic Acid (SRFA), a reference DOC isolate obtained from the International Humic Substances Society (IHSS), served as a terrestrial end-member of DOC representing carbon derived from decomposed plant matter and soils (http://humic-substances.org). SRFA solutions were prepared by dissolving freeze-dried solid SRFA in air-equilibrated MilliQ water. The SRFA solution had a final pH of 5.2, a DOC concentration of

2310 μM, and 60 μM Fe(II) added in the form of ferrous ammonium sulfate. The pH of the SRFA solution and the ratio of DOC to Fe(II) were similar to soil waters sampled in the field (Table 2.1). A range of H_2O_2 concentrations was added to the SRFA + Fe(II) solution (5 to 300 μM H_2O_2), and compared to a control with no H_2O_2 added. After 24-hour oxidation, CO_2 and relative •OH production were measured as described above.

2.4.6 Soil core collection

Soil cores were collected with a SIPRE coring auger from six different sites during summer 2015. Seven cores were collected at each site (Fig. 2.2) to yield a minimum of 4 kg wet soil per depth analyzed. Soils collected from cores were split by depth into the annually thawed, shallow organic mat (5-50 cm; the "active layer"), and the deeper permafrost layer that included both organic and mineral soil horizons (95-105 cm). Immediately after collection soils were placed into Ziploc bags and frozen at -20 ^{o}C until thawed for further experiments.

2.4.7 Soil leachates

Frozen soil (250 grams) was added to 1 L of MilliQ water and allowed to incubate in the dark at room temperature in an anoxic glove box for two weeks. The amount of soil added and incubation time were chosen to generate soil leachates that contained similar chemistry (pH and conductivity) and concentrations of Fe(II), EDC, and DOC comparable to soil waters collected in the field. Following incubation, soil water leachates were 0.2 μm filtered (Sterivex), split into initial, control, and treatment triplicate subsamples, and analyzed for EDC, total iron, Fe(II), •OH, and CO_2 as described above. Soil water leachates were tested alongside soil waters sampled in the field to increase the dataset of CO_2 and relative •OH production in this study.

2.5 Results

2.5.1 Surface and soil water chemistry

On average, soil waters were mildly acidic (pH 5.6 ± 0.7) and contained low O_2 (29 ± 5 μM DO) (Table 2.1). The average specific conductivity in soil waters was 408 ± 104 μS cm^{-1} (Table 2.1), and the average concentration of DOC was 1769 ± 262 μM (Table 2.1). Average iron concentrations were 245 ± 57 μM for total iron and 225 ± 56 μM for Fe(II) (Table 2.1). The average EDC upon introduction of air to soil waters was 192 ± 30 μM electrons released (Table 2.1). Waters leached from soils incubated in the lab (i.e., soil leachates) had lower conductivity, but similar pH and similar concentrations of DOC, EDC, and iron as compared with soil waters collected in the field (Table 2.1). On average, surface waters had higher pH (6.7 ± 1.7; Table 2.1), higher DO concentrations, lower specific conductivity, and lower concentrations of DOC, EDC, and iron compared to soil waters sampled in the field and soil water leached in the laboratory (Table 2.1).

The change in EDC upon addition of O_2 to soil waters relative to the initial value was a measure of electrons released from oxidation of reduced constituents (Fig. 2.4). Likewise, the change in Fe(II) concentration upon introduction of air to soil waters relative to the initial value was a measure of electrons released from Fe(II) oxidation (Fig. 2.4). There was a significant, positive correlation between electrons released from Fe(II) oxidation and total number of electrons released from oxidation of all reduced constituents (slope = 0.72 ± 0.02, $p < 0.0001$; Fig.2. 4), suggesting that Fe(II) was the main source of electrons released upon oxidation.

2.5.2 Trends in •OH production

Production of •OH ranged from undetectable to 20 ± 7.9 μM (N = 77) for soil waters oxidized by O_2 (air; Fig. 2.3), and from undetectable to 50 ± 0.3 μM (N = 93) for soil waters

oxidized with H_2O_2. •OH production was significantly, positively correlated with the initial EDC ($R^2 = 0.70$, $p < 0.0001$; Fig. 2.5A) and initial Fe(II) in soil waters tested ($R^2 = 0.66$, $p < 0.0001$; Fig. 2.5B). However, there was no significant correlation between •OH production and Fe(II) oxidation over the 24-hour aeration period (Fig. 2.S2). There was also no significant correlation between •OH production and other water chemistry parameter (e.g., conductivity, carbonate; data not shown). •OH production was higher on average from soil waters sampled on older or fluvial land surfaces compared to younger surfaces or the coastal plain (Table 2.S1). Surface water samples had low production of •OH upon introduction of O_2, consistent with the relatively high dissolved O_2, low EDC, and low Fe(II) concentrations in these waters compared to soil waters (Table 2.1; Fig. 2.5A, B).

2.5.3 H_2O_2 concentrations in soil waters

The average H_2O_2 concentration after one hour oxidation by O_2 in soil waters was 21 ± 11 μM. H_2O_2 concentration in soil waters after oxidation by O_2 was generally higher for soil waters with low initial O_2 concentration (Fig. 2.6). As a qualitative confirmation of H_2O_2 production from aeration of soil waters, H_2O_2 concentrations were compared between a filtered soil water leachate oxidized by O_2 in the presence and absence of catalase, an enzyme that rapidly decomposes H_2O_2 to water and O_2. In the absence of catalase, the soil water produced 2.7 ± 0.40 μM H_2O_2 after one hour exposure to air (data not shown). In the presence of catalase, there was no detectable H_2O_2 produced from the soil water.

2.5.4 •OH and CO_2 production from soil waters amended with H_2O_2

All soil waters amended with H_2O_2 showed significant production of relative •OH compared to the control (no H_2O_2 addition; Figs. 2.3, 2.7A, 2.7B). For soil waters amended with a range of H_2O_2 concentrations, relative •OH production was positively, linearly correlated with

the concentration of H_2O_2 added (Fig. 2.7A). The slope of the relationship between H_2O_2 added and relative •OH produced varied between the soil waters and leachates tested, ranging from 0.08 ± 0.01 ($p < 0.01$) to 0.01 ± 0.002 ($p < 0.01$) (Fig. 2.7A). •OH production was significantly higher in the soil water amended with H_2O_2 in the absence of catalase, compared to unamended soil waters and to the soil water containing H_2O_2 and catalase (Fig. 2.8).

Most soil waters amended with H_2O_2 showed a significant increase in DIC (i.e., CO_2 produced) compared to control soil waters (65% of 92 soil waters tested, Fig. 2.S3). The remaining soil waters showed no detectable production of CO_2 (35% of soil waters tested). The production of CO_2 from all soil waters was not significantly correlated with EDC, total iron and Fe(II), or •OH production (Fig. 2.S3). However, CO_2 produced was significantly, positively correlated with increasing concentrations of H_2O_2 added to four soil waters (Fig. 2.7B). The slope of the linear relationship between H_2O_2 added and CO_2 produced differed by soil water, ranging from 0.39 ± 0.09 ($p < 0.1$) to 0.04 ± 0.002 ($p < 0.0001$) (Fig. 2.7B). There was no systematic pattern between the slopes of the linear relationship of CO_2 produced and H_2O_2 added for soil waters by date, site, or between soil water versus soil leachate. For the solution of Suwannee River Fulvic Acid (SRFA) containing Fe(II), there was also a significant, positive correlation between CO_2 produced and H_2O_2 added (Fig. 2.7B). The slope of the relationship for CO_2 produced and H_2O_2 added for SRFA + Fe(II) was within the range of slopes observed for the natural soil waters containing similar concentrations of DOC and Fe(II) and amended with the same range of H_2O_2 concentrations (Fig. 2.7B).

For any soil water amended with H_2O_2, both relative •OH production and CO_2 production increased with increasing H_2O_2 concentration added (Fig. 2.7A, 2.7B). Therefore, for all sample types, sites, and dates, CO_2 production was significantly positively correlated with the

•OH produced by adding H_2O_2 (Fig. 2.9). The slopes of the relationship between CO_2 production and relative •OH production varied between the soil waters and leachates, and SRFA + Fe(II) solution, as did the slopes representing relative •OH production and H_2O_2 added to different soil waters (Fig. 2.7A, 2.7B).

2.6 Discussion

2.6.1 Conditions favorable for dark •OH production in arctic soil waters

Overall, our main results (1) extend the findings of •OH production by aeration of soil or surface water to a wider range of water chemistry, (2) demonstrate that Fe(II) is the dominant electron donor supporting •OH production, and (3) provide direct, multiple lines of evidence for the production of CO_2 from the oxidation of DOC by •OH in natural waters. The first main result is consistent with prior work demonstrating that •OH is produced from aeration of soil or lake waters containing reduced constituents [10,11]. These findings support the conceptual model proposing •OH production from the oxidation of Fe(II) or reduced DOC by dissolved O_2 (Fig. 1) [9]. Consistent with this conceptual model and prior work [10], in this study there was little •OH production in oxic surface waters containing lower EDC, lower Fe(II), and lower DOC, while in low-O_2 waters with higher EDC, higher Fe(II), and higher DOC the •OH production was significantly, positively correlated with initial EDC and Fe(II) (Fig. 2.5A, 2.B).

Our first result demonstrates that reducing conditions (i.e., high EDC and thus high concentrations of electron donors) that support •OH production can be found across a wider range of pH and conductivity in anoxic and low-O_2 arctic soil waters than previously observed [10]. In this study, the subset of soil waters sampled on the Arctic Coastal Plain and adjacent to glacially-fed rivers (Fig. 1) had significantly higher pH and specific conductivity than soil waters sampled near Toolik in this and prior work (Table 2.S1; Fig. 2.S4) [10]. Soil waters of the

Coastal Plain and adjacent to glacial-fed rivers had higher pH and specific conductivity due to calcareous loess deposits [28]. Reducing conditions are observed across a range of pH and conductivity in arctic soil waters due to the presence of permafrost at a shallow depth and flat topography that prevents drainage of water and leads to saturated, low-O_2 soils [35,36]. Anoxic or low-O_2 soils lead to strongly reducing conditions that accelerate the buildup of high concentrations of electron donors such as Fe(II) in arctic soils. For example, previous work showed that arctic soil waters spanning a wide range of pH and conductivity contain concentrations of reduced Fe(II) ranging from 100 to 10,000 μM [10,16,26,37-39].

The yield of •OH from the oxidation of reduced constituents such as Fe(II) or reduced DOC may depend strongly on pH. At circumneutral pH, the oxidation of Fe(II) may yield oxidants other than •OH [39]. For example, at pH 7, oxidation of Fe(II) may result in production of ferryl iron (Fe(IV)) as well as •OH, which would lower the ratio of •OH produced per mol Fe(II) oxidized [7,40]. Studies of the •OH production from Fe(II) oxidation suggest that at low pH (~5), production of •OH from Fe(II) oxidation is more likely than production of Fe(IV) [40]. In contrast to Fe(II) oxidation, the effect of pH on the yield of •OH from oxidation of reduced DOC has not been studied. It has been shown that at high pH the oxidation of reduced moieties within DOC is more favorable than at low pH [17], suggesting that oxidation of DOC to produce •OH might be more likely at higher pH. Overall, the yield of •OH from oxidation of Fe(II) or reduced DOC is expected to be higher in natural waters with low pH than in waters with higher pH where there could be production of ferryl ion in addition to •OH. Consistently, in our study •OH production was generally higher in mildly acidic soil waters (pH ~ 6; Fig. 2.S4), while •OH production was generally lower in soil waters with pH > 7.5 (Fig. 2.S4).

2.6.2 Oxidation of Fe(II) controls •OH production in arctic soil waters

2.6.2.1 Fe(II) was the main electron donor to O_2

The second main result of this study provides strong evidence that Fe(II) was the main electron donor to O_2 upon aeration of soil waters, and thus the main control on •OH production in soil waters of the Alaskan Arctic. The significant, linear correlation between the total electrons released and the electrons released from Fe(II) oxidation upon addition of air to soil waters (Fig. 2.4) suggests the oxidation of Fe(II) accounts for the total electrons released during the oxidation. Assuming one mole of Fe(II) oxidized contributes one mole of electrons, the change in Fe(II) concentration should correspond 1:1 with the electrons released upon aeration. The relationship between moles of electrons released from Fe(II) oxidation per moles of total electrons released supported this expectation, and had a slope of 0.72 ± 0.02 ($p < 0.0001$) (Fig. 2.4), suggesting that 7 out of 10 moles of electrons released came from Fe(II).

2.6.2.2 Limitations of the EDC method to detect electrons released from Fe(II) oxidation

Some soil waters had a lower EDC than expected based on the amount of Fe(II) oxidized, and plotted substantially below the 1:1 line in Figure 4. This is likely due to interference in the EDC method that uses a phosphate buffer to minimize changes in pH [17]. In the presence of high concentrations of Fe(II) in soil waters, a greater proportion of Fe(II) may complex with phosphate in the buffer solution, which may slow the oxidation of Fe(II) [41]. Thus, complexation of Fe(II) with phosphate may result in a lower EDC than expected based on the concentration of Fe(II) present. For example, when Fe(II) as the electron donor was added to MilliQ water in the form of ferrous ammonium sulfate, the EDC was lower than the concentration of Fe(II) when Fe(II) concentrations exceeded 50 µM (less than 1 mol of total electrons released per 1 mol of electrons released from Fe(II); see *methods* and Fig. 2.S1). This

result suggests that at high Fe(II) concentrations some of the iron complexes with phosphate, resulting in a lower EDC than expected based on the initial Fe(II) concentration. Because phosphate buffer was used only for the subset of soil waters analyzed for EDC, and was not used to quantify Fe(II) oxidation upon addition of air, there was no interference for the quantification of the oxidation of Fe(II). Thus, together these results strongly indicate that for the 78% of soil waters plotting on or below the 1:1 line for the electrons released from Fe(II) oxidation versus total electrons released (Fig. 4), Fe(II) was the most important electron donor upon oxidation of soil waters.

2.6.2.3 Contribution from other electron donors to •OH production

For the ~ 20% of soil waters plotting above the 1:1 line, electron donors other than Fe(II) may have contributed to the EDC upon aeration of soil water (Fig. 2.4). While oxidized iron could be reduced and re-oxidized multiple times (*section 2.5.4.1.*), most of the soil waters that plotted significantly above the 1:1 line had low Fe(II) concentrations suggesting the presence of electron donors other than iron (Fig. 2.4). Based on estimates of the fraction of DOC that may be reduced and on the concentrations of total manganese (Mn) in these soil waters, previous work proposed that alternate electron donors may include reduced DOC or Mn (Table 2.1) [10]. Sulfide could be an additional electron donor [18]; however, concentrations of sulfide in the soil waters of this study are too low for sulfide to be a substantial source of electrons to produce •OH [10]. The expected reductants within the DOC pool are reduced quinone moieties, which may produce •OH upon oxidation by air via an organic Fenton reaction, with H_2O_2 expected to be an intermediate, similar to Fe(II) oxidation (Fig. 2.1) [9]. Assuming the same fraction of reduced DOC in our samples as that determined for similar samples by Page et al. [10], DOC could have accounted for 25% of the EDC on average from the soil waters in this study. Concentrations of

total Mn were on average five-fold lower than total iron in these soil waters (Table 2.1) [10], suggesting that Mn was likely less important than Fe(II) or DOC as an electron donor to O_2 yielding •OH in most soil waters. However, at one site, concentrations of Fe(II) were significantly lower than the EDC (Fig. 2.4) and lower than total dissolved Mn (49 μM), suggesting that the oxidation of reduced Mn could have contributed to the EDC.

2.6.3 H_2O_2 production is consistent with a Fenton source of •OH

Here we show for the first time that H_2O_2 is produced upon introduction of O_2 to anoxic or low-O_2 soil waters (Fig. 2.6). H_2O_2 may be present in soils as a result of fungal activities that may produce H_2O_2 to degrade lignin by the Fenton reaction [42]. While H_2O_2 has not been measured directly in soils before, others have reported dark H_2O_2 production or H_2O_2 concentrations in ponds, lakes, and coastal waters [34,43,44]. Dark H_2O_2 production in low Fe(II), oxic surface waters was attributed to biological activity [34,43,44]. H_2O_2 production in this study was not likely due to biological processes because soil waters were filtered to minimize microbial activity prior to oxidation (see *methods*). In addition, H_2O_2 likely reacts rapidly with the high Fe(II) concentrations in these soil waters (Table 2.1, Fig. 2.1), and thus any H_2O_2 biologically produced prior to filtration should not be stable. High concentrations of H_2O_2 similar to those in this study (μM range; Table 2.1; Fig. 2.6) have been reported for aerated sediments amended to contain high concentrations of Fe(II), where production of up to ~ 4 μM H_2O_2 in the amended sediments was attributed to the oxidation of Fe(II) by O_2 [45]. Thus, this direct evidence for the production of H_2O_2 upon aeration of soil waters rich in reduced constituents (Fig. 2.1, 2.6) is also evidence for an abiotic source of H_2O_2.

H_2O_2 production from aeration of soil waters was higher at low initial O_2 concentrations, suggesting that H_2O_2 production resulted from oxidation of reduced constituents such as Fe(II) or

DOC (Fig. 2.6). This result is consistent with the well-studied production of H_2O_2 during the oxidation of Fe(II) or reduced DOC by O_2 [9,13,14,19,46]. H_2O_2 produced by the oxidation of Fe(II) or reduced DOC likely subsequently oxidized Fe(II) in these high-iron soil waters, leading to production of •OH [47].

2.6.4 Controls on the production of •OH from iron oxidation in arctic soil waters

2.6.4.1 The yield of •OH from Fe(II)

Evidence from this study strongly suggests that Fe(II) oxidation is the main source of •OH produced upon aeration of soil waters (Fig. 2.4). However, the large variability in the amount of •OH produced from soil waters with the same initial concentration of Fe(II), or the same amount of Fe(II) oxidized upon aeration (Fig. 2.5, 2.S2), suggests that factors other than the initial amount of Fe(II) present can influence the production of •OH. Given that •OH production and oxidation of Fe(II) were each measured over the same time period (24 hours) for all waters, we interpret differences in •OH production per oxidation of Fe(II) to be due to differences in the yield of •OH per mol Fe(II) oxidized. Differences in •OH yield per mol Fe(II) oxidized may be due to the large variability in soil water chemistry (pH, initial Fe(II), DOC) that influenced both the rate of Fe(II) oxidation and the production of specific intermediates and products formed during Fe(II) oxidation [19,33,48,49]. In water containing only dissolved O_2 and iron, the expected (net) stoichiometry is one mole •OH produced for every three moles Fe(II) oxidized (Fig. 2.S2) [40], because the oxidation of iron proceeds by a series of one electron transfer reactions to O_2 producing a suite of reactive oxygen species [13]. However, in natural waters varying widely in chemistry, the molar yield of •OH per mol Fe(II) oxidized may be substantially different than the expected 1:3 ratio because iron may undergo rapid redox cycling.

Previous work in simulated sediment pore waters reported that iron redox cycles varied widely as a function of pore water chemistry. Burns et al. [8] reported that the number of Fe(II) / Fe(III) cycles may vary between 10 – 22000, resulting in 3 to 750 mol •OH produced per mol Fe(II). Thus, in natural soil waters it may be possible to generate > 1 mol •OH per 3 mol Fe(II) oxidized if there are many cycles of Fe(II) / Fe(III) [8].

The controls on the number of iron redox cycles yielding •OH in natural waters are not yet well understood. In this study, few soil waters exhibited greater than the expected 1 mol •OH produced per 3 mol Fe(II) oxidized (Fig. 2.S2) if there were many cycles of Fe(II) / Fe(III). Most soil waters exhibited less than 1 mol •OH produced per 3 mol Fe(II) oxidized (Fig. 2.S2). We expect in these DOC-rich soil waters for DOC to have the greatest influence on the iron redox cycling (Table 2.1). DOC can influence the iron redox cycling and thus •OH production by (1) forming complexes with iron and by (2) playing a role in iron oxidation and reduction.

2.6.4.2 Complexation of Fe(II) with DOC

Complexation of Fe(II) with DOC ligands has been suggested to affect the rate of Fe(II) oxidation [19,49]. In the predominately acidic to mildly acidic soil waters in this study, organic ligands within DOC were most likely to form complexes with Fe(II) given that these waters contain high DOC concentrations and low concentrations of other ligands such as sulfide or carbonate (Table 1) [10]. Given that concentrations of Fe(II) and Fe(III) were much higher than expected based on equilibrium with the amount of dissolved oxygen at the specific pH of the soil water (Table 2.1, Fig. 2.S4), it is likely that interactions between Fe(II) and DOC influenced the stability of Fe(II) [50,51,52]. Alternatively, DOC may influence iron redox cycling by increasing rates of Fe(II) oxidation. For example, Voelker and Sulzberger [19] found faster oxidation of Fe(II) by H_2O_2 in the presence of DOC. Fe(II) and DOC concentrations are

strongly, positively correlated in soil waters in this study ($p < 0.05$; data not shown), and there is evidence for an association between iron and DOC in soil waters [38,53]. However, it is currently not possible to predict the specific effects of DOC on iron redox cycling, and thus on the •OH production during aeration of natural waters, due to lack of information on the identity, abundance, and acidity of DOC ligands for iron.

DOC in arctic soil waters is derived mostly from the degradation of plant and soil matter, and thus this DOC pool contains abundant carboxyl and phenolic moieties [54,55]. Herndon et al. [38,56] showed that both Fe(II) and Fe(III) present in arctic soil waters were complexed with DOC, and Daugherty et al. [57] suggested that carboxyl ligands within DOC are most important for complexing Fe(II). These findings are consistent with prior work suggesting that carboxyl and phenolic moieties may serve as ligands to complex with both Fe(II) and Fe(III) [7,19,50,52]. In carboxyl and phenolic rich DOC soil waters from our study, DOC is expected to complex with Fe(II), but how this complexation may either speed up or slow down Fe(II) oxidation, or influence the number of Fe(II) / Fe(III) redox cycles and thus influence •OH production, remains an open question.

2.6.4.3 The role of DOC in iron oxidation and reduction

In addition to the role of DOC in complexing with iron, DOC likely influences iron redox cycling and •OH production by acting as a source of reactive oxygen species involved in iron oxidation and reduction, or as a reductant of Fe(III). Oxidation of reduced DOC could produce H_2O_2 [9], the key reactant in Fenton-mediated Fe(II) oxidation that yields •OH (Fig. 2.1, 2.6). Interactions of iron with DOC may also influence the balance of reactive intermediates and products formed during iron redox cycling [19,40]. For example, in the presence of terrestrially-derived DOC (e.g., SRFA), Voelker and Sulzberger [19] found that •OH reacted with DOC to

produce an organic radical. The organic radical reduced O_2 to yield superoxide that then oxidized Fe(II) to Fe(III) and regenerated H_2O_2. DOC can also reduce Fe(III) to Fe(II) [7,19], thereby enhancing iron redox cycling by regenerating Fe(II) that had been oxidized by O_2 or by reactive oxygen species. Thus, by acting as a source of reactive oxygen species or as a reductant of Fe(III), DOC may have influenced the number of iron redox cycles or rate of Fe(II) oxidation, affecting the range of •OH production per mol Fe(II) oxidized in the study waters (Fig. 2.5, 2.S2).

2.6.5 •OH oxidation of DOC and CO_2 production

2.6.5.1 CO_2 production in soil waters

The third main result is that more than half the soil waters tested showed production of CO_2 within 24 hours after addition of H_2O_2. Increasing CO_2 production with increasing H_2O_2 (Fig. 2.7) and increasing relative •OH (Fig. 2.9) is consistent with the oxidation of DOC to CO_2 by •OH [8,19,24]. DOC is likely the main sink for •OH in soil waters due to high DOC concentrations and low concentrations of quenching anions like chloride and bromide [4,10] that can scavenge •OH [58]. Carbonate can also scavenge •OH to produce low energy radicals at a slower rate than •OH reacts with DOC [20]. However, while some of the soil waters or soil leachates contained relatively high DIC (i.e., high carbonate alkalinity), at the pH of these soil waters there were still too few carbonate ions to compete with DOC as a sink for •OH (Table 2.1) [4,20]. Therefore, oxidation of DOC by •OH in the soil waters tested here is expected to be the main source of CO_2 produced.

The linear increase in both relative •OH and CO_2 production with increasing concentrations of H_2O_2 added to soil waters containing Fe(II) strongly supports the model of •OH oxidation of DOC as the source of the CO_2 (Fig. 2.9). Alternative pathways for CO_2

production from soil waters include aerobic microbial respiration of DOC or anaerobic fermentation. However, soil waters were filtered to remove microbes prior to H_2O_2 addition, thus minimizing CO_2 production from microbes.

Another line of evidence for oxidation of DOC by •OH as the source of CO_2 is the experiments with SRFA + Fe(II). Previous work showed that addition of H_2O_2 to solutions of SRFA + Fe(II) resulted in production of •OH [19], as we observed in this study (Fig. 2.7). This •OH is expected to oxidize DOC to CO_2, as shown directly here with CO_2 production increasing with increasing relative •OH in SRFA + Fe(II) solutions. Production of CO_2 in microbe-free solutions of SRFA + Fe(II) comparable to production in soil waters suggests that in both cases the source of CO_2 is oxidation of DOC by •OH (Fig. 2.9).

2.6.5.2 Variability in CO_2 production

The results suggest that for the same amount of •OH produced there can be large variability in CO_2 production from the oxidation of DOC by •OH. For example, there were differences in the yield of CO_2 produced per relative •OH produced between soil waters amended with a range of H_2O_2 concentrations (Fig. 2.9). Consistently, there was high variability in yield of CO_2 per relative •OH produced in all soil waters oxidized by H_2O_2 (Fig. 2.S3). Differences in DOC composition between the soil waters studied could influence whether CO_2 versus other products are formed from the oxidation of DOC by •OH [22,59,60]. It is expected that within the broad range of aromatic and aliphatic fractions of DOC shown to react with •OH, the abundance of the moieties that react most rapidly with •OH are expected to control the rate of DOC oxidation and thus the rate of CO_2 production [22,23]. In addition to DOC composition, other factors can influence the amount of CO_2 produced during the series of iron oxidation reactions that yield •OH, including the production of alternate oxidants (i.e., ferryl iron) [7,40].

Therefore, the range in the concentrations of CO_2 produced by DOC in the presence of •OH (Fig. 2.9) is consistent with the variable chemistry and DOC composition between the soil waters tested (Table 2.1) [55].

2.6.5.3 Underestimation of •OH production

Greater yield of CO_2 produced from oxidation of DOC by •OH in this study than a previously measured laboratory yield [5] may be evidence of underestimation of •OH produced in our study. Two methodological constraints may have contributed to an underestimation of •OH. First, as described in the *methods* and *results*, CO_2 production was quantified from undiluted soil water exposed to the same concentration of H_2O_2 as diluted soil water used to quantify •OH production. Due to differences in the methodological constraints for detection of CO_2 versus •OH, there was a larger ratio of Fe(II) and DOC to H_2O_2 present in the subset of (undiluted) soil waters used to quantify CO_2 production versus the subset of (diluted) soil waters used to quantify •OH. Higher concentrations of Fe(II) and DOC in undiluted soil waters could lead to a greater number of Fe(II) / Fe(III) redox cycles [8], and thus more •OH and CO_2 produced compared to diluted waters. In contrast to undiluted soil waters, in diluted soil waters containing low Fe(II) and DOC relative to the H_2O_2 present, Fe(II) may be unable to complete the redox cycle to produce •OH, or •OH may react with excess H_2O_2 (instead of DOC) to produce less reactive radicals [61]. Thus, the values of relative •OH produced reported here may be conservative, and there may have been more •OH produced in the undiluted soil water used to quantify CO_2 produced versus the same diluted soil water used to quantify •OH produced.

Second, assumptions about the yield for reaction of the TPA probe used to quantify •OH produced may lead to an underestimation of •OH produced from soil waters. Specifically, TPA reacts with •OH to produce hTPA, with a yield of 35% demonstrated in simulated natural waters

[60]. However, Charbouillot et al. [62] reported that the yield of hTPA produced per mol •OH in aqueous solutions decreased with decreasing pH between pH 7.5 to 3.9. Because the pH range of the soil waters studied here ranged from 7.6 to 4.5, applying a constant yield of 35% could underestimate the concentrations of •OH produced if the yield of hTPA produced per mol •OH present was lower. Although it is not possible to determine controls on the yield of •OH across the range of water chemistries studied here, a yield of 0.35 mol hTPA per 1 mol •OH has been proposed to be an upper limit [62,63]. Assuming the yield varies from 0.10 to 0.35 mol hTPA per 1 mol •OH [62], concentrations of •OH could be almost four times greater in some soil waters than reported here. Therefore, the multiple methodological limitations in •OH detection suggest that •OH produced from soil waters is likely a conservative estimate. While it was not possible to know with confidence the absolute •OH produced from oxidation of soil waters by O_2 or H_2O_2, the findings from this study strongly suggest that when •OH is produced, it oxidizes DOC to CO_2 (Fig. 2.9).

2.7 Conclusions and implications

Results from this study show for the first time that Fe(II) was the main electron donor upon aeration of soil waters, and that H_2O_2 is likely produced from aeration of natural waters with reduced species such as iron and DOC. Prior work and our results strongly indicate Fe(II) oxidation as the predominant pathway for •OH production when O_2 is introduced to arctic soil waters. This study also is the first to directly demonstrate that CO_2 is produced from natural soil waters in proportion to •OH produced, likely due to the oxidation of DOC by •OH. Thus, this study demonstrates that the dark, chemical oxidation of DOC by •OH may be an important source of CO_2 produced in arctic soils. Direct evidence for CO_2 from •OH oxidation of DOC in

this study supports prior work in tropical soils, where a correlation between CO_2 production and Fe(II) oxidation was suggested to be due in part to oxidation of DOC by •OH [24].

However, the quantitative importance of •OH in soil carbon cycling depends on the *in-situ* •OH production as redox constituents in soil waters cycle between reducing and oxidizing conditions. Waterlogged soils result in the accumulation of Fe(II) [16] that can be oxidized by the introduction of O_2. O_2 can be introduced through a change in the water table depth, slow diffusion to the oxic-anoxic interface, rain events, or downslope flow of anoxic soil waters into oxic surface streams. Introduction of O_2 by any of these pathways to Fe(II) rich soil waters could trigger the oxidation of DOC by •OH to CO_2 or to low molecular weight organic compounds [5] at these redox interfaces. Interestingly, Herndon et al. [38] reported the presence of low molecular weight compounds like acetate at redox interfaces in arctic soils. Therefore, understanding (1) the frequency of oxygenation events, (2) the rates of production of reduced species after oxygenation, (3) the variability in Fe(II) concentrations and *in-situ* •OH production, and (4) the controls on the production of CO_2 from oxidation of DOC by •OH, are the next steps needed to understand the role of dark •OH in soil carbon cycling.

Understanding iron-mediated •OH production is important because increased thaw depth in a warming Arctic may increase the abundance of Fe(II) in arctic and boreal soils [26,37,38,39,64]. For example, Barker et al. [65] reported the highest concentrations of total dissolved iron in arctic streams in late fall, which they attributed to deeper thaw into the mineral layer of the soils. Previous work has shown that minerals in permafrost soils contain leachable iron [26], but information from broad geographic settings is limited.

In addition to greater iron availability with increasing thaw depth, thawed permafrost soils contain tremendous stores of soil carbon [66] susceptible to oxidation by •OH. Oxidation

of DOC by •OH may be less selective than microbial oxidation and degradation of DOC [55], suggesting that even if annual rates of DOC oxidation by •OH to CO_2 are much less than microbial production of CO_2 from arctic and boreal soils, •OH oxidation of DOC may influence microbial respiration of DOC. For example, •OH may oxidize a fraction of DOC that would otherwise be relatively resistant to microbial degradation, or produce low molecular weight acids that are more labile to microbes [5]. Thus, iron-mediated •OH production and its oxidation of organic carbon could influence the conversion of the vast stores of organic carbon in permafrost soils to CO_2 on relatively short time scales, and potentially contribute to an accelerating feedback to global warming [e.g.,67].

2.8 Acknowledgements

We thank K. Yuhas, J. Dobkowski, C. Ward, C. Cook, M. Findley, A. Deely, and researchers, technicians, and support staff of the Toolik Lake Arctic LTER and Toolik Lake Field Station (GIS, J. Stuckey) for assistance in the field and laboratory. Thanks to Anne Giblin and three anonymous reviewers for helpful feedback on the manuscript. Research was supported by NSF CAREER-1351745, DEB-1026843 and 1637459, PLR-1504006, and NSF GRFP to A. Trusiak.

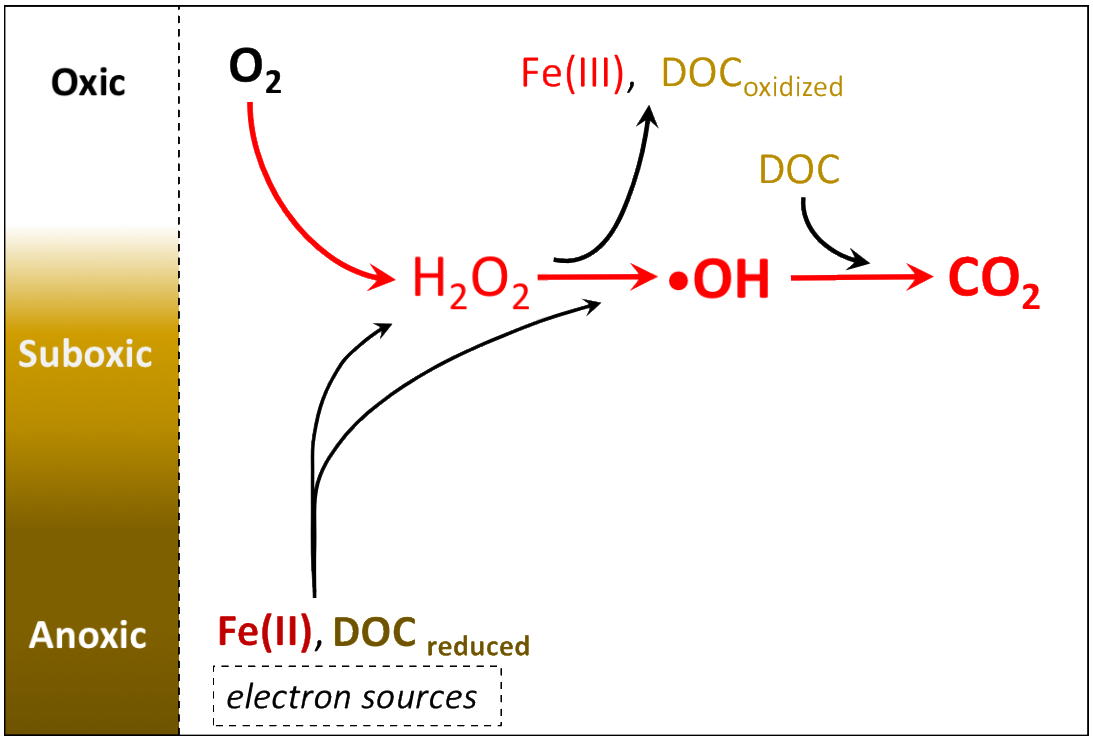

Figure 2.1. Summary of expected iron and DOC redox reactions upon introduction of air (O_2) to soil waters in this study. Species in red or maroon were measured directly (see Methods). Oxidation of Fe(II) and reduced DOC by O_2 produces H_2O_2. H_2O_2 can oxidize the remaining Fe(II) and reduced DOC to produce •OH. •OH in turn can oxidize DOC to produce CO_2.

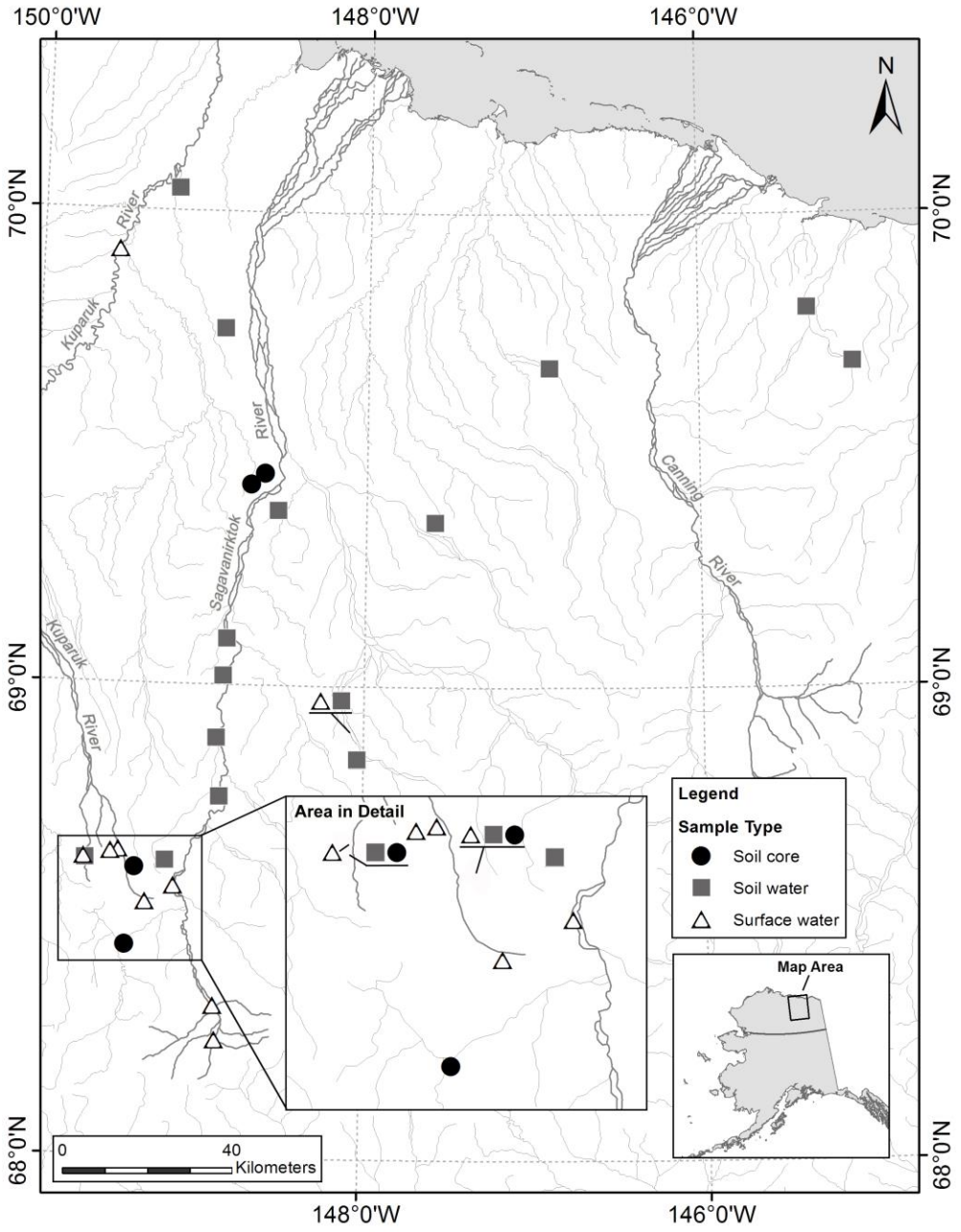

Figure 2.2. Map of sampling sites across the North Slope of Alaska where soil (triangles) and surface waters (squares), and soil cores (circles) were collected for this study. Sites north of ~69.7º latitude are on the Arctic Coastal Plain.

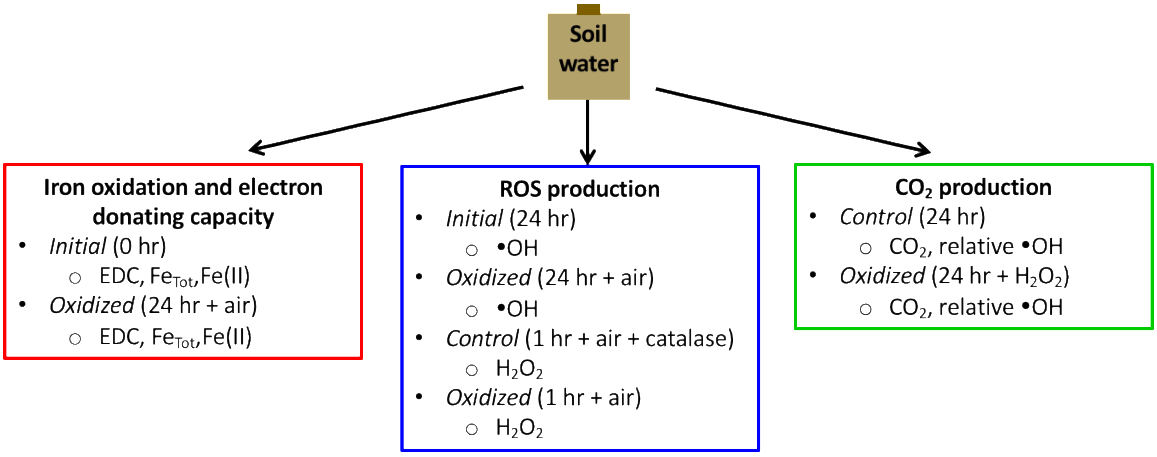

Figure 2.3. Summary of experimental design to quantify the role of iron oxidation in the production of reactive oxygen species (ROS) and CO_2 from arctic soil waters (see methods for details). Analysis of each analyte required different dilution factors and ways of introducing the oxidant (air or H_2O_2). Thus, subsamples of filtered soil water were placed into vials depending on requirements for analyte concentration and measurement volume, grouped here by experimental objective. Oxidation of iron and other reduced constituent were quantified by measuring the change in total iron and Fe(II), and the change in electron donating capacity, respectively, between the initial soil water (at 0 hours) and after 24 hours oxidation by O_2 (i.e., aeration). •OH and H_2O_2 produced during aeration were quantified after 24 or 1 hour aeration, respectively, by addition of soil water to aerated reagents. Due to method constraints, the aeration time for H_2O_2 analysis was shorter than other analyses (see Methods 3.4). CO_2 and relative •OH production were quantified 24 hours after addition of H_2O_2 to soil water compared to a control (i.e., no H_2O_2 added to the soil water). The ratio of H_2O_2 added per mol Fe(II) in sample waters was higher in the subsamples used to quantify •OH production compared to the subsamples used to quantify changes in CO_2 (see Methods 3.5). Measurements were done in triplicate for oxidized, and control and initial subsamples of each soil water.

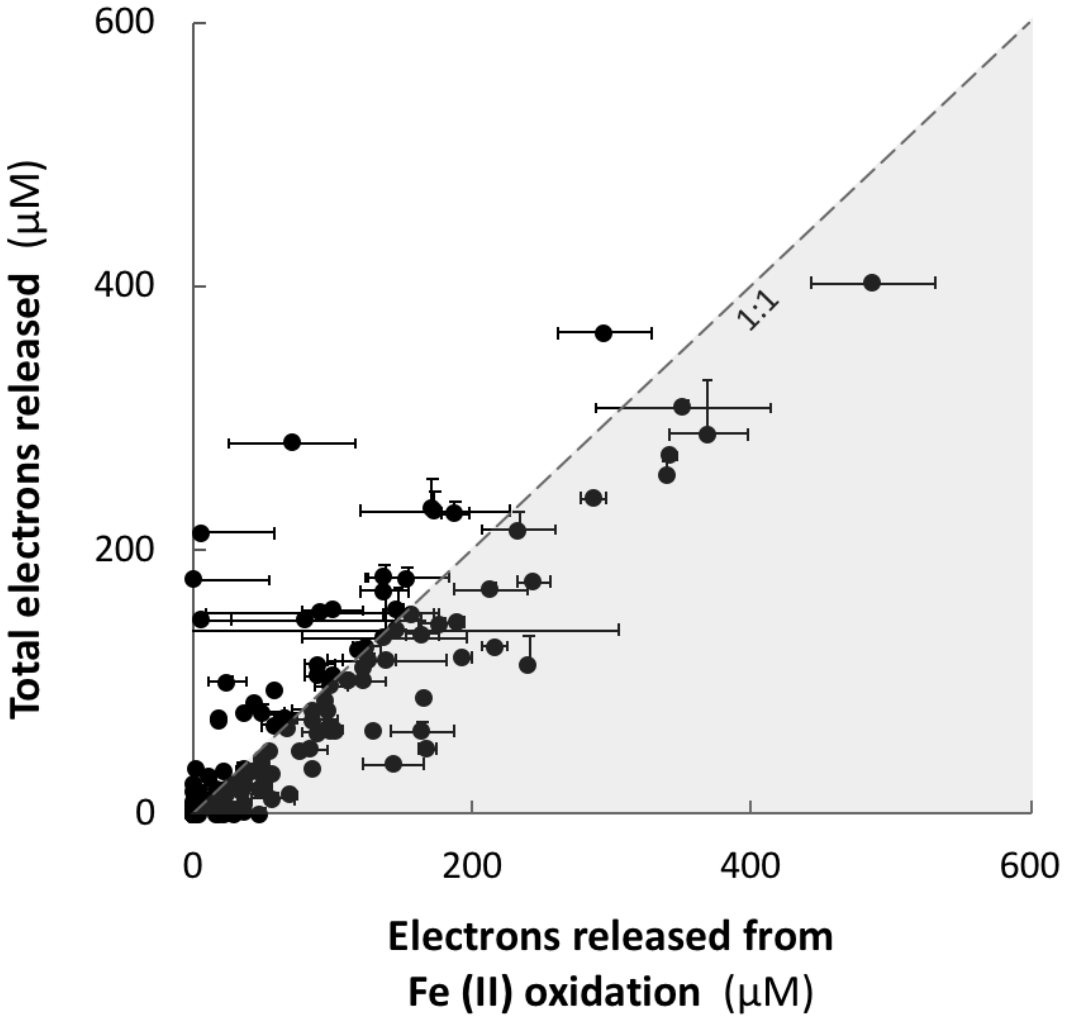

Figure 2.4. Electrons released from Fe(II) oxidation versus electrons released from oxidation of all reduced constituents. In 78% of soil and surface waters and soil leachates, electrons released from Fe(II) oxidation by O_2 (air) account for the total electrons released (change in electron donating capacity between oxidized and control waters). The majority of samples plotted on or below the 1:1 (shaded gray area), strongly suggesting that Fe(II) was the most important electron donor in all waters tested. The data were fit using least-squares regression, where total electrons released (μM) = [0.72 ± 0.02] × electrons released from Fe(II) oxidation (μL) + [17 ± 10], R^2 = 0.84; $p < 0.0001$.

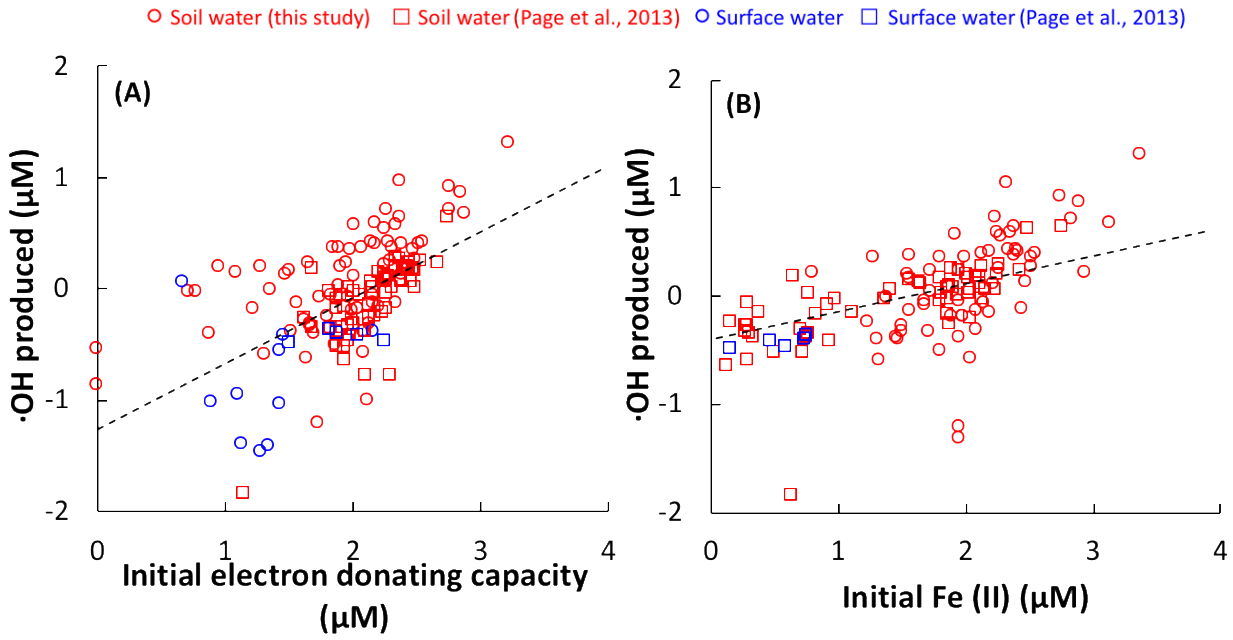

Figure 2.5. •OH production upon oxidation of soil waters by air is correlated with initial electron donating capacity **(A)** and initial Fe(II) concentration **(B)** of the soil and surface waters, and soil leachates. Values plotted are log values of measured concentrations. Soil waters shown in red and surface waters in blue. **(A)** •OH produced over 24 hour oxidation by O_2 versus the initial electrons donating capacity. All data were fit using least-squares regression, where •OH produced (µM) = [0.001 ± 0.0005] × initial electron donating capacity (µM) - [0.03 ± 0.1], R^2 = 0.70, $p < 0.0001$. **(B)** •OH produced over 24 hour oxidation by O_2 versus initial Fe(II) concentration in the water sample. All data were fit using least-squares regression, where •OH produced (µmol L^{-1}) = [0.007 ± 0.0004] × initial Fe(II) (µL) + [0.6 ± 0.1], R^2 = 0.66, $p < 0.0001$.

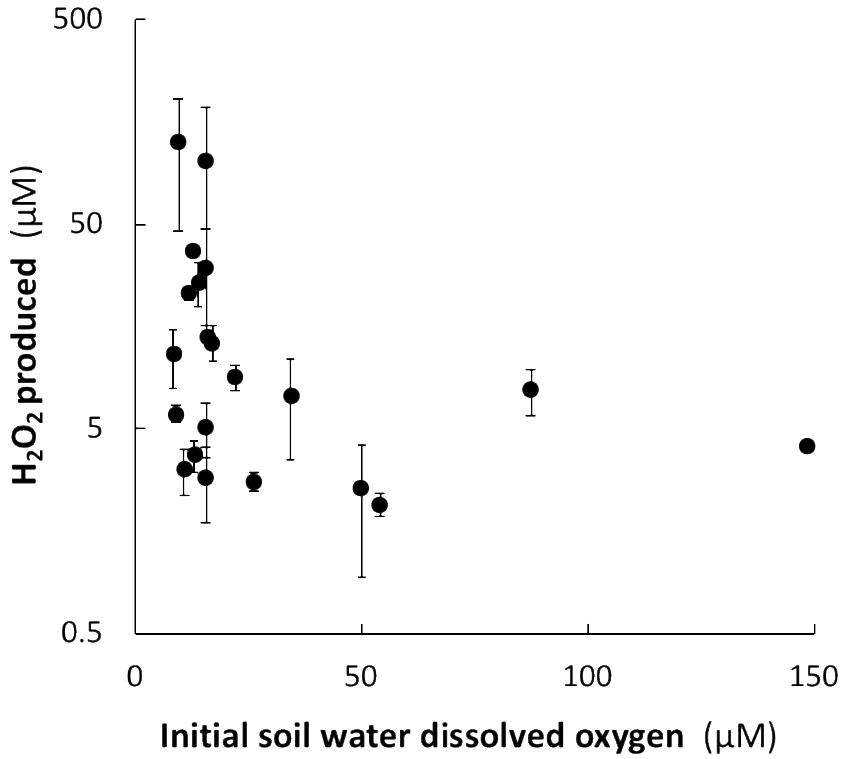

Figure 2.6. H_2O_2 production (μM) during a 1-hour oxidation by O_2 (air) versus initial dissolved oxygen concentrations in soil waters. H_2O_2 production is higher in soil waters with low dissolved oxygen than in oxic soil waters.

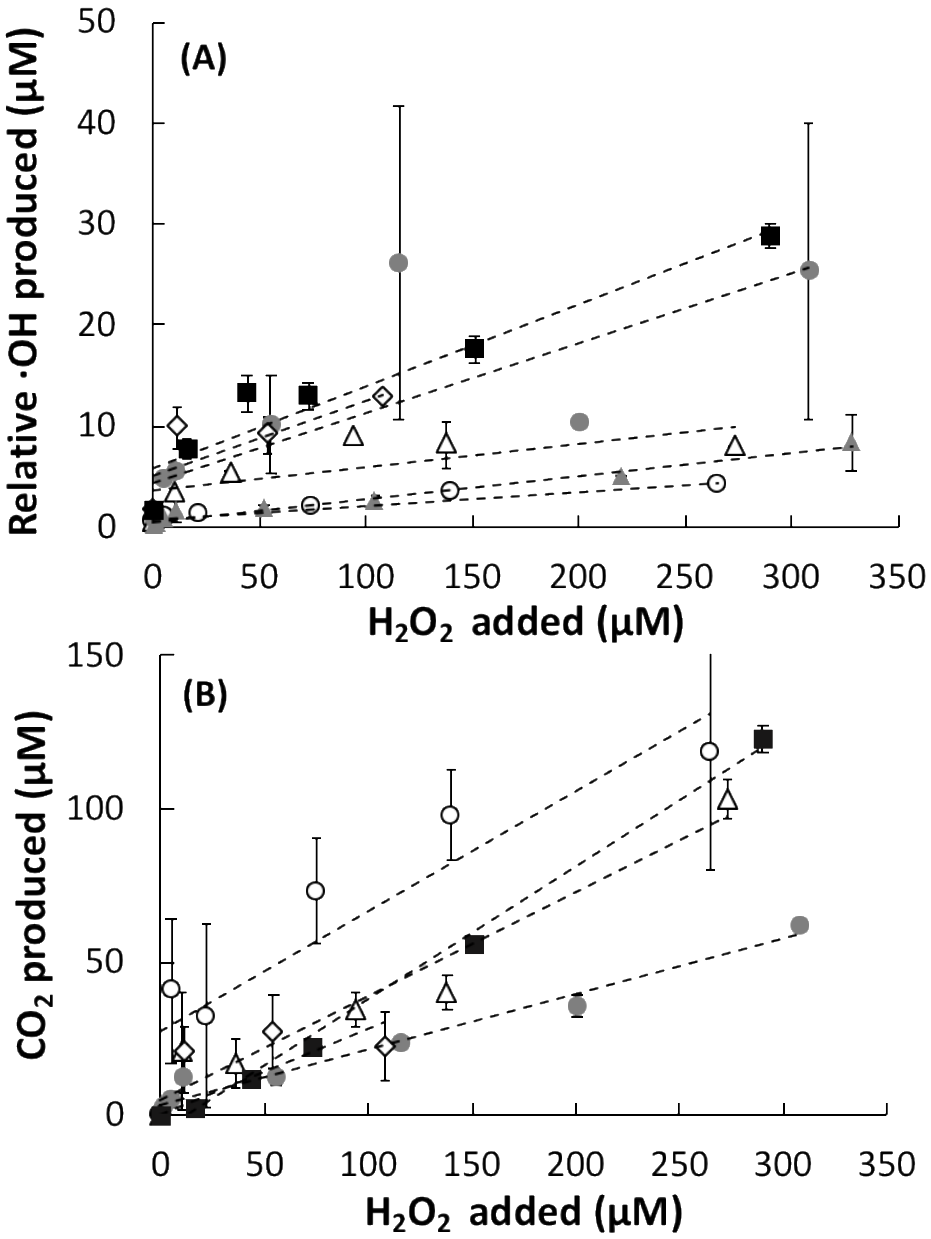

Figure 2.7. Relative •OH and CO_2 production by H_2O_2 oxidation in soil waters (white), soil leachates (grey), or Suwannee River fulvic acid (SRFA, black). Both •OH **(A)** and CO_2 **(B)** production were positively correlated with concentrations of H_2O_2 added. **(A)** The slope of the relationship between H_2O_2 added and relative •OH produced varied between the soil waters and leachates tested, ranging from 0.08 ± 0.01 ($p < 0.01$) to 0.01 ± 0.002 ($p < 0.01$). Circle = Imnavait wet sedge soil water, $p < 0.01$, 11 August 2016; diamond = Imnavait wet sedge, $p < 0.25$, 18 July 2016; triangle = Imnavait wet sedge, $p < 0.1$, 11 August 2016; circle = Imnavait wet sedge leachate, $p < 0.1$, core collected 15 June 2015; triangle = Toolik wet sedge leachate, $p < 0.00001$, core collected 23 May 2015; square = SRFA with ferrous ammonium sulfate, $p < 0.01$. **(B)** CO_2 production from soil waters (white), soil leachates (grey), or Suwannee River fulvic acid (SRFA) containing ferrous ammonium sulfate (black) oxidized by a range of H_2O_2

concentrations. Slopes of the linear relationship between added H_2O_2 and CO_2 produced differed by soil water, ranged from 0.39 ± 0.09 ($p < 0.1$) to 0.04 ± 0.002 ($p < 0.0001$). Circle = Imnavait wet sedge soil water, $p < 0.01$, 11 August 2016; diamond = Imnavait wet sedge, $p < 0.4$, 18 July 2016; triangle = Imnavait wet sedge, $p < 0.001$, 11 August 2016; circle = Imnavait wet sedge leachate, $p < 0.0001$, core collected 15 June 2015; square = SRFA with ferrous ammonium sulfate, $p < 0.0002$.

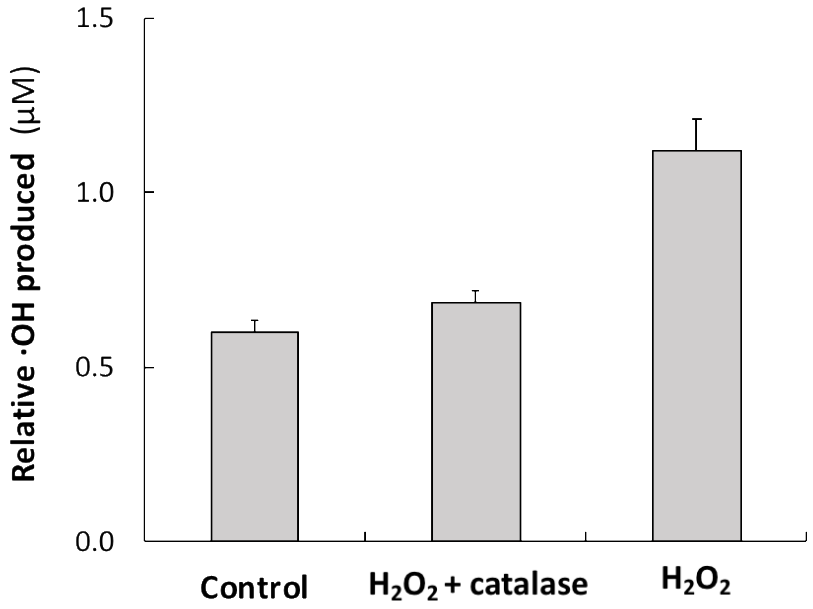

Figure 2.8. •OH production in control soil waters (no H_2O_2 added), compared to the same soil waters oxidized by H_2O_2 + catalase or by H_2O_2 (see Methods 3.4). Addition of H_2O_2 to soil waters produced significantly greater •OH than the control and the H_2O_2 + catalase sample ($p < 0.001$). There was no statistically significant difference in •OH produced between control and H_2O_2 + catalase soil water ($p = 0.96$).

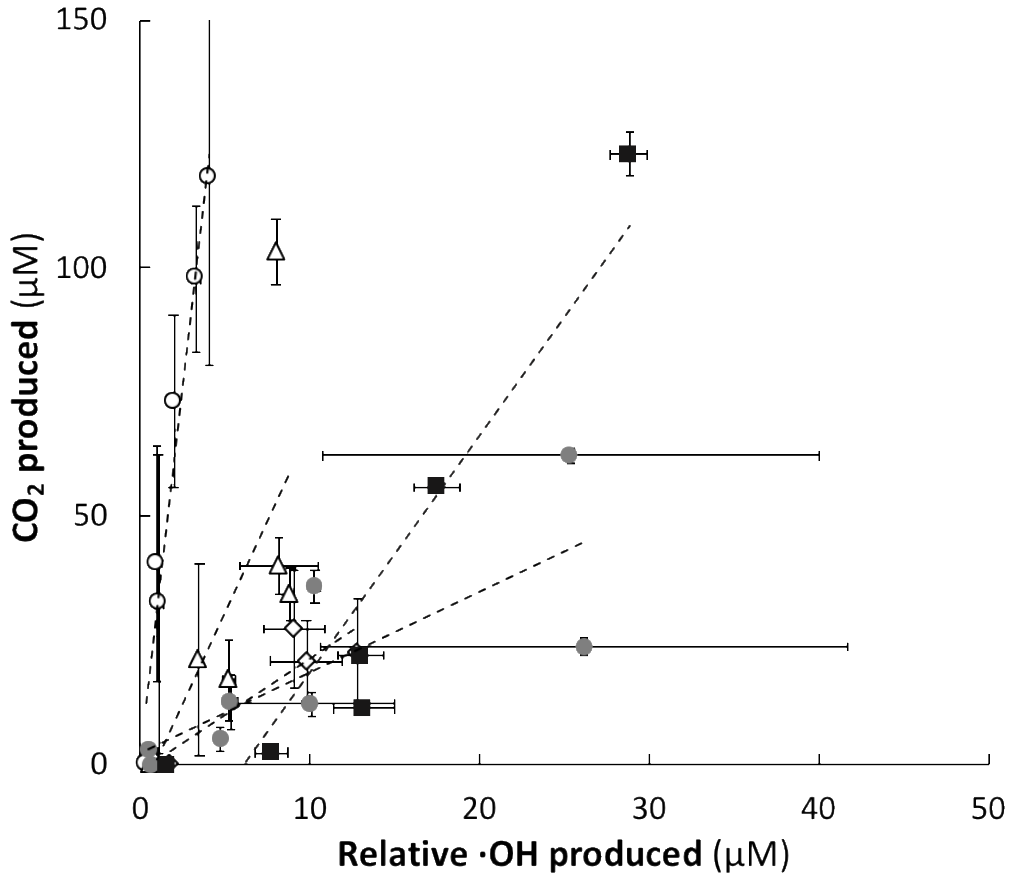

Figure 2.9. Effect of increasing H_2O_2 concentration on relative •OH production and CO_2 production for soil waters (white), soil leachates (grey), or Suwannee River fulvic acid (SRFA). Relative •OH and CO_2 were measured on the same soil waters oxidized with the same amount of H_2O_2, but the ratio of reduced constituents to H_2O_2 in soils waters differed due to method constraints (see Methods 2.6). Slopes of the linear relationship between CO_2 production and relative •OH production ranged from 29 ± 3.2 ($p < 0.001$) to 2.3 ± 0.86 ($p < 0.15$). Circle = Imnavait wet sedge soil water, $p < 0.001$, 11 August 2016; diamond = Imnavait wet sedge, $p < 0.15$, 18 July 2016; triangle = Imnavait wet sedge, $p < 0.15$, 11 August 2016; circle = Imnavait wet sedge leachate, $p < 0.00001$, core collected 15 June 2015; square = SRFA with ferrous ammonium sulfate, $p < 0.01$.

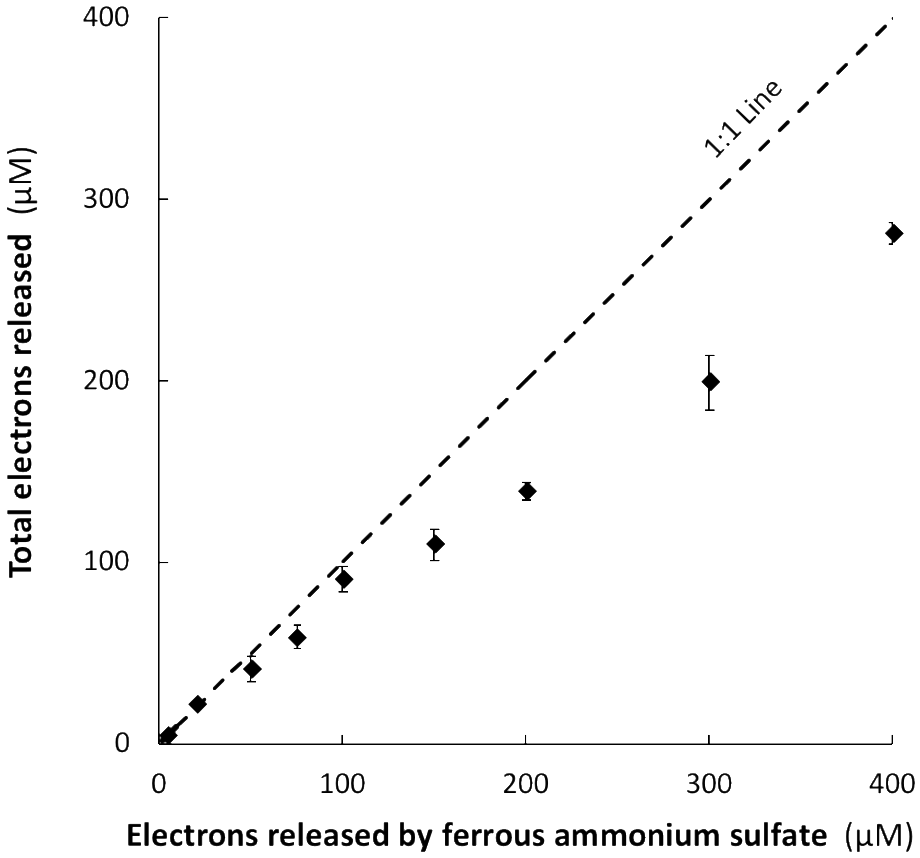

Figure 2.S1. Measurements of the total number of electrons released over a range of ferrous ammonium sulfate concentrations show that $ABTS^{+\bullet}$ did not detect all Fe(II) present, i.e., it underestimated the electrons released by Fe(II). For waters with Fe(II) above ~50 μM, ABTS+• did not detect all the potential electrons released upon oxidation, leading to lower electron concentrations than Fe(II) concentrations measured.

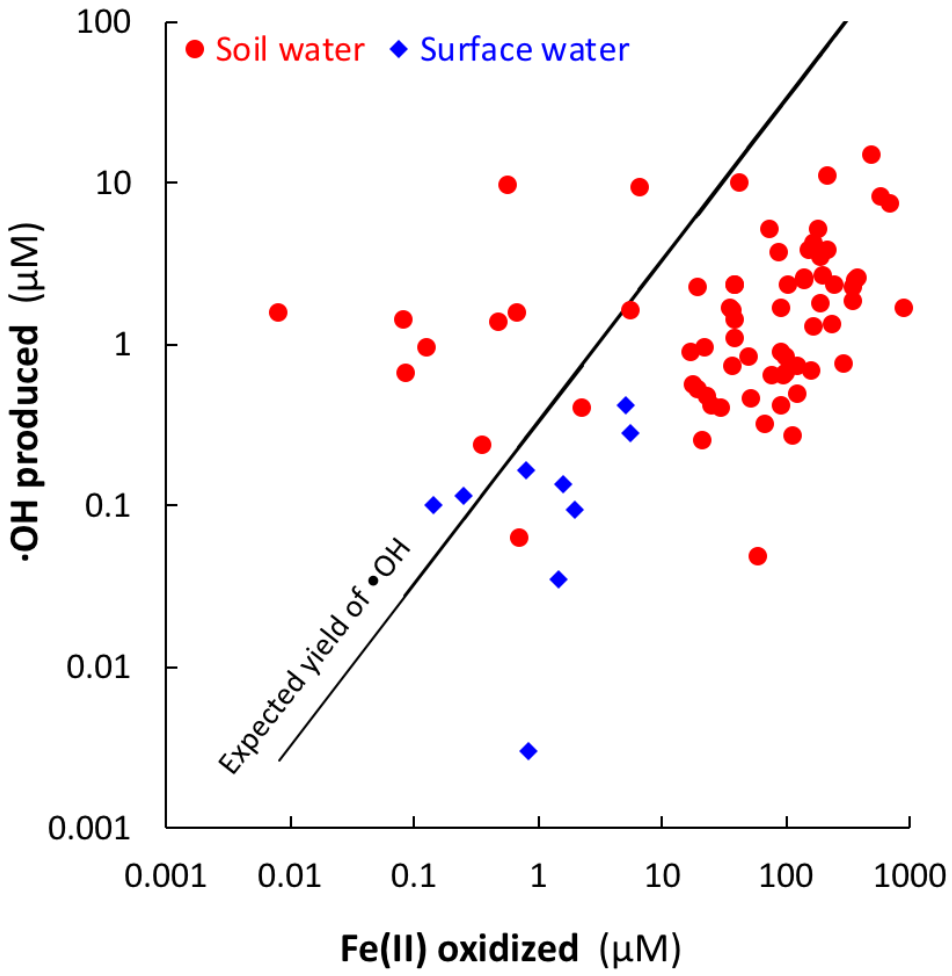

Figure 2.S2. There was no correlation in •OH production with Fe(II) oxidized during the 24 hour oxidation by O_2. Black line is the expected yield of 1 mol of •OH produced per 3 moles of Fe(II) oxidized.

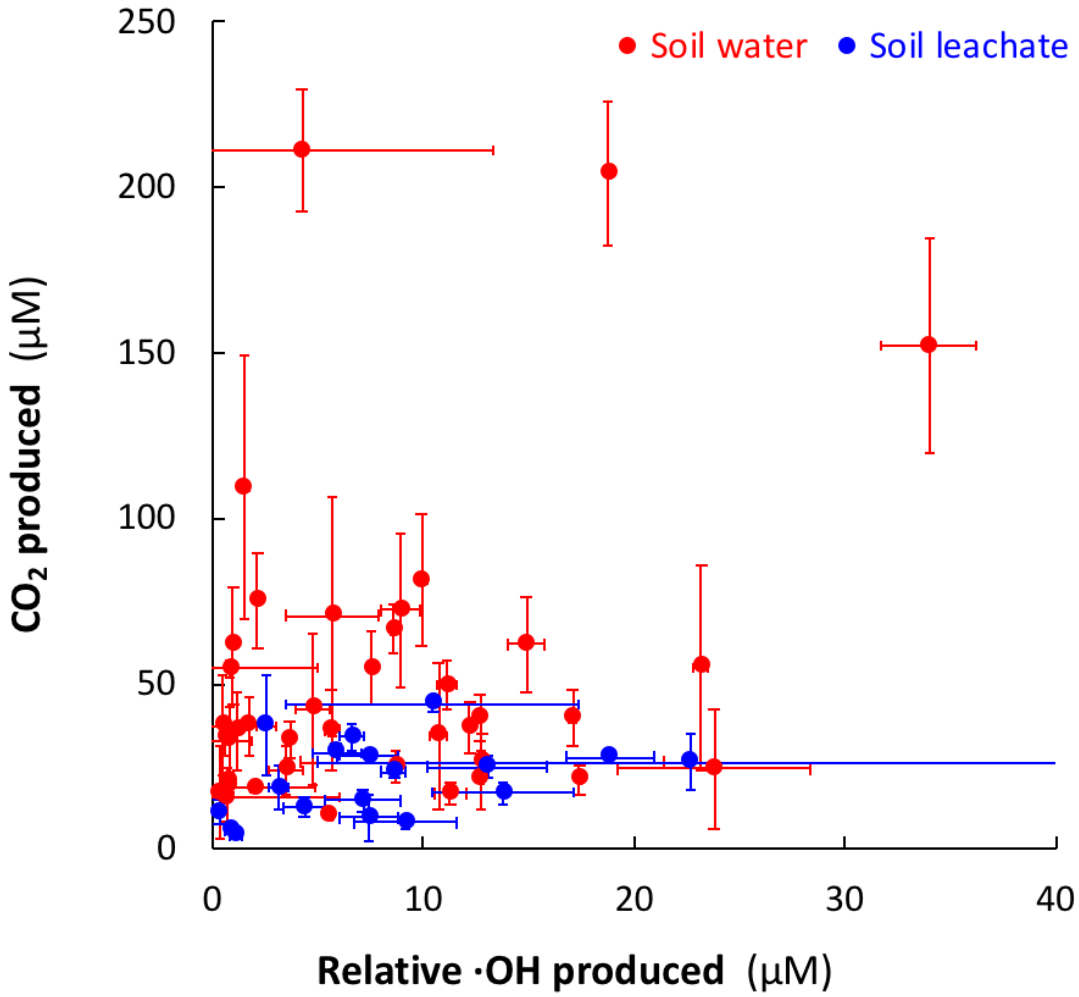

Figure 2.S3. CO_2 production versus relative •OH production in soil waters (red) and soil leachates (blue) upon introduction of H_2O_2. Both CO_2 and •OH production were measured after a 24 hour oxidation by H_2O_2 versus relative to controls (no H_2O_2 added). 65% of the soil waters and leachates (N = 93) produced detectable CO_2 and those are the waters plotted in the figure.

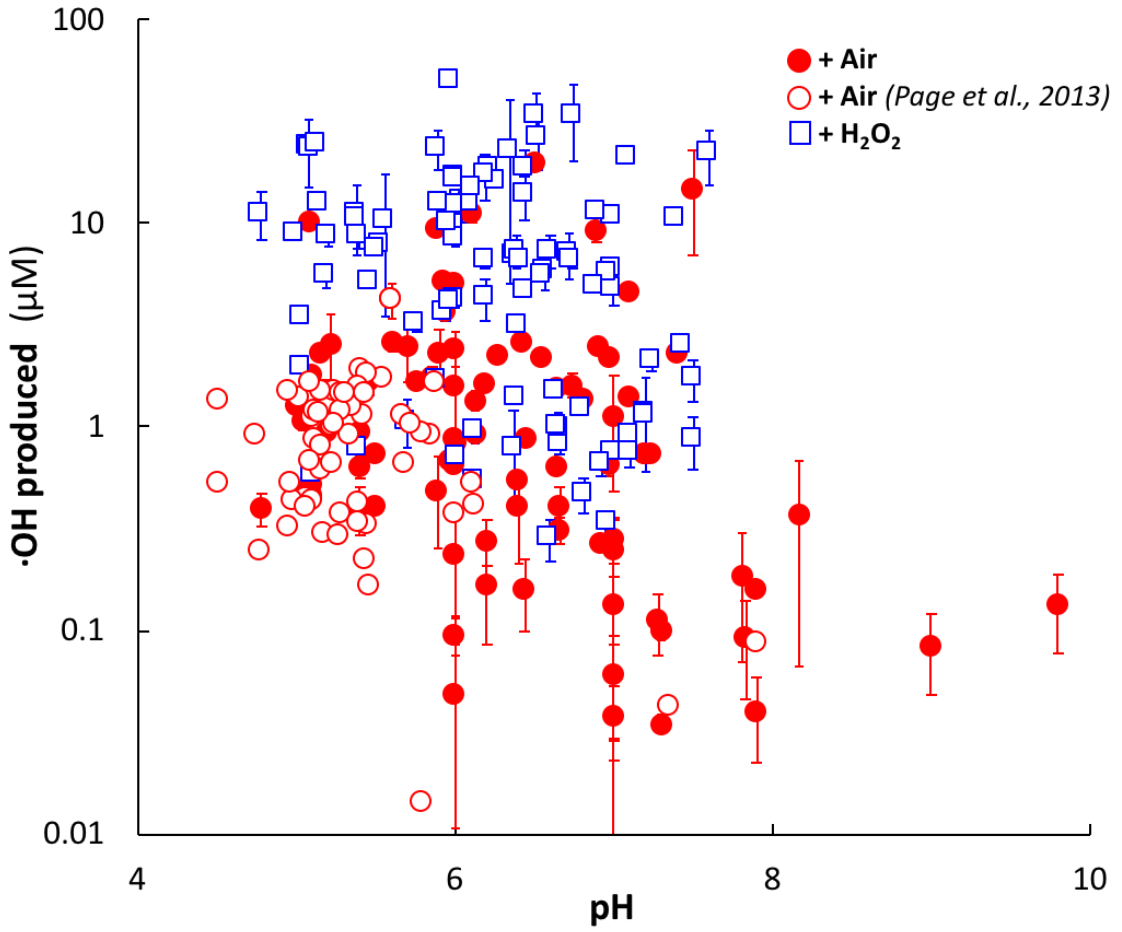

Figure 2.S4. •OH production from oxidation by O_2 as a function of initial pH of the water including surface and soil water, and soil leachates. •OH production at higher pH (pH > 8) is lower as expected because at high pH production of other reactive species (for example Fe(IV)) is expected. Plot includes data from 2012, 2015, and 2016 field seasons.

Variable	Surface water	Soil water	Soil leachate
pH	6.7 ± 1.6 (17) *6.0-9.8*	5.6 ± 0.7 (70) *4.8-7.6*	6.3 ± 1.4 (24) *5.6-7.6*
Specific conductivity ($\mu S\ cm^{-1}$)	77 ± 18 (17) *8-234*	408 ± 104 (70) *12-6040*	102 ± 24 (24) *1-522*
Dissolved oxygen (μM)	302 ± 15 (15) *125-344*	29 ± 5 (62) *7-219*	25 ± 6 (23) *7-100*
•OH (μM)	0.2 ± 0.1 (17) *ND-1.1*	1.7 ± 0.6 (80) *ND-19.9*	0.7 ± 0.2 (23) *0.3-59.4*
H_2O_2 (μM)		21 ± 11 (20) *1-137*	
Electron donating capacity (μM)	19 ± 8 (17) *ND-145*	183 ± 30 (77) *ND-1681*	179 ± 56 (25) *ND-1119*
Total Fe (μM)	1.1 ± 0.7 (17) *ND-10*	237 ± 65 (70) *ND-3292*	176 ± 75 (26) *ND-1496*
Fe(II) (μM)	ND (17)	230 ± 58 (77) *ND-3511*	142 ± 61 (26) *ND-1120*
DOC (μM)	389 ± 58 (17) *93-952*	1769 ± 262 (70) *66-12320*	2281 ± 325 (26) *141-6759*
[α] Estimated electrons released from DOC (μM)	8 ± 1 (16) *2-22*	29 ± 4 (77) *1-201*	55 ± 8 (26) *3-162*
Mn (μM)		60 ± 26 (56)	14 ± 10 (17)
[β] SO_4^{2-} (μM)	107.5 ± 43.4 (17)	2.0 ± 1.0 (17)	
Cl^- (μM)	10.1 ± 2.5 (17)	2.3 ± 0.7 (17)	
HCO_3^- (μM)	443 ± 112 (17)	74 ± 15 (17)	
DIC (μM)		3178 ± 298 (80) *168-10405*	945 ± 219 (26) *23-4910*

[α] Estimated following Page et al. (2013) assuming (1) quinones are the main redox moieties within DOC, and (2) the same fraction of quinone-C is present in all soil water DOC.

[β] Not representative of average sulfate concentrations around Toolik Lake previously reported (~4 μM, Kling et al., 2000). Sulfate averages reported in the surface waters here are higher due to the influence of three Sagavanirktok river water samples from headwater stations in the Brooks Range (Fig. 2) that had sulfate concentrations of 435, 478, and 553 μM.

Table 2.1. Chemistry of surface water, soil water, and soil leachate samples analyzed in this study. Shown are the mean ± standard error with the number of samples (N) in parentheses, and the minimum to maximum range of values below in italics. ND = not detected.

	Old Landscape [α]	Young Landscape [β]	Coastal Plain [γ]	Fluvial Landscape [δ]
pH	5.6 ± 1.3 (17) *5.0-6.0*	5.6 ± 1.3 (17) *5.0-7.0*	6.2 ± 2.1 (9) *5.9-7.1*	6.0 ± 1.1 (27) *4.8-7.6*
Specific conductivity ($\mu S\ cm^{-1}$)	35 ± 6 (17) *13-76*	138 ± 29 (17) *23-431*	362 ± 65 (9) *56-625*	829 ± 249 (27) *54-6040*
Dissolved oxygen (μM)	41 ± 11 (13) *8-148*	16 ± 1 (14) *13-34*	13 ± 2 (9) *8-26*	35 ± 10 (26) *7-219*
DOC (μM)	1332 ± 112 (17) *721-2345*	767 ± 96 (17) *424-2150*	2221 ± 378 (9) *725-3758*	2525 ± 629 (27) *66-12320*
Electron donating capacity (μM)	149 ± 35 (17) *6-694*	149 ± 23 (17) *21-333*	58 ± 13 (9) *12-112*	275 ± 75 (27) *ND-1681*
Total Fe (μM)	99 ± 25 (17) *2-329*	165 ± 27 (17) *26-391*	51 ± 15 (9) *4-109*	431 ± 160 (27) *ND-3510*
Fe(II) (μM)	155 ± 38 (24) *ND-794*	155 ± 26 (17) *21-356*	34 ± 13 (17) *ND-99*	408 ± 158 (27) *ND-3510*
$\bullet OH$ (μM)	3.1 ± 0.6 (24) *0.4-10.1*	1.2 ± 0.2 (17) *0.3-2.6*	1.2 ± 0.2 (17) *0.2-2.3*	3.2 ± 1.9 (27) *ND-19.9*

[α] Older surface (Sagavanirktok, ~250,000 yr BP).
[β] Younger glacial surface (Itkillik I, ~60,000 yr BP and Itkillik II, ~14,000 yr BP.
[γ] Soil waters collected on the Arctic Coastal Plain.
[δ] Soil waters collected on the Arctic Coastal plain adjacent to glacial-fed rivers receiving calcareous loess deposits (Walker and Everett, 1991).

Table 2.S1. Chemistry of soil waters by landscape age or type. Shown are the mean ± standard error with the number of samples (N) in parentheses, and the minimum to maximum range of values below in italics. ND = not detected. Soil waters sampled from the younger and older landscape ages as well as from next to the Sagavanirktok River were collected from upland tussock tundra and lowland wet sedge tundra. The vegetation above all soil waters collected on the coastal plain was wet sedge. Soil waters collected from the Saviukviak River were collected beneath birch-willow vegetation.

2.9 References

1. Faust, B. C., and Hoigné, J. (1990). Photolysis of Fe(III)-hydroxy complexes as sources of •OH in clouds, fog and rain. *Atmospheric Environment Part A, General Topics* 24, 79–89.

2. Mopper, K., and Zhou, X. (1990). Hydroxyl radical photoproduction in the sea and its potential impact on marine processes. *Science* 250, 661–4.

3. Vaughan, P. P., and Blough, N. V. (1998). Photochemical formation of hydroxyl radical by constituents of natural waters. *Environ. Sci. Technol.* 32, 2947–2953.

4. Page, S. E., Logan, J. R., Cory, R. M., and McNeill, K. (2014). Evidence for dissolved organic matter as the primary source and sink of photochemically produced hydroxyl radical in arctic surface waters. *Environ. Sci. Processes & Impacts* 16, 807–822.

5. Goldstone, J. V., Pullin, M. J., Bertilsson, S., and Voelker, B. M. (2002). Reactions of hydroxyl radical with humic substances: Bleaching, mineralization, and production of bioavailable carbon substrates. *Environ.Sci. Technol* 36, 364–372.

6. Southworth, B. A., and Voelker, B. M. (2003). Hydroxyl Radical Production via the Photo-Fenton Reaction in the Presence of Fulvic Acid. *Environ. Sci. Technol*. 37(6), 1130–1136.

7. Vermilyea, A. W., and Voelker, B. M. (2009). Photo-fenton reaction at near neutral pH. *Environ. Sci. Technol.* 43, 6927–6933.

8. Burns, J. M., Craig, P. S., Shaw, T. J., and Ferry, J. L. (2010). Multivariate examination of Fe(II) / Fe(III) cycling and consequent hydroxyl radical generation. *Environ. Sci. Technol.* 44, 7226–7231.

9. Page, S. E., Sander, M., Arnold, W. A., and McNeill, K. (2012). Hydroxyl radical formation upon oxidation of reduced humic acids by oxygen in the dark. *Environ. Sci. Technol.* 46, 1590–1597.

10. Page, S. E., Kling, G. W., Sander, M., Harrold, K. H., Logan, J. R., McNeill, K., and Cory, R. M. (2013). Dark formation of hydroxyl radical in arctic soil and surface waters. *Environ. Sci. Technol.* 47, 12860–12867.

11. Minella, M., De Laurentiis, E., Maurino, V., Minero, C., and Vione, D. (2015). Dark production of hydroxyl radicals by aeration of anoxic lake water. *Science of the Total Environment* 527–528, 322–327.

12. Tong, M., Yuan, S., Ma, S., Jin, M., Liu, D., Cheng, D., and Wang, Y. (2016). Production of Abundant Hydroxyl Radicals from Oxygenation of Subsurface Sediments. *Environ. Sci. Technol.* 50, 214–221.

13. Haber, F., and Weiss, J. (1932). Uber die Katalyse des Hydroperoxydes. *Die Naturwissenschaften* 20, 948–950.

14. Stumm, W., and Lee, F. G. (1961). Oxygenation of ferrous iron. *Industrial and engineering chemistry* 53, 143–146.

15. Klapper, L., McKnight, D. M., Fulton, J. R., Blunt-Harris, E. L., Nevin, K. P., Lovley, D. R., and Hatcher, P. G. (2002). Fulvic acid oxidation state detection using fluorescence spectroscopy. *Environ. Sci. Technol*. 36, 3170–3175

16. Lipson, D. a., Jha, M., Raab, T. K., and Oechel, W. C. (2010). Reduction of iron (III) and humic substances plays a major role in anaerobic respiration in an Arctic peat soil. *J. Geophys. Res. Biogeosciences* 115, 1–13.

17. Aeschbacher, M., Graf, C., Scwarzenbach, R. P., and Sander, M. (2012). Antioxidant properties of humic substances. *Environ. Sci. Technol.* 46, 4916–4925.

18. Wallace, G., Sander, M., Chin, Y.P., and Arnold, W. (2017). Quantifying the electron donating capacities of sulfide and dissolved organic matter in sediment pore waters of wetlands. *Environ. Sci.: Processes Impacts* 19, 1–10.

19. Voelker, B. M., and Sulzberger, B. (1996). Effects of fulvic acid on Fe(II) oxidation by hydrogen peroxide. *Environ. Sci. Technol.* 30, 1106–1114.

20. Buxton, G. V., Greenstock, C. L., Helman, W. P., and Ross, A. B. (1988). Critical review of rate constants for reactions of hydrated electrons, hydrogen atoms and hydroxyl radical in Aqueous Solution. *Journal of Physical and Chemical Reference Data* 17, 513–886.

21. Sulzberger, B., and Durisch-Kaiser, E. (2009). Chemical characterization of dissolved organic matter (DOM): A prerequisite for understanding UV-induced changes of DOM absorption properties and bioavailability. *Aquatic Sciences* 71, 104–126.

22. Westerhoff, P., Aiken, G., Amy, G., and Debroux, J. (1999). Relationships between the structure of natural organic matter and its reactivity towards molecular ozone and hydroxyl radicals. *Water Research* 33, 2265–2276.

23. Waggoner, D. C., Chen, H., Willoughby, A. S., and Hatcher, P. G. (2015). Formation of black carbon-like and alicyclic aliphatic compounds by hydroxyl radical initiated degradation of lignin. *Organic Geochemistry* 82, 69–76.

24. Hall, S. J., and Silver, W. L. (2013). Iron oxidation stimulates organic matter decomposition in humid tropical forest soils. *Global Change Biology*, *19*(9), 2804–2813.

25. Hobbie, J. E. and G. W. Kling, editors. (2014). A Changing Arctic: Ecological Consequences for Tundra, Streams, and Lakes. *Oxford University Press*, 331

26. Keller, K., Blum, J. D., and Kling, G. W. (2007). Geochemistry of Soils and Streams on Surfaces of Varying Ages in Arctic Alaska. *Arctic, Antarctic, and Alpine Research* 39(1), 84–98.

27. Hamilton, T. D. (2003). Glacial Geology of the Toolik Lake and Upper Kuparuk River Regions. *Biological Papers of the University of Alaska* 1–24.

28. Walker, D. A., and Everett, K. R. (1991). Loess Ecosystems of Northern Alaska: Regional Gradient and Toposequence at Prudhoe Bay. *Ecological Monographs* 61, 437–464.

29. Muller, S. V., Racoviteanu, A. E., and Walker, D. A. (1999). Landsat MSS-derived land-cover map of northern Alaska: Extrapolation methods and a comparison with photo-interpreted and AVHRR-derived maps. *International Journal of Remote Sensing* 20, 2921–2946.

30. Kling, G. W., Kipphut, G. W., Miller, M. M., and O'Brien, W. J. (2000). Integration of lakes and streams in a landscape perspective: The importance of material processing on spatial patterns and temporal coherence. *Freshwater Biology* 43, 477–497.

31. Stookey, L. L. (1970). Ferrozine a new spectrophotometric reagent for iron. *Analytical Chemistry* 42, 779–781.

32. Page, S. E., Arnold, W. A., and McNeill, K. (2010). Terephthalate as a probe for photochemically generated hydroxyl radical. *Journal of Environmental Monitoring* 12, 1658–1665.

33. Burns, J. M., Cooper, W. J., Ferry, J. L., King, D. W., DiMento, B. P., McNeill, K., and Waite, T. D. (2012). Methods for reactive oxygen species (ROS) detection in aqueous environments. *Aquatic Sciences* 74, 683–734.

34. Cory, R. M., Davis, T. W., Dick, G. J., Johengen, T., Denef, V. J., Berry, M., and Kling, G. W. (2016). Seasonal dynamics in dissolved organic matter, hydrogen peroxide, and cyanobacterial blooms in Lake Erie. *Frontiers in Marine Science*, 3, 54.

35. Lipson, D. A., Zona, D., Raab, T. K., Bozzolo, F., Mauritz, M., and Oechel, W. C. (2012). Water-table height and microtopography control biogeochemical cycling in an Arctic coastal tundra ecosystem. *Biogeosciences* 9, 577–591.

36. Lipson, D. A., Raab, T. K., Goria, D., and Zlamal, J. (2013). The contribution of Fe (III) and humic acid reduction to ecosystem respiration in drained thaw lake basins of the Arctic Coastal Plain. *Global Biogeochemical Cycles* 27, 399–409.

37. Pokrovsky, O. S., Shirokova, L. S., Kirpotin, S. N., Kulizhsky, S. P., and Vorobiev, S. N. (2013). Impact of western Siberia heat wave 2012 on greenhouse gases and trace metal concentration in thaw lakes of discontinuous permafrost zone. *Biogeosciences* 10, 5349–5365.

38. Herndon, E. M., Yang, Z., Bargar, J., Janot, N., Regier, T. Z., Graham, D. E., and Liang, L. (2015). Geochemical drivers of organic matter decomposition in arctic tundra soils. *Biogeochemistry* 126, 397–414.

39. Reyes, F. R., and Lougheed, V. L. (2015). Rapid Nutrient Release from Permafrost Thaw in Arctic Aquatic Ecosystems. *Arctic, Antarctic, and Alpine Research* 47, 35–48.

40. Remucal, C. K., and Sedlak, D. L. (2011). The Role of Iron Coordination in the Production of Reactive Oxidants from Ferrous Iron Oxidation by Oxygen and Hydrogen Peroxide. *Aquatic Redox Chemistry*, 178–197.

41. Van der Grift, B., Behrends, T., Oste, L. A., Schot, P. P., Wassen, M. J., and Griffioen, J. (2016). Fe hydroxyphosphate precipitation and Fe(II) oxidation kinetics upon aeration of Fe(II) and phosphate-containing synthetic and natural solutions. *Geochim. Cosmochim. Acta* 186, 71–90.

42. Baldrian, P., and Valášková, V. (2008). Degradation of cellulose by basidiomycetous fungi. *FEMS Microbiology Reviews* 32, 501–521.

43. Vermilyea, A. W., Dixon, T. C., and Voelker, B. M. (2010). Use of H2 18O2 to measure absolute rates of dark H2O2 production in freshwater systems. *Environ. Sci. Technol.* 44, 3066–3072.

44. Zhang, T., Hansel, C. M., Voelker, B. M., and Lamborg, C. H. (2016). Extensive Dark Biological Production of Reactive Oxygen Species in Brackish and Freshwater Ponds. *Environ. Sci. Technol.* 50, 2983–2993.

45. Murphy, S. A., Solomon, B. M., Meng, S., Copeland, J. M., Shaw, T. J., and Ferry, J. L. (2014). Geochemical production of reactive oxygen species from biogeochemically reduced Fe. *Environ. Sci. Technol.* 48, 3815–3821.

46. Klüpfel, L., Piepenbrock, A., Kappler, A., and Sander, M. (2014). Humic substances as fully regenerable electron acceptors in recurrently anoxic environments. *Nature Geoscience* 7, 195–200.

47. Petigara, B. R., Blough, N. V., and Mignerey, A. C. (2002). Mechanisms of Hydrogen Peroxide Decomposition in Soils. *Environ. Sci. Technol.* 36, 639–645.

48. Chang, C. Y., Hsieh, Y. H., Cheng, K. Y., Hsieh, L. L., Cheng, T. C., and Yao, K. S. (2008). Effect of pH on Fenton process using estimation of hydroxyl radical with salicylic acid as trapping reagent. *Water Science and Technology* 58, 873–879.

49. Fujii, M., Rose, A. L., Waite, T. D., and Omura, T. (2010). Oxygen and superoxide-mediated redox kinetics of iron complexed by humic substances in coastal seawater. *Environ. Sci. Technol.* 44, 9337–9342.

50. Miller, C. J., Rose, A. L., & Waite, T. D. (2009). Impact of natural organic matter on H2O2-mediated oxidation of Fe(II) in a simulated freshwater system. *Geochim. Cosmochim. Acta* 73, 2758–2768.

51. Pham, A. N., and Waite, T. D. (2008). Modeling the kinetics of Fe(II) oxidation in the presence of citrate and salicylate in aqueous solutions at pH 6.0-8.0 and 25C. *Journal of Physical Chemistry* 112, 5395–5405.

52. Jones, A. M., Griffin, P. J., and Waite, T. D. (2015). Ferrous iron oxidation by molecular oxygen under acidic conditions: The effect of citrate, EDTA and fulvic acid. *Geochimica et Cosmochimica Acta* 160, 117–131.

53. Sundman, A., Karlsson, T., Laudon, H., and Persson, P. (2013). XAS study of iron speciation in soils and waters from a boreal catchment. *Chemical Geology* 364, 93–102.

54. Drake, T.W., Wickland, K.P., Spences, R.G.M, McKnight, D.M., and Striegl, R.M. (2015). Ancient low molecular weight organic acids in permafrost fueld rapid carbon dioxide production upon thaw. *Proceedings of the National Academy of Sciences* 112(45), 13946-13951

55. Ward, C. P., and Cory, R. M. (2015). Chemical composition of dissolved organic matter draining permafrost soils. *Geochim. Cosmochim. Acta* 167, 63–79.

56. Herndon, E., AlBashaireh, A., Singer, D., Roy Chowdhury, T., Gu, B., and Graham, D. (2017). Influence of iron redox cycling on organo-mineral associations in Arctic tundra soil. *Geochimica et Cosmochimica Acta* 207, 210–231.

57. Daugherty, E. E., Gilbert, B., Nico, P. S., and Borch, T. (2017). Complexation and Redox Buffering of Iron(II) by Dissolved Organic Matter. *Environmental Science & Technology* 51(19), 11096–11104.

58. Qian, J., Mopper, K., and Kieber, D. J. (2001). Photochemical production of the hydroxyl radical in Antarctic waters. *Deep-Sea Research Part I: Oceanographic Research Papers* 48, 741–759.

59. Zepp, R. G., Faust, B. C., and Holgne, J. (1992). Hydroxyl Radical Formation in Aqueous Reactions (pH 3-8) of Iron (II) with Hydrogen Peroxide: The Photo-Fenton Reaction. *Environ. Sci. Technol*. 26, 313–319.

60. Brezonik, P. L., and Fulkerson-Brekken, J. (1998). Nitrate-induced photolysis in natural waters: Controls on concentrations of hydroxyl radical photo-intermediates by natural scavenging agents. *Environ. Sci. Technol.* 32, 3004–3010.

61. Ciotti, C., Baciocchi, R., and Tuhkanen, T. (2009). Influence of the operating conditions on highly oxidative radicals generation in Fenton's systems. *Journal of Hazardous Materials* 161, 402–408.

62. Charbouillot, T., Brigante, M., Mailhot, G., Maddigapu, P. R., Minero, C., and Vione, D. (2011). Performance and selectivity of the terephthalic acid probe for hydroxyl radical as a function of temperature, pH and composition of atmospherically relevant aqueous media. *Journal of Photochemistry and Photobiology A: Chemistry* 222, 70–76.

63. Fang, X., Mark, G., and von Sonntag, C. (1996). Hydroxyl radical formation by ultrasound in aqueous solutions Part I: the chemistry underlying the terephthalate dosimeter. *Ultrasonics Sonochemistry* 3, 57–63.

64. Vonk, J. E., Tank, S. E., Bowden, W. B., Laurion, I., Vincent, W. F., Alekseychik, P., and Wickland, K. P. (2015). Reviews and syntheses: Effects of permafrost thaw on Arctic aquatic ecosystems. *Biogeosciences* 12, 7129–7167.

65. Barker, A. J., Douglas, T. A., Jacobson, A. D., McClelland, J. W., Ilgen, A. G., Khosh, M. S., and Trainor, T. P. (2014). Late season mobilization of trace metals in two small Alaskan arctic watersheds as a proxy for landscape scale permafrost active layer dynamics. *Chemical Geology* 381, 180–193.

66. Ping, C. L., Michaelson, G. J., Jorgenson, M. T., Kimble, J. M., Epstein, H., Romanovsky, V. E., and Walker, D.A. (2008). High stocks of soil organic carbon in the North American Arctic region. *Nature Geoscience* 1, 615–619.

67. MacDougall, A. H., Avis, C. a., and Weaver, A. J. (2012). Significant contribution to climate warming from the permafrost carbon feedback. *Nature Geoscience* 5, 719–721.

Chapter 3
The Controls of Iron and Oxygen on Hydroxyl Radical (•OH) Production in Soils[1]

3.1 Abstract

Hydroxyl radical (•OH) is produced in soils from oxidation of reduced iron (Fe(II)) by dissolved oxygen (O_2) and can oxidize dissolved organic carbon (DOC) to carbon dioxide (CO_2). Understanding the role of •OH on CO_2 production in soils requires knowing whether Fe(II) production or O_2 supply to soils limits •OH production. To test the relative importance of Fe(II) production versus O_2 supply, we measured changes in Fe(II) and O_2 and in situ •OH production during simulated precipitation events and during common, waterlogged conditions in mesocosms from two landscape ages and the two dominant vegetation types of the Arctic. The balance of Fe(II) production and consumption controlled •OH production during precipitation events that supplied O_2 to the soils. During static, waterlogged conditions, •OH production was controlled by O_2 supply because Fe(II) production was higher than its consumption (oxidation) by O_2. An average precipitation event (4 mm) resulted in 200 μmol •OH m^{-2} per day produced compared to 60 μmol •OH m^{-2} per day produced during waterlogged conditions. These findings suggest that the oxidation of DOC to CO_2 by •OH in arctic soils, a process potentially as important as microbial respiration of DOC in arctic surface waters, will depend on the patterns and amounts of rainfall that oxygenate the soil.

[1] Trusiak A., Treibergs L.A., Kling G.W., and Cory R.M, *Soil Syst.*, 2019

3.2 Introduction

Oxidation of dissolved ferrous iron (Fe(II)) by oxygen (O_2) produces hydroxyl radical (•OH) in soil waters [1–3]. •OH is an unselective oxidant capable of oxidizing dissolved organic carbon (DOC) to carbon dioxide (CO_2) [3,4]. Preliminary estimates indicated that on a landscape scale the oxidation of DOC to CO_2 by •OH in Alaskan Arctic soil waters is on the same order of magnitude as microbial respiration of DOC in the surface waters draining the same soils [2]. Thus, this iron-mediated abiotic oxidation of DOC may be an important component of local and regional carbon budgets in the Arctic [2,3] or at any terrestrial-aquatic interface with waterlogged soils and strong redox gradients [5–7]. However, the preliminary estimates of •OH's impact on DOC oxidation in arctic soil waters were based on two untested assumptions [2]. First, it was assumed that Fe(II) in the often waterlogged, low O_2 soil waters is continuously exposed to enough O_2 to support the estimated daily rates of Fe(II) oxidation and •OH production. Second, it was assumed that Fe(II) production in soil waters is fast with respect to its oxidation.

It is the balance of O_2 supply and Fe(II) availability that will control •OH production (Figure 1). For example, if O_2 supply is slower than Fe(II) production, then O_2 supply will limit •OH production. Conversely, if O_2 supply is faster than Fe(II) production, then Fe(II) production will limit •OH production. O_2 in soil waters is consumed by redox reactions and microbial respiration and can be supplied to soils by introduction of oxygenated rain water during precipitation events, by diffusion from the atmosphere, by lowering of the water table height and by plant aerenchyma (Figure 3.1) [8–14]. Fe(II) in soil waters is consumed by redox reactions and produced by the microbial reduction of Fe(III) [14] and mineral dissolution and desorption of Fe(II) [15–17]. In general, the waterlogged, low O_2 soils commonly found in arctic lowlands

contain high Fe(II) concentrations [2,3,18,19], suggesting more production than consumption of Fe(II).

The processes that produce Fe(II) in soil waters (e.g., predominately microbial reduction) have been shown to depend on DOC concentration and composition [14,15,17,23]. For example, quinone moieties within the aromatic fraction of DOC are thought to aid microbial reduction of Fe(III) to Fe(II) (Figure 1) [14,20-22]. The strong correlations between Fe(II) and DOC concentrations across arctic and boreal regions [2,3,24,25] support the role of aromatic DOC in reducing Fe(III) to produce Fe(II). Thus, the aromatic content of the DOC may be an important control on Fe(II) production.

In addition to the aromatic content of the DOC, the processes that produce Fe(II) may vary between soils of different landscape ages and vegetation types [3,26,27]. In the foothills of the Alaskan Arctic (and near our study sites), glaciations have produced young and old land surfaces (~14,000 to >250,000 years BP) [28] that have otherwise been exposed to the same climate conditions [29]. These differences in the soil age lead to varying thickness of organic soil layers, water saturation and contact with mineral soils between older and younger landscapes. On each landscape age there are two dominant vegetation types that vary by landscape position. Tussock tundra is found in the uplands and wet sedge tundra is typical of lowland areas [26,30]. Tussock tundra is characterized by a relatively lower water table resulting in wet but not consistently saturated soils with better drainage, resulting in more oxidizing conditions [26,30,31]. Tussock tundra soils are also characterized by the presence of a deeper mineral layer in the summer-time, unfrozen active layer of the soil. The lowland wet sedge areas are characterized by more waterlogged soils (higher water table), poorer drainage, more reducing conditions and higher organic matter content in the soils because mineral layer is not shallow enough to be thawed during

summer [26,30,31]. These differences in landscape age, position and vegetation type lead to differences in redox conditions and soil chemistry that are expected to affect the Fe(II) production rate but this has yet to be studied.

In this study we tested whether the O_2 supply rate or the Fe(II) production rate was most important for the •OH production in soils under different conditions. To integrate the effects of O_2 supply and Fe(II) production on the in situ •OH production, we used intact soil mesocosms representative of natural conditions and processes in the plant-soil system through time because they integrate a relatively large surface area and typical depths of thawed soil. This approach contrasts with the prior studies on the •OH production [2,3] that aerated soil water withdrawn at one time and one location. Soil mesocosm experiments were used to determine how vegetation type and landscape age, coupled with varying O_2 supply rate during precipitation events or during static waterlogged conditions, affected the •OH production and subsequent oxidation of DOC to CO_2 by •OH. Our hypothesis is that the in situ •OH production in arctic soil waters is limited by Fe(II) production when O_2 supply is high during precipitation events and by O_2 supply when O_2 supply is low during static, waterlogged conditions in the soils.

3.3 Materials and Methods

3.3.1 Tundra soil cores collection

A total of 24 intact soil-plant cores (cores 28 cm diameter; length 30 ± 1 cm; Table 3.1, Figure 3.S1) were collected near Toolik Lake, Alaska (68°38′00″ N, 149°36′15″) in July 2017. The soil cores were collected from two dominant landscape ages in this region (~14,000 to 100,000 years BP for Toolik, the younger landscape; and ~250,000 years BP for Imnavait, the older landscape). On each of the two landscape ages, soil cores were collected from the two dominant vegetation types (wet sedge and tussock tundra, representing ~75% of the low Arctic landscape)

[32]. Wet sedge tundra is found in valleys or lowland areas near stream or lake margins where the water table is high. Wet sedge tundra is dominated by *Carex chordorrhize*, *C. rotundata*, *Eriphorum aquatilis* and *E. angustifolium* [31]. Upland from wet sedge is tussock tundra vegetation, where the water table fluctuates with precipitation but soils are often saturated due to the water holding capacity of the surface organic mat. Tussock tundra vegetation is dominated by sedges (*Eriophorum vaginatum*), dwarf shrubs (*Betuna nana*, *Vaccinium vitus idaea*, *Ledum palustre*) and mosses (*Sphagnum* spp., *Hylocomium* spp., *Aulacomium* spp.) [31].

3.3.2 Mesocosm design

The soil cores were used for two mesocosm experiments (Figure 3.S1). The first experiment consisted of two acclimation periods (to mimic static, waterlogged conditions) and two flushing periods (to mimic precipitation events). The first acclimation period (static) preceded the first flushing period, followed by a second acclimation period and subsequent flushing on the same cores. The second experiment used a different set of cores and consisted of only one acclimation and one flushing period. For each of the two experiments, three replicate soil cores were collected for each of the two landscape ages and each of the two vegetation types (Figure 3.S1). The soil cores were flushed with ~10 L of oxic deionized water (DI) immediately after core collection to establish similar conditions in each mesocosm at the start of the experiment. After the initial flush, each soil core was transferred to a 20 L plastic bucket to establish a mesocosm. Soil mesocosms were housed in large plastic coolers (46 cm × 46 cm × 84 cm). Each cooler contained three mesocosms surrounded by an ice-filled water bath to keep the temperature relatively constant and within the temperature range of soils in the summer at the field site. The water bath covered about 80% of the soil mesocosm depth and helped simulate natural conditions at and near the permafrost boundary where the soil temperatures range from 0 to 10 °C [32]. Soil temperatures were

measured at two depths in the mesocosm (at the bottom of the soil and at 10 cm below the soil surface) over the acclimation and flushing periods until the end of the experiments using iButton® data loggers. The data loggers were wrapped in whirlpacks and placed in the soil when the mesocosms were established. The soil temperatures at these depths ranged from 5 to 20 °C in all of the mesocosms (measured at 60 min intervals; N = 672 and N = 336 soil temperatures made from each mesocosm of each landscape age and vegetation type age over the average 14 and 7 days of the experiments, respectively; Figure 3.S1). The ambient air temperatures ranged from −7 °C to 23 °C (average 9 ± 0.2 SE °C) during the study period (Environmental Data Center, Toolik Field Station).

The soil mesocosms were open to the atmosphere at the top and sealed at the bottom; O_2 could diffuse into the soils from the top of each mesocosm. The mesocosms were acclimated under static waterlogged conditions (i.e., no flowing water) in the water bath for four to ten days to generate the reducing conditions observed in intact soils in the field [2,3]. DI water (1–2 L) was added to the soil mesocosms during the acclimation period to account for evapotranspiration and keep the water table constant in the mesocosms.

The soil water sampled at the end of the acclimation period just before DI was added during the flushing period was assumed to represent conditions in the mesocosms during the acclimation period. After the acclimation period, each set of triplicate mesocosms for each of the two landscape ages and for each of the two vegetation types was flushed with an average of 16.8 ± 0.9 L of DI water (N = 36, average ± SE) over one to 3 h, called the "flushing period" (Figure 3.S1). The flushing period consisted of ten individual flushes where ten soil water samples were collected every 0.2 to 2 L of DI flushed from each replicate mesocosm. The total volume of water flushed was chosen to represent precipitation events up to and in excess of the natural precipitation patterns

near Toolik Field Station (Table 3.S1). Thus, the flushing mimicked the effects of brief and rapid changes in redox conditions on concentrations of DOC and iron, their export during precipitation events and their effect on •OH production in the soil waters. During the flushing period the mesocosms were drained from the bottom and DI was added to the top to keep the water level constant. After the flushing period, each set of triplicate mesocosms was acclimated again for five to seven days under the same conditions as during the first acclimation period. After the second acclimation period each mesocosm was flushed with 12.5 ± 0.2 L (average ± SE) of DI water during the second flushing period. As in the first flushing period, ten soil water samples were collected with each volume of DI added during the second flushing period.

At the end of the experiment, subsamples were collected from each soil core from organic and mineral (if present) layers for soil moisture, bulk density, porosity and organic carbon content [33]. Soil moisture was measured as the difference in mass of a subsample of the soil before and after draining the gravimetric water and then drying the soil for two days at 105 °C in an oven. Bulk density of the soil was determined as the mass of dry soil in an entire core divided by the soil volume (dimensions of the soil contained in the core). Porosity of the soil was calculated from the volume of soil core occupied by water versus soil. The volume of soil water was determined by draining a known volume of the soil core and measuring the volume of drained (gravimetric) water. The volume of the soil was determined from the dimensions of the soil core. Organic carbon content was determined from combusting a subsample of dried soil for one day at 550 °C, assuming the mass of organic matter lost during ignition was 50 % carbon. Values are reported as an average ± SE (N = 9 for each landscape age and vegetation type, corresponding to three replicate mesocosms measured after each of the two acclimation periods for the first experiment and after the only acclimation period for the second experiment; Figure 3.S1).

3.3.3 Soil water collection and characterization

Soil water was collected from each mesocosm through a drain in the bottom of the bucket with 0.5 cm radius Tygon tubing flowing directly into 60 mL BOD bottles wrapped with aluminum foil until overfilled by at least one bottle volume. Temperature, pH, conductivity and dissolved oxygen were measured on unfiltered soil water in each BOD bottle immediately after soil water collection, before and then during the flushing period. pH was measured using a WTW SenTix pH 3210 meter and probe. Temperature and conductivity were measured with a WTW Cond 3210 meter and probe. Dissolved oxygen was measured (optical probe, YSI) in the soil water collected in BOD bottles and also measured on the DI water before it was flushed through the mesocosms during the simulated precipitation events to determine how much O_2 was added with flushing (DI contained average 0.3 ± 0.01 SE mmol O_2 L^{-1}, N = 9).

Subsamples of soil water from each BOD bottle were filtered for analysis of dissolved organic carbon (DOC) using pre-combusted and sample-rinsed Whatman GF/F filters. DOC samples were preserved with 6 N trace-metal grade HCl and stored in the dark at 4 °C until analysis on a Shimadzu TOC-V analyzer (Coefficient of Variation ~5% on duplicate samples or standards) [34]. Subsamples of soil water from each BOD bottle were analyzed for electron donating capacity, colored and fluorescence dissolved organic matter characterization (CDOM and FDOM, respectively), total iron and Fe(II) and •OH as described below. All values for soil water chemistry are reported as the average ± standard error (SE) from the triplicate mesocosms of each landscape age and vegetation type measured after each of the two acclimation periods for the first experiment and after the only acclimation period for the second experiment (N = 9; Figure 3.S1).

3.3.4 EDC and iron concentrations

Unfiltered triplicate soil waters were analyzed immediately for EDC, total iron and Fe(II). For the EDC measurements, we used colorimetric detection following the protocol from Trusiak et al. (2018) [2]. Total iron and Fe(II) concentrations were quantified by the ferrozine method [35] following Trusiak et al. (2018). Particulate-rich samples were centrifuged for 3 min at 32,000 rpm to separate particulates from the soil water. The settling of particulates could lead to underestimation of the amount of EDC, total iron and Fe(II) present in the soil water of the mesocosms. Absorbance for both EDC and iron was measured on a Horiba Aqualog Spectrofluorometer in 1-cm pathlength methacrylate cuvettes.

3.3.5 CDOM and FDOM analysis

Soil water subsamples for CDOM and FDOM analysis were filtered using pre-combusted Whatman GF/F filters and analyzed approximately one hour after the sample collection in the field using a Horiba Aqualog Spectrofluorometer [36]. CDOM and FDOM were analyzed on the soil waters in a 1-cm pathlength quartz cuvette. Fluorescence excitation-emission matrices (EEMs) of the soil water were collected over excitation and emission ranges of 240–600 nm by excitation/emission increments of 5/1.64 nm/nm, respectively. Integration times ranged from 2 to 3 s. When necessary, the soil water was diluted 2 to 6-fold with MilliQ water to less than 0.6 absorbance units (A) at 254 nm prior to the analysis [37]. EEMs were corrected for inner-filter and instrument-specific excitation and emission effects in Matlab (version 2015b). Blank EEMs were collected using MilliQ water and were subtracted from soil water EEMs to minimize the influence of water Raman peaks. Intensities of corrected soil water EEMs were converted to Raman units. Dominant peaks in the corrected soil water EEMs were identified following Cobble [38]: Peak A (λex = 250 nm; λem = 380–460 nm), Peak C (λex = 350; λem = 420–480 nm) and

Peak T (λex = 275 nm; λem = 340 nm). The fluorescence index (FI) [39,40] was calculated as the ratio of emission intensity at 470 nm to emission intensity at 520 nm at an excitation wavelength of 370 nm.

3.3.6 •OH concentrations

•OH was quantified using terephthalate (TPA) [41] as a probe for •OH as previously used in arctic soil waters [2,3]. •OH was quantified by adding an unfiltered soil water subsample to O_2-free (stored in O_2-free atmosphere in a glove box) MilliQ water containing excess TPA. •OH present was allowed to react with TPA for 24 h prior to analysis of the product of the TPA reaction with •OH (2-hydroxyterephthalic acid, hTPA) [41]. •OH concentrations were determined using standard additions of 0, 25 and 50 nM hTPA to account for matrix effects. hTPA was quantified on an Acquity Ultra High Performance H-Class LC (uPLC; Waters, Inc., Milford, MA, USA; Mississauga, Ontario, Canada) with fluorescence detection (excitation 250 nm, emission 410 nm) on an Acquity uPLC BEH C_{18} column (2.1 × 50 mm; 1.7 µm). The yield for hTPA formation from •OH reaction with TPA was assumed to be 35% [41].

3.3.7 EDC, DOC and iron production

EDC, DOC, total iron and Fe(II) production was calculated as the respective concentrations in the soil waters from the initial soil water collection (after the acclimation period) divided by the number of days of the acclimation period. Preliminary measurements of soil water collected before the first acclimation period showed no detectable EDC, total iron or Fe(II). Thus, to calculate EDC, total iron and Fe(II) production rates we assumed values of zero for each of these constituents at the start of the first acclimation period. To calculate the DOC production rate, we subtracted the average DOC concentration in soil water at the end of the first flushing period from the DOC concentration measured at the end of the first acclimation period. To calculate production

rates after the second acclimation period, concentrations of EDC, DOC, total iron and Fe(II) at the end of the first flushing period were subtracted from the concentrations in soil water collected after the second acclimation period. For the mesocosms where the concentrations of EDC, DOC, total iron and Fe(II) were higher after the first or second individual flush than during the initial soil water collection, the average of the first two to three individual flushes was used as the initial EDC, DOC, total iron and Fe(II) concentration. The EDC, DOC, total iron and Fe(II) production was normalized to the dry mass of soil in each mesocosm. The dry mass of soil was obtained by drying a subsample a volume of soil from the mesocosm at 105 °C for 48 h and determining the loss of soil mass after drying. The difference in the mass of the soil before and after drying is the mass of water originally contained in the soil.

3.3.8 Dissolved O_2 consumption

Dissolved O_2 consumption was calculated as the difference in the O_2 concentration before the acclimation period and the O_2 concentration in soil waters at the end of the acclimation period divided by the number of days of the acclimation period. This approach likely yields minimum estimates of O_2 consumption because it does not account for O_2 consumed during the slow diffusion of O_2 into the stagnant boundary layer of the soil core. In addition, if all O_2 consumption happened before the end of the acclimation period then rates of O_2 consumption were faster than estimated. Dissolved O_2 consumption was then normalized to the dry mass of soil in each mesocosm (Section 3.3.7).

3.3.9 •OH production

•OH production during the flushing period was calculated as •OH concentration after the first flush volume (corresponding to up to 15 mm of precipitation) divided by the amount of O_2 introduced to the mesocosms (based on the volume of DI added and O_2 concentrations in DI, giving

•OH per O_2 added), assuming a constant yield of •OH per O_2 supplied for all precipitation events up to 15 mm rain. This yield of •OH per O_2 supplied was then multiplied by the amount of O_2 supplied from a 4 mm per day precipitation event, the average amount of precipitation received in one day during the summer at Toolik Field Station, to give a •OH production rate per day during precipitation events. •OH production during static, waterlogged, low O_2 conditions was calculated as the •OH concentration in soil water collected at the end of the acclimation period minus a starting concentration of zero (see below). •OH production during the acclimation period was divided by the number of days of the acclimation period to estimate a daily •OH production rate, which was assumed to be constant during the acclimation period. As with EDC and Fe(II) above, preliminary measurements of soil water showed no detectable •OH production prior to the start of the first acclimation period. Thus, we used a concentration of zero •OH at the beginning of the first acclimation period in order to calculate •OH production over time. For the second acclimation period, •OH concentrations at the end of the first flushing period were subtracted from the concentrations in the soil water collected after the second acclimation period and divided by the number of days of the second acclimation period.

A number of assumptions were made to estimate •OH production. First, we assumed that •OH concentrations were the values measured by the chemical probe (Section 3.3.6). This assumption likely results in conservative estimates of •OH production because the measured •OH during each period of the experiment is a net of •OH production and consumption given fast quenching and reaction rates of •OH with soil constituents [42]. In addition, considering that •OH was measured only from soil water flushed from the soils, •OH production from colloids or particles retained in the soils [7] was likely not detected. Thus, it is likely that more •OH was produced in the soil waters than detected during both periods of the experiment. Finally, •OH

concentration in the soil water sampled from the bottom of the mesocosm was assumed to be representative of all soil water in the mesocosm (i.e., each mesocosm was assumed to be homogenous).

3.4 Results

3.4.1 Soil and soil water chemistry differed by landscape age and vegetation type

The chemical and physical properties of the soil cores differed in organic carbon content, soil moisture, porosity and bulk density between the landscape ages and vegetation types, as expected. Soil cores from the older landscape had higher soil organic carbon content, soil moisture and porosity than soil cores collected from the younger landscape (Table 3.1). Soil cores from wet sedge vegetation were characterized by a thick organic layer, while the cores from tussock vegetation contained both organic and mineral layers (Table 3.1). Wet sedge soils had lower bulk density and higher soil organic carbon, soil moisture content and porosity than tussock soils (Table 3.1).

All soil waters were mildly to fairly acidic, low in conductivity and dissolved oxygen and high in EDC, DOC and Fe(II) (Table 3.2), as expected from the previous work [2,3]. On average, Fe(II) accounted for 52 ± 3% of the EDC and 74 ± 9% of the total dissolved iron in soil waters, again consistent with previous work [2]. EDC and Fe(II) concentrations were strongly correlated (R^2 = 0.9, $p < 0.05$, data not shown). Thus, Fe(II) concentrations are shown in Figure 3.2 to represent changes over time in both Fe(II) and EDC (not shown). Soil waters from the older landscape had higher EDC, DOC and Fe(II) concentrations compared to soil waters from the younger landscape. On each landscape, there were generally no significant differences in EDC, DOC, total iron and Fe(II) concentrations between the two vegetation types (*t*-test, Table 3.2).

Similar to the initial differences in soil water chemistry presented above, there were some significant differences in the DOC composition between landscape age and vegetation type (Table 3.3). The ratio of peak A to peak T intensity of FDOM (T/A) differed significantly by landscape age for each vegetation type. That is, when comparing soil waters from tussocks, the T/A ratio was significantly higher for soil water DOC from the younger than the older landscape soils (Table 3.3). Similarly, for wet sedge soil waters, the T/A ratio was significantly higher for DOC from the younger than the older landscape soils (Table 3.3). The DOC in soil water from older tussock soils had a significantly lower slope ratio than DOC from younger tussock soils (Table 3.3). The fluorescence index (FI) of DOC from older wet sedge soils was significantly higher than the FI of DOC from younger wet sedge soils (Table 3.3). Of the DOC from younger soils, the FI was significantly higher from tussock than from wet sedge soils (Table 3.3).

3.4.2 Change in soil water chemistry during precipitation events

O_2 concentrations decreased to low levels during the acclimation period of the experiment and increased with the amount of water flushed through the mesocosms (Figure 3.2). For example, following the acclimation period, the initial soil water collected from the mesocosms had low O_2 (52 ± 9 µM, average ± SE, N = 36; Table 3.2). During the first flushing period, soil water O_2 concentrations increased with increasing volume of DI water added (i.e., increased with flush volume; Figure 2) to average 230 ± 14 SE µM (N = 36; Figure 3.2). During the second acclimation period following the first flushing period, O_2 in soil waters was consumed and returned to the low concentrations observed after the first acclimation period (Figure 3.2). The increase in O_2 concentrations during the second flushing period was similar to that in the first flushing period (Figure 3.2).

During the first acclimation period, Fe(II) concentrations increased as O_2 concentrations decreased in each mesocosm (shaded portions of Figure 3.2). Thus, Fe(II) concentrations were the highest in the soil waters just after each acclimation period (i.e., within the first or second flush; Figure 2) with an exception. For wet sedge soil waters, Fe(II) concentrations decreased during the second acclimation period and remained relatively constant during the first and second flushing periods. For tussock soil waters, Fe(II) concentrations decreased during the first and second flushing periods. Fe(II) concentrations generally decreased with increasing flush volume until concentrations were 10 µM or less, at which point they remained relatively constant or decreased less with increasing flushing (Figure 3.2).

Similar to Fe(II), DOC concentrations were the highest at the end of each acclimation period and generally decreased with flushing (Figure 3.2). An exception was wet sedge soil water, where the DOC concentrations remained relatively constant during the first and second flushing periods (Figure 3.2). DOC composition changed during the flushing as well. Although there was high variability in FI of the DOC between replicate mesocosms, there was a significant decrease in the FI of the DOC with flushing from each mesocosm (i.e., slope significantly less than zero; $p < 0.05$; data not shown). When averaged by landscape age and vegetation type, there was a significant decrease in the FI of the DOC with flushing (Figure 3.3). As the volume of water flushed through the soil increased, the DOC exported was thus likely more aromatic (i.e., lower FI) [39].

Changes in •OH concentration during the precipitation events and static waterlogged conditions generally followed the changes in O_2, DOC and Fe(II) in the tussock soil waters (Figure 3.2). In the tussock soil waters, •OH was higher after the acclimation periods when O_2 was low and when DOC and Fe(II) were high (Figure 3.2). •OH concentrations generally decreased with

flushing of the tussock soil waters concurrent with increases in O_2 and decreases in DOC and Fe(II). In the wet sedge soil waters, changes in •OH were less clearly coupled to changes in O_2, DOC and Fe(II) (Figure 3.2). •OH decreased in the older landscape wet sedge soil water with flushing as O_2 increased but there was less change in •OH with increasing O_2 in the younger landscape wet sedge soil water. •OH increased during the second acclimation period (corresponding to the decrease in O_2) in the wet sedge soil waters when DOC and Fe(II) decreased or stayed the same (Figure 3.2).

3.4.3 Consumption and production from waterlogged soils

O_2 consumption was higher in the older landscape wet sedge soil waters than in the younger landscape tussock soil waters (Table 3.4). O_2 consumption was not significantly different between the first and second acclimation periods for all mesocosms, except in the older landscape wet sedge soil water where O_2 consumption was lower during the second acclimation period than during the first acclimation period (Table 3.4).

Fe(II) and DOC were generally produced during the acclimation period and their production was positively correlated (Figure 3.4A,B). One exception to Fe(II) production was the net consumption of Fe(II) from wet sedge soil waters on the older landscape during the second acclimation period (Table 3.4, Figure 3.4B, negative values). During the first acclimation period, Fe(II) production rates were significantly higher from the soil waters on the older than the younger landscapes (Figure 3.4A). During the second acclimation period Fe(II) production rates were generally lower than or within the same range as during the first acclimation period for all soil waters, except for the tussock soil waters on the older landscape (Table 3.4, Figure 3.4B). For the older landscape tussock soil waters, Fe(II) production during the second acclimation period was significantly higher than during the first acclimation period (Figure 3.4B).

•OH production rates were strongly, positively correlated with Fe(II) production rates (Figure 3.5). Therefore, there were significant differences in •OH production between landscape ages and vegetation types. •OH production was higher from the soil waters on the older, high-iron landscapes than from the younger landscapes and higher from the soil waters in tussock than from wet sedge vegetation (Figure 3.5).

3.5 Discussion

Our results demonstrate that either Fe(II) or O_2 availability could control •OH production, depending on the soil and environmental conditions that are affected by landscape age and vegetation type. For example, during precipitation events when upland soils are rapidly flushed with O_2, there is high potential for •OH production due to the consumption of Fe(II) by O_2. This potential may be limited by the Fe(II) production rate because Fe(II) is consumed by oxidation when soils are flushed. During static, waterlogged conditions characterized by low O_2 and relatively high Fe(II) concentrations, •OH production may be limited by the O_2 supply rate to oxidize Fe(II). By relating •OH production to the O_2 supply and consumption and to the Fe(II) production and consumption, we assess the limits on •OH production (and its oxidation of DOC to CO_2) during different redox regimes in soils occurring during precipitation events and waterlogged conditions.

3.5.1 The balance of Fe(II) production and consumption controls •OH production during precipitation events

During precipitation events, Fe(II) exported from the soil can decrease due to dilution by rain water or consumption by oxidation or increase by production. Correcting Fe(II) export for the addition of simulated rain water (i.e., DI water containing no detectable Fe(II)) rules out a decrease in Fe(II) from dilution (Figure 3.6). Once corrected for dilution, Fe(II) export was

relatively constant with increasing O_2 added during the flushing period in all soil waters except for the older tussock (Figure 3.6). In older tussock soil waters, Fe(II) export corrected for dilution decreased and then was relatively constant as more O_2 was supplied during the flushing period (Figure 3.6). Thus, these results suggest that Fe(II) production was in balance with its consumption as O_2 was supplied in all soils except older tussock soils (Figure 3.6).

Fe(II) production with increasing O_2 supplied is not expected given that Fe(II) oxidation by O_2 is a sink for Fe(II) [43]. However, one process that could produce Fe(II) in the presence of O_2 is the reduction of Fe(III) by reduced DOC [14,22,23,44–47]. Two lines of evidence suggest that reduction of Fe(III) by DOC could produce Fe(II) as O_2 was supplied. First, the electron donating capacity (EDC) of the DOC exported from the soils likely increased during flushing. This is because the EDC of DOC increases as the DOC aromatic fraction increases [44] and the DOC flushed from soils at higher O_2 was increasingly aromatic (lower FI, Figure 3.3). Second, the DOC export (corrected for dilution; Figure 3.S2), was relatively constant with flushing. Together, these results suggest export of increasingly reduced DOC at higher O_2 supplied (Figures 3.3 and 3.A2). The export of increasingly reduced DOC at higher O_2 could offset the loss of reduced DOC by its oxidation by O_2 [44–46]. Flushing aromatic DOC with a relatively higher EDC from the soils (per g DOC; Figures 3.3 and 3.A2) may have regenerated Fe(II) that was oxidized by O_2, thereby contributing to the constant Fe(II) export with increasing O_2 supply during precipitation events (Figure 3.6). Thus, DOC composition likely influenced the balance of Fe(II) production and consumption during precipitation events.

The balance of Fe(II) production and consumption limits •OH during precipitation events. •OH export corrected for dilution by rain water were generally relatively constant with increasing O_2 supplied, which is consistent with Fe(II) production (Figure 3.6). For example, the relatively

constant •OH export in all soil waters during a large precipitation event (≥ 3.8 mmol O_2 m^{-2} corresponding to ≥ 15 mm of rain) [26] was likely due to the balance between Fe(II) production and consumption where there was no net change in Fe(II) concentrations (Figure 3.6).

3.5.2 O_2 supply limits •OH production during waterlogged conditions

•OH production rates quantified during the acclimation period were likely representative of •OH production rates in the soil waters during static, waterlogged conditions. During the acclimation period, the O_2 supply rates to soil mesocosms were likely similar to the O_2 supply rates to natural soils (e.g., O_2 was supplied to the soil by diffusion or via plant roots). In addition, there was net Fe(II) production in most soil waters during the acclimation period (Figure 4) at rates comparable to field studies in other arctic soils [14] and in temperate-zone northern peatlands [12,13]. Thus, we assume that the •OH production rate measured during the acclimation period approximates a constant daily rate at which •OH is produced from the Fe(II) oxidation by O_2 supplied to the soils.

Field observations suggest that the O_2 supply may limit •OH production during static, waterlogged conditions. Generally during summer in the Alaskan arctic tundra, the shallow impermeable barrier of permafrost in soils results in waterlogged and reducing conditions as indicated by low dissolved O_2 and high Fe(II) concentrations [2,3,48,49]. High Fe(II) concentrations suggest that Fe(II) production outpaces its consumption by O_2 (and thus outpaces the O_2 supply rate) during static, waterlogged conditions. However, the oxidative consumption of Fe(II) by O_2 is the source of •OH [2,3,7]. Thus, if the O_2 supply rate was similar to the Fe(II) production rate, then the •OH production could be higher compared to conditions when O_2 supply rates are lower than Fe(II) production. The former scenario is indicated by relatively constant •OH production at relatively constant Fe(II) (the net of Fe(II) production and consumption after

correction for dilution; Figure 3.6). If O_2 supply is a limit on the •OH production in static waterlogged soils, identifying the dominant supplies of O_2 to soils is crucial for understanding •OH production.

O_2 supply can be much faster than Fe(II) production in any soil water, where net Fe(II) production may be up to 10 mmol Fe(II) m^{-2} day^{-1} (Table 3.4). First, the average O_2 diffusion from the atmosphere into soil air pore spaces has been reported to be 46 ± 2.4 mmol O_2 m^{-2} day^{-1} for tussock soils and 34 ± 5.5 mmol O_2 m^{-2} day^{-1} for wet sedge soils [31]. Second, a 1 cm drop in the water table in an organic mat soil with a typical porosity of 60–80% would result in an increase in O_2 of 60 to 80 mmol O_2 m^{-2} for wet sedge and tussock soil waters, respectively. Changes in water table height from 1 mm up to 1 cm per day have been observed in soils underlain by permafrost [50–52]. Thus, a daily drop in water table height of 1 mm to 1 cm could result in a rate of O_2 supply from 1–12 mmol O_2 m^{-2} d^{-1}. Third, O_2 supply from plant roots for wetland species has been reported to be 10–130 ng O_2 cm^{-2} root surface min^{-1} depending on the vegetation and the distance from the root [53]. Assuming a live fine root area index of 5 m^2 root surface per m^2 area of tundra [54] results in an O_2 supply to the soils of 23–304 mmol O_2 m^{-2} day^{-1}. If Fe(II) oxidation is the only sink for O_2, then faster O_2 supply than Fe(II) production suggests that Fe(II) should be oxidized and not accumulate in the soil waters during static, waterlogged conditions.

There are large and fast O_2 sinks other than Fe(II) oxidation that could result in limited availability of O_2 in waterlogged soils. For example, respiration contributes to O_2 consumption [9,31,48,55,56] and microbial respiration in arctic soil waters at our study sites has been reported to produce 2.76 ± 1.06 mol CO_2 m^{-2} day^{-1} [26]. Ecosystem respiration rates in arctic and boreal soils have been reported to produce 0.2 to 0.3 mol CO_2 m^{-2} day^{-1} [30,57]. In addition, O_2 supplied may also be consumed during the oxidation of particulate organic matter and reduced minerals

[58–61] that may not result in •OH production. Given that the respiration rates are likely much faster than the O_2 supply rates, it is unlikely that all O_2 supplied to the soils is used for Fe(II) oxidation and •OH production. Thus, fast O_2 supply and large sinks for O_2 support our results suggesting that O_2 availability limits •OH production under static, waterlogged conditions.

3.5.3 •OH mediated oxidation of DOC to CO_2 Dduring precipitation versus static conditions

Results from this study show that •OH is produced from soils during precipitation events where O_2 is introduced to the soil waters, as well as during static, waterlogged conditions (Figure 3.2). DOC is the main sink for •OH in arctic soil waters [42] and •OH oxidizes DOC to CO_2 [3]. Here we compare the summer-time amount of CO_2 that could be produced by •OH oxidation of DOC during precipitations events versus during static, waterlogged conditions. •OH production during a typical precipitation event was calculated using the yield of •OH per O_2 supplied during flushing (Figure 3.6), assuming a constant yield of •OH per O_2 supplied for all precipitation events up to 15 mm rain (using the average slope between the first two data points in Figure 3.6 for all landscape age and vegetation types). The yield of •OH per O_2 supplied was then multiplied by the amount of O_2 supplied from a 4 mm per day precipitation event, the average amount of precipitation received in one day during the summer at Toolik Field Station, resulting in a rate of •OH production per day during precipitation events (Table 3.5). The average •OH production rate from all landscape ages and vegetation types quantified during the acclimation period (Figure 5) was assumed to be the daily •OH production rate from waterlogged soils during the summer. These calculations result in rates of •OH production of 200 ± 70 µmol •OH m^{-2} day^{-1} and 60 ± 20 µmol •OH m^{-2} day^{-1} during precipitation events and during waterlogged conditions, respectively (Table 3.5; Appendix 3.8.1 and 3.8.2). Assuming a yield of 1 mol CO_2 per 3 mol •OH [4], the range of

CO_2 that could be produced from •OH oxidation of DOC is 60 ± 20 μmol CO_2 m^{-2} day^{-1} and 20 ± 6 μmol CO_2 m^{-2} day^{-1} during precipitation events and during waterlogged conditions, respectively (Table 3.5).

Assuming that the soils receive precipitation on half of the summer days and during the remaining half of the summer the soils can be characterized as static and waterlogged, then precipitation events may generate up to two to three times more •OH and CO_2 production, respectively, over the summer compared to static, waterlogged conditions (Table 3.5; Appendix 3.8.1 and 3.8.2). The amount of •OH and CO_2 produced by precipitation events is the same order of magnitude as the prior, preliminary estimate based on the unlimited O_2 supply to Fe(II)-rich soil waters [2]. Similar •OH and CO_2 production from precipitation events as from conditions in soils where •OH production is not limited by O_2 is consistent with the fact that O_2 was not likely limiting •OH production during precipitation events (Figure 3.6). The amount of •OH and CO_2 produced during waterlogged conditions is about five times less than the prior, preliminary estimate based on the unlimited O_2 supply to Fe(II)-rich soil waters [2], consistent with the fact that O_2 supply likely limits •OH production during these conditions (Figure 3.2). While these first comparisons of •OH and CO_2 production from precipitation events versus static waterlogged conditions suggest that precipitation events may produce more •OH (and CO_2), there is greater uncertainty in the production of •OH and CO_2 during precipitation versus waterlogged conditions because the variation in production with the rate of O_2 supply is unknown. Using the yield of •OH production per O_2 supplied from the flushing period of the experiment (Figure 3.6) to calculate the •OH production rate during precipitation events requires an assumption that the yield of •OH per O_2 supplied does not depend on the rate of O_2 supplied during a precipitation event. That is, we assume the same yield of •OH per O_2 supplied is independent of whether the O_2 was supplied to

the soils in a few h versus over the course of the day. Finally, both current (Table 3.5) and previous [2] landscape-scale estimates of •OH and CO_2 production do not account for differences due to landscape age or vegetation type (Figure 3.5). Scaling the estimates of •OH and CO_2 produced to the landscape requires an assessment of the landscape controls on Fe(II) and •OH production.

3.5.4 Landscape controls on Fe(II) and •OH production

Given that the magnitude of •OH production is generally controlled by the magnitude of Fe(II) production (Figure 3.5), it follows that •OH production is expected to be higher from tussock soils on the older landscapes that supported higher Fe(II) production (Table 3.4, Figure 3.5). Fe(II) production was highest in the older landscape tussock soil waters for two reasons. First, the mineral layer present in tussock soils was likely a source of Fe(II) from dissolution or microbial reduction (Table 3.1) [14,19,62]. Second, soil minerals on the older landscapes have been more extensively weathered than on the younger landscapes and thus, more carbonate has been removed from the soils on the older than on the younger landscapes [62]. Less carbonate in the older versus younger soils results in a lower pH in soil waters on the older versus younger landscapes [2,3,61] and lower pH slows the Fe(II) oxidation [43,46,62]. In addition to differences in carbonate and pH, the higher DOC concentrations in soil waters on older landscapes buffer these soils at a lower pH than soils buffered by carbonate on younger landscapes (Table 3.2) [63,64]. Lower pH and higher DOC in soil waters on older landscapes facilitates higher Fe(II) production by supporting mineral dissolution, desorption and microbial reduction of Fe(III) to Fe(II) [17]. Together, differences in soil chemistry between landscape ages explain why Fe(II) production was higher in tussock soil waters on older versus younger landscapes, despite the presence of a mineral layer in tussock soils on both landscapes. These results suggest that in the field, •OH production should

be highest in tussock soils on older landscapes where Fe(II) production was the highest (Table 3.4, Figure 3.5).

The higher •OH production in tussock soils with higher Fe(II) production (Table 3.4, Figure 3.5) is contrary to previous studies showing the highest •OH production in wet sedge soil waters, not tussock soil waters [2,3]. In the previous studies the high •OH production from wet sedge soil waters was due to the higher Fe(II) concentrations compared to tussock soil waters, opposite of the difference in Fe(II) concentrations between wet sedge and tussock in the mesocosms (Figure 3.4, Table 3.2). Those two previous studies analyzed water withdrawn from the soil at one time, compared to the time course of analyses in intact mesocosms used in this study that integrate a larger surface area and greater depth of soil. However, while the mesocosms are much more representative of natural conditions in the bulk soil and processes through time than the methods used in prior work [2,3], they restrict the horizontal, downslope flow of water and constituents that occurs on the landscape. It is this hydrologic connectivity between upland tussock and lowland wet sedge that allows for the transfer and buildup of constituents such as Fe(II) in wet sedge soil waters [65–67]. Little production or even consumption of Fe(II) after the acclimation period in the wet sedge mesocosms suggests that in the field, the upland tussock soils supply dissolved constituents such as Fe(II) to the lowland wet sedge soils [2,3].

The differences in Fe(II) production and O_2 supply between tussock and wet sedge soils (Table 3.4) suggest that •OH production will vary between these vegetation types representing differences in soil mineral layers and landscape position. The results from this study show that tussock soils have a larger reservoir of reducible iron than wet sedge soils. In addition, the upland tussock soils are better drained and experience more frequent oxidizing conditions than do wet sedge soils. Together, these characteristics of tussock soils suggest that •OH production in tussock

soil waters may be dependent on the rate at which Fe(III) can be reduced to Fe(II). In contrast to tussock soil waters, wet sedge soil waters accumulate Fe(II) draining from upland tussock soils and lowland wet sedge habitats are typically poorly drained, have consistently more reducing conditions and have greater O_2 consumption (Table 3.4) than do tussock soils. This combination of higher Fe(II) concentrations and lower O_2 availability suggests that in wet sedge soil waters the supply of O_2 may limit •OH production. Thus, •OH production from wet sedge soils may be greatest when precipitation events introduce O_2 to a high-iron, reducing environment.

3.6 Conclusions

Results from this study combined with the field observations of waterlogged soils across the Arctic suggest that O_2 supply is likely the predominant limit on •OH production under waterlogged conditions in arctic soils. As O_2 is supplied to soils, the magnitude of •OH production that can be sustained in turn depends strongly on the Fe(II) concentration, which this study showed to depend on soil chemistry (corresponding to landscape age) and on the presence of a mineral layer (tussock soils). The capacity to sustain •OH production as O_2 is supplied to soils may also depend strongly on the chemical composition and thus capacity of DOC to regenerate Fe(II) via reduction of Fe(III).

Given that the •OH (and subsequent CO_2) produced by precipitation events may be about three times greater than by static, waterlogged conditions (Table 3.5), quantifying the importance of DOC oxidation to CO_2 by •OH depends strongly on changes in the hydrologic regime in a warming Arctic. There is a high potential for DOC and Fe(II) export from reduced soils to oxic surface waters during storms or floods [this study and work 66–69 and the frequency of heavy precipitation and inundation may increase in some regions of the arctic and subarctic in the future [70,71]. On the other hand, ice-wedge degradation occurring on the Arctic coastal plain as the

permafrost thaws is predicted to alter the water balance of lowland tundra by decreasing inundation and increasing runoff [72]. In addition, most studies suggest that warming in the Arctic will result in lower water table heights [18,73–75] and thus increasingly oxic conditions at deeper depths in the soils than at present. This shift may also lower the depth of the oxic-anoxic interface at which Fe(II) oxidation occurs. However, •OH production from Fe(II) oxidation should continue to be important in a warming Arctic given the high abundance of iron at deeper depths in permafrost soils [63,76].

Finally, while estimates from this study indicate that CO_2 produced from •OH oxidation of DOC is much less than CO_2 produced by soil respiration, this process should not be discounted as unimportant in carbon budgets. For example, oxidation of DOC to CO_2 at terrestrial-aquatic interfaces is a critical component of global carbon cycling e.g., [29,77–79]. Our results suggest that the •OH oxidation of DOC to CO_2 may contribute to the high rates of element cycling and greenhouse gas production at redox gradients common at terrestrial-aquatic interfaces. These terrestrial-aquatic interfaces are currently poorly understood and poorly represented in Earth-system models. In addition, in boreal waters where DOC and dissolved iron mainly as Fe(II) have been increasing over the past 30 years [80], the availability of Fe(II) to produce •OH may be increasing. Here we show that changes in hydrology and precipitation amounts and the forms of iron and composition of DOC exported from soils, will strongly govern the CO_2 production rates by this abiotic, redox-sensitive reaction involving •OH.

3.7 Acknowledgments

We thank J. Dobkowski, C. Cook, A. Deely, K. Romanowicz and researchers, technicians and support staff at the Toolik Lake Arctic LTER and Toolik Lake Field Station for assistance in the field and laboratory.

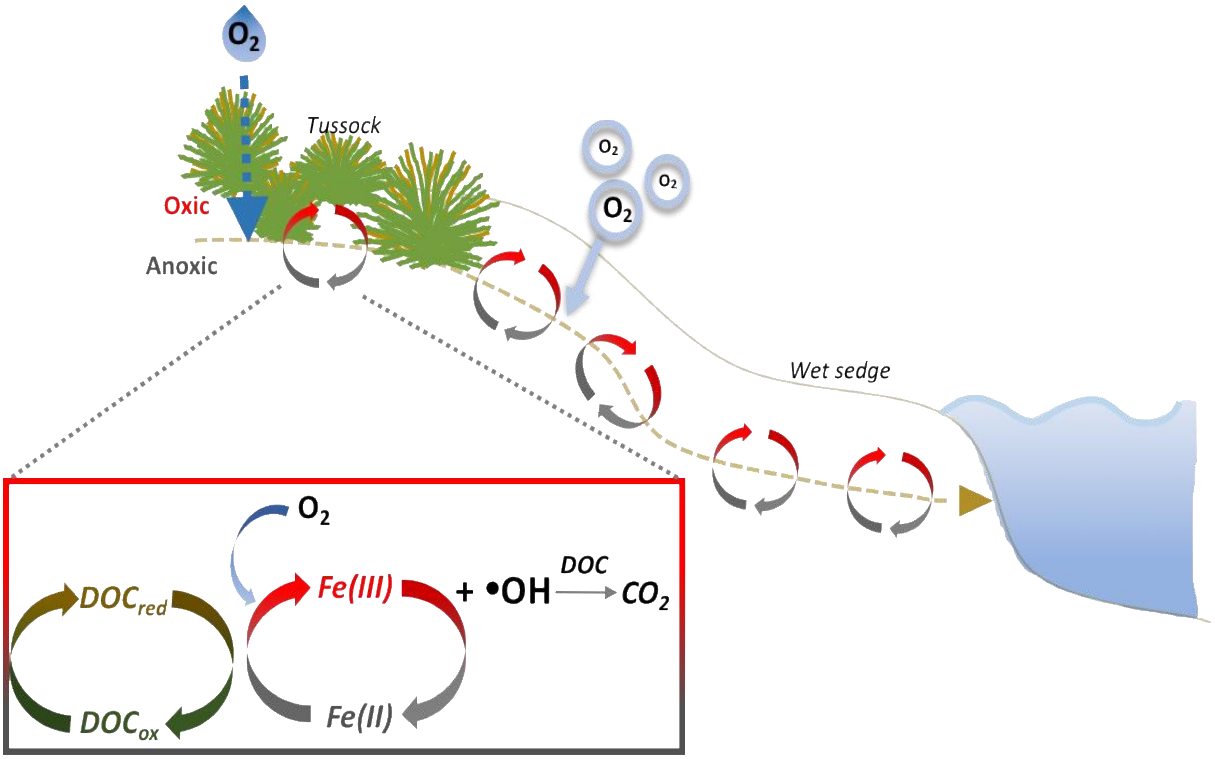

Figure 3.1. O_2 is supplied to soils through the downslope flow of oxygenated water during precipitation events, by diffusion from the atmosphere, by lowering of the water table height and by plant aerenchyma. O_2 leads to the oxidation of dissolved Fe(II) to Fe(III) in the soil waters at oxic-suboxic interfaces, resulting in the production of •OH [2,3]. •OH can then oxidize DOC to CO_2. Fe(II) can be regenerated by the DOC-mediated reduction of Fe(III) [14,20–22].

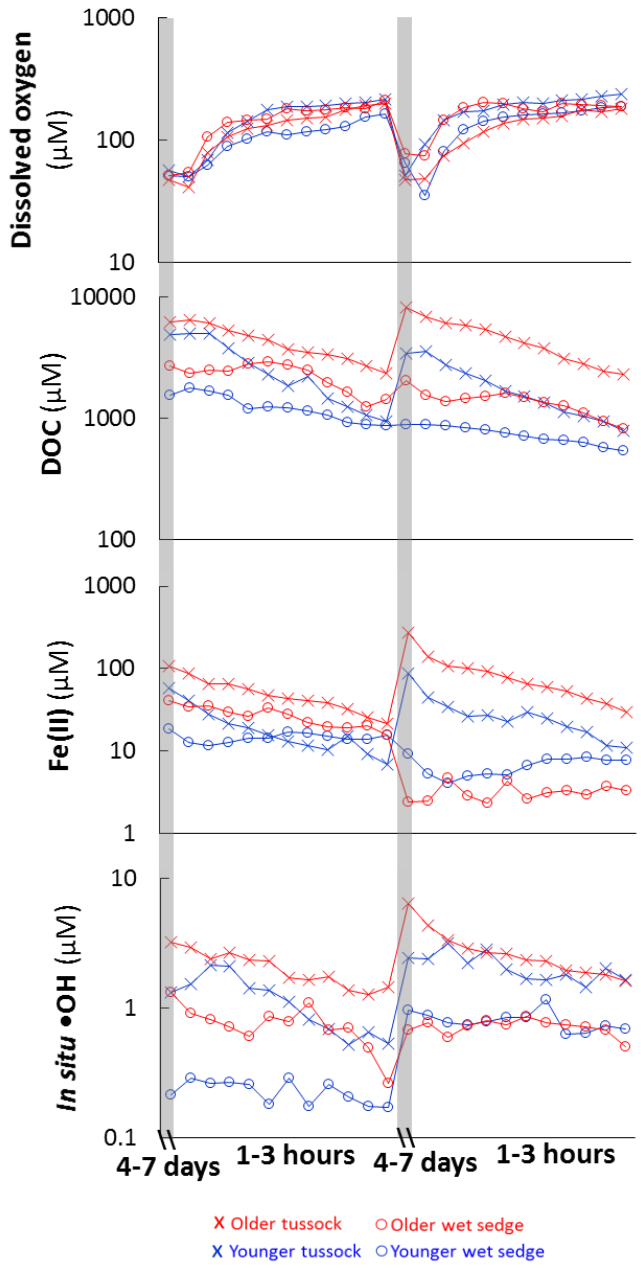

Figure 3.2. Dissolved O_2, DOC, Fe(II) and •OH concentrations during the experiments. Soil mesocosms were acclimated under waterlogged conditions for four to ten days to generate the reducing conditions observed in the field (acclimation periods shaded in grey). DI water was flushed through the soil mesocosms over one to 3 h during the flushing period (white area). EDC and Fe(II) concentrations were strongly correlated ($R^2 = 0.9$, $p < 0.05$, thus EDC data are not shown because Fe(II) concentrations represent changes in both Fe(II) and EDC). For the first acclimation and flushing period, values shown are averages of triplicate mesocosms from the two experiments (N = 6; error bars not shown; Figure 3.S1), while for the second acclimation period and flushing period values are averages from triplicate mesocosms from one experiment (N = 3; error bars not shown; Figure S1).

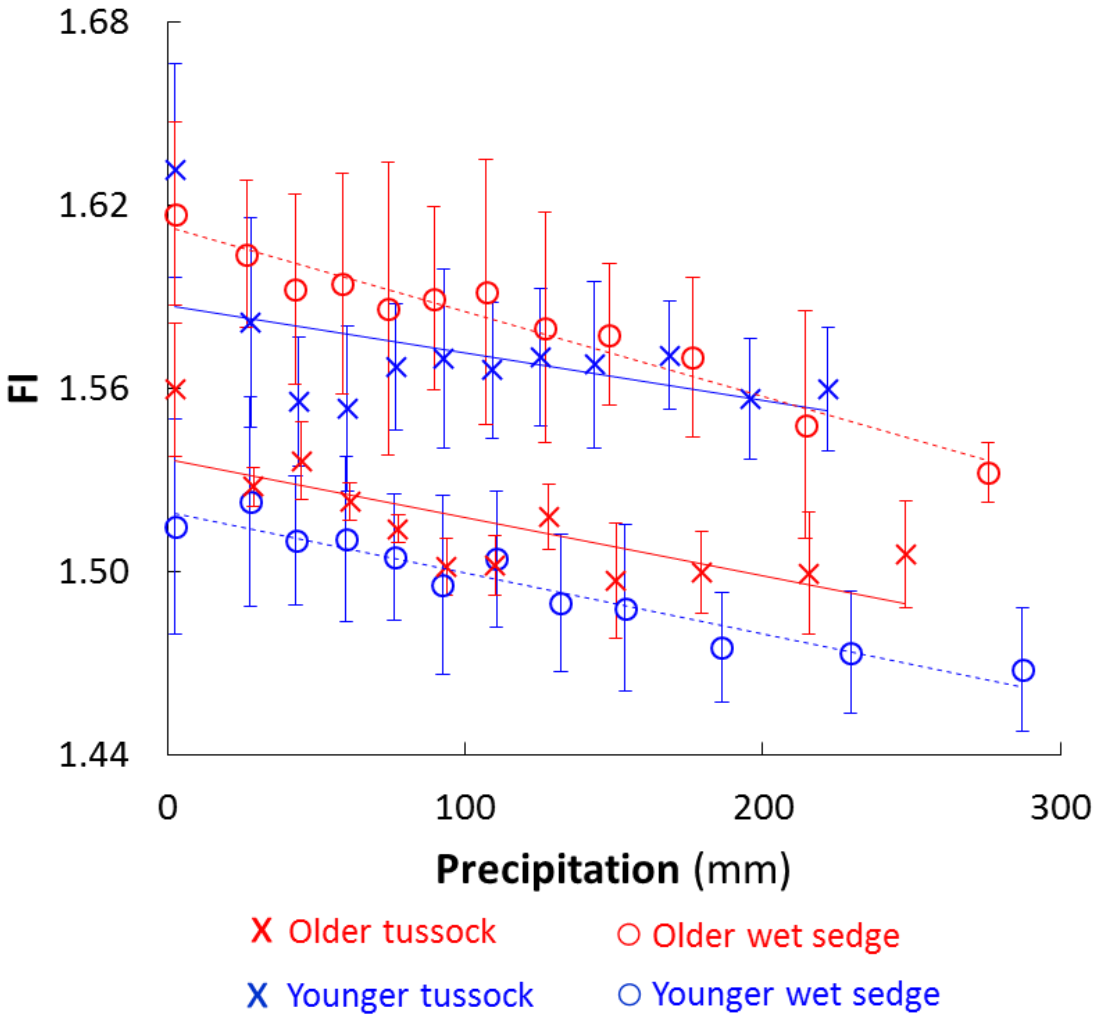

Figure 3.3. Fluorescence index (FI) of the DOC versus precipitation (mm). Values shown are averages ± SE of triplicate mesocosms from the two experiments (N = 9; Figure 3.S1). Dashed best-fit lines are for wet sedge while solid lines are for tussock. The slope of the relationship between FI and precipitation ranged from −0.00028 ± 0.000022 ($p < 0.0001$) to −0.00016 ± 0.000082 ($p < 0.1$) across landscape ages and vegetation types. Younger wet sedge $p < 0.00001$, older wet sedge $p < 0.00001$, younger tussock $p < 0.1$, older tussock $p < 0.005$.

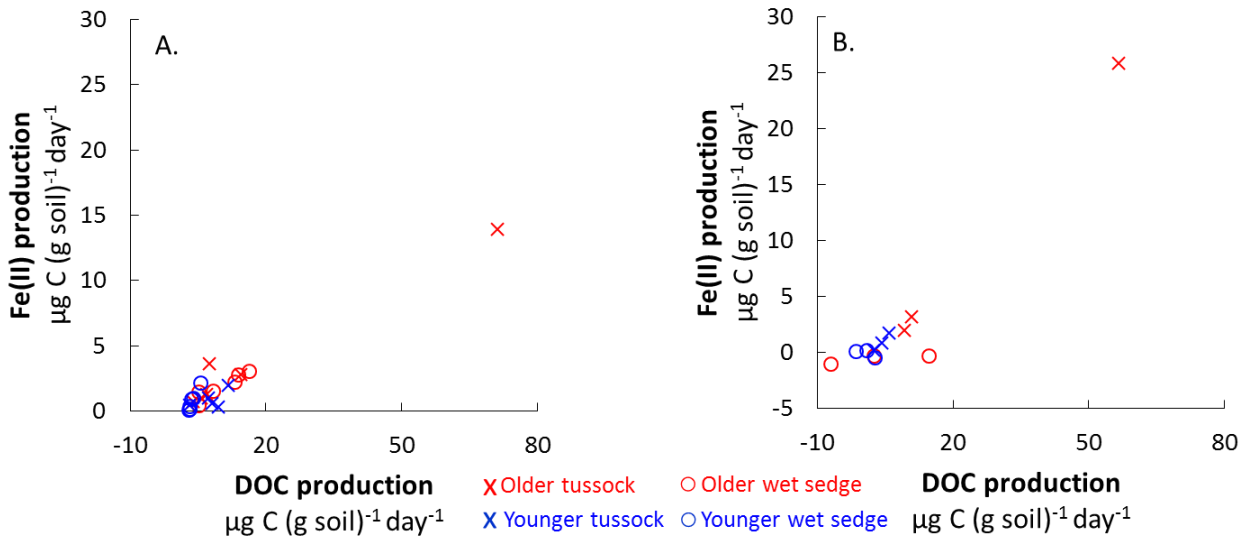

Figure 3.4. Average Fe(II) production versus average DOC production in all soil mesocosms after the first (**A**) and second (**B**) acclimation periods. For the first acclimation period, values are shown for each mesocosms from the two experiments (N = 24), while for the second acclimation period values are shown for each mesocosm from one experiment (N = 12; Figure 3.S1). There was a positive relationship between Fe(II) and DOC production in soils of all landscape ages and vegetation types. **A:** Fe(II) production (µg (g soil)$^{-1}$ (day)$^{-1}$) = 0.2 ± 0.04 × DOC production (µg C (g soil)$^{-1}$ (day)$^{-1}$) + 0.03 ± 0.3, R^2 = 0.79, $p < 0.05$; **B:** Fe(II) production (µg (g soil)$^{-1}$ (day)$^{-1}$) = 0.1 ± 0.06 × DOC production (µg C (g soil)$^{-1}$ (day)$^{-1}$) + 0.1 ± 0.4, R^2 = 0.3, $p < 0.05$). These regressions did not include the highest point in the upper right of each figure.

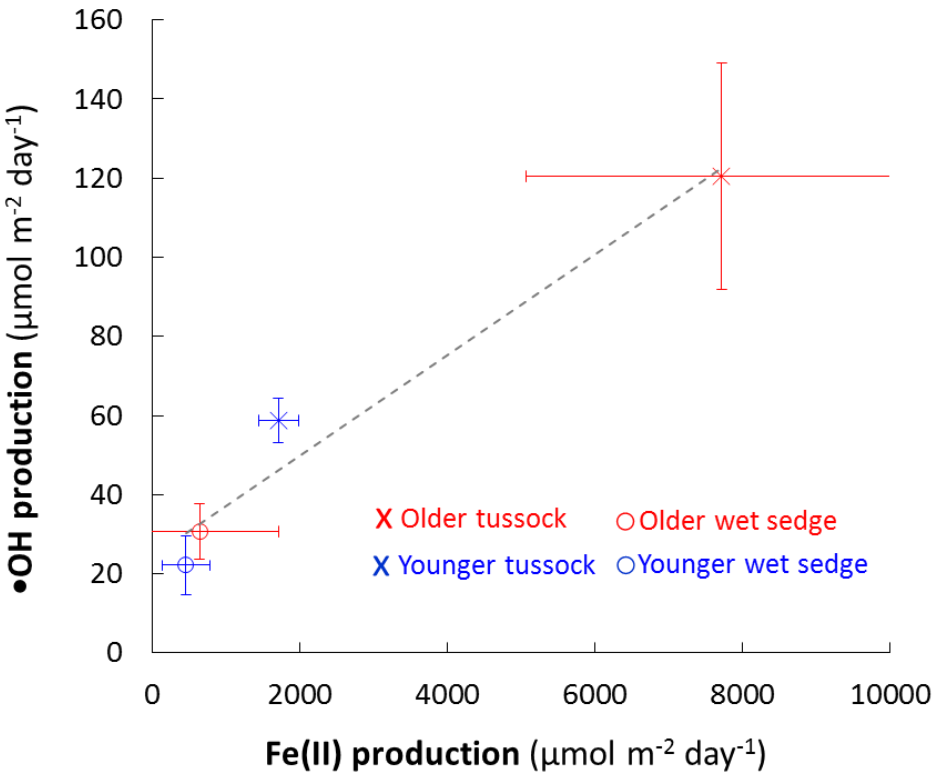

Figure 3.5. •OH production versus Fe(II) production. Values shown are averages ± SE of triplicate mesocosms from two acclimation periods for the first experiment and one acclimation period for the second experiment (N = 9; Figure 3.S1). There was a significant, positive relationship between •OH and Fe(II) production in soil waters when considering all landscape ages and vegetation types. The data were fit using least-squares regression, where •OH production (µmol m^{-2} day^{-1}) = 0.013 ± 0.002 × Fe(II) production (µmol m^{-2} day^{-1}) + 25 ± 7.2, $R^2 = 0.96$, $p < 0.01$.

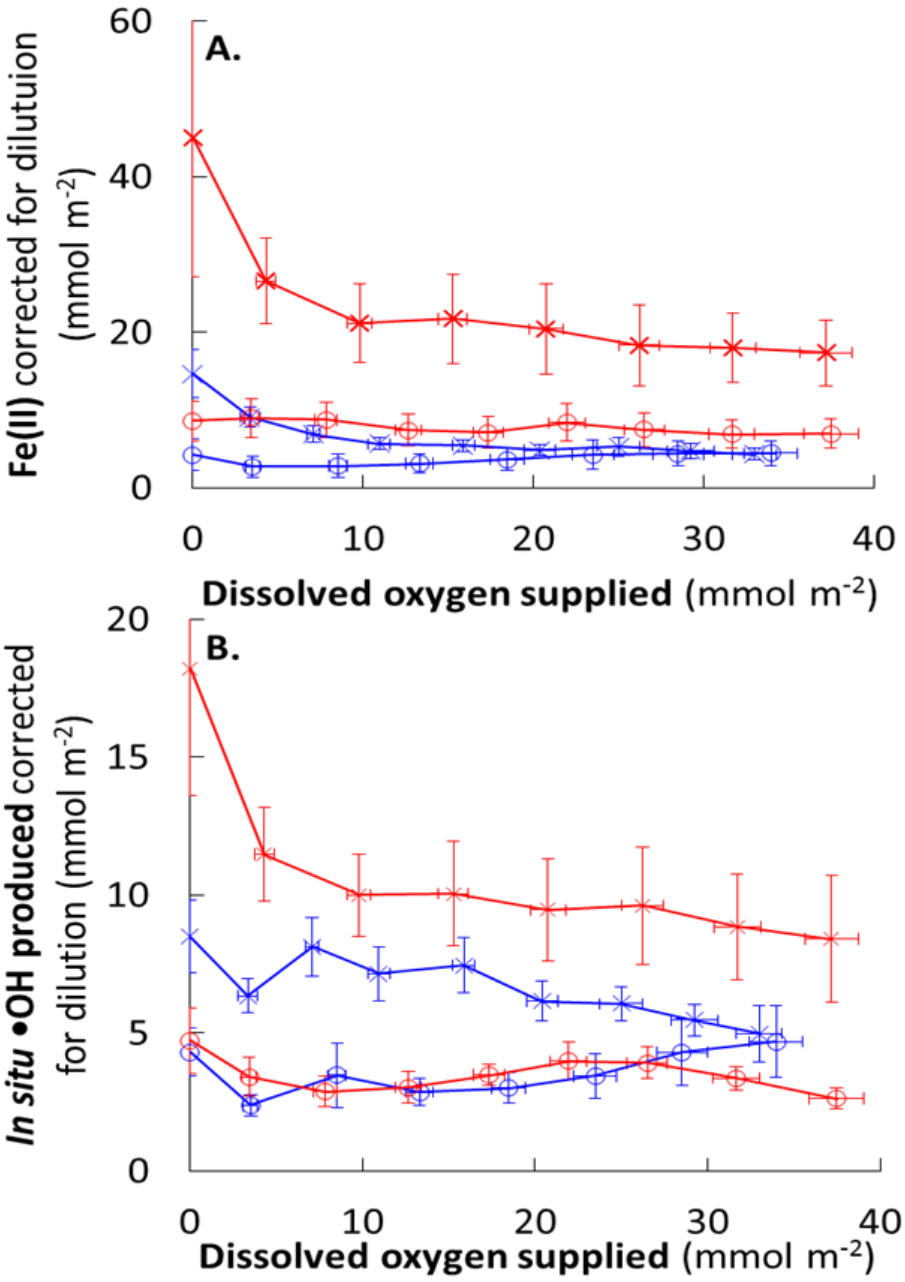

Figure 3.6. Fe(II) (**A**) and •OH export (**B**) versus dissolved oxygen supplied. Data plotted are averages ± SE from triplicate mesocosms from the two experiments for all acclimation (static waterlogged) and flushing (simulated precipitation) periods (N = 9; Figure S1). Export of Fe(II) and •OH were calculated from the concentration measured from the soil water after each flush multiplied by the total volume of water in each of the soil mesocosms plus the volume of DI water added with each flush (i.e., concentrations were corrected for dilution by the DI water used to flush the soils). The mole of each constituent exported in the soil water was then divided by the surface area of the soil mesocosm.

Variable	Older (Imnavait)			Younger (Toolik)		
Vegetation	Tussock		Wet sedge	Tussock		Wet sedge
Horizon	Organic	Mineral	Organic	Organic	Mineral	Organic
Depth (cm)	19 ± 8	9 ± 4	27 ± 1	15 ± 7	18 ± 8	30 ± 1
Bulk density (g dry soil cm^{-3})	0.3 ± 0.04^{A}		0.2 ± 0.01^{B}	0.4 ± 0.08^{A}		0.2 ± 0.01^{B}
Soil organic carbon (%)	40 ± 3^{A}	5 ± 0^{A}	$40 \pm 1^{B,C}$	30 ± 6^{A}	6 ± 1^{A}	$35 \pm 1^{B,D}$
Moisture (% water)	82 ± 3^{A}	30 ± 2^{A}	83.1 ± 1.2^{B}	70 ± 7^{B}	38 ± 5^{B}	82 ± 0^{B}
Porosity (% of total soil volume)	80 ± 3^{A}	30 ± 2^{A}	90 ± 6^{B}	70 ± 7^{B}	40 ± 5^{B}	80 ± 6^{B}

Letters A and B indicate significant differences ($p < 0.05$) between the same landscape ages but different vegetation types. Letters C and D indicate significant differences ($p < 0.05$) between different landscape ages and the same vegetation type.

Table 3.1. Properties of bulk soils of older and younger landscape age tussock and wet sedge mesocosms (average ± SE; N = 6) from the triplicate mesocosms of each landscape age and vegetation type measured after the second flushing period for the first experiment and after the only flushing period for the second experiment (Figure 3.S1). Bulk density is the average bulk density of the soil core including organic and mineral layers. Soil moisture was quantified as the volumetric water content of the soils.

Variable	Older (Imnavait)		Younger (Toolik)	
Vegetation	Tussock	Wet Sedge	Tussock	Wet Sedge
pH	5.0 ± 0.1^{A}	$5.4 \pm 0.1^{B,C}$	4.9 ± 0.1^{A}	$6.4 \pm 0.1^{B,D}$
Conductivity ($\mu S\ cm^{-1}$)	46 ± 3	34 ± 6^{C}	44 ± 6^{A}	$151 \pm 10^{B,D}$
Dissolved oxygen (μM)	47 ± 9	46 ± 4	49 ± 11	65 ± 12
Electron donating capacity $\mu mol\ (kg\ dry\ soil)^{-1}$	530 ± 210^{C}	370 ± 90	120 ± 40^{D}	190 ± 30
DOC $\mu g\ C\ (g\ dry\ soil)^{-1}$	120 ± 45	100 ± 16^{C}	48 ± 7.1	49 ± 6.8^{D}
Fe(tot) $\mu g\ (g\ dry\ soil)^{-1}$	22 ± 8.9	26 ± 6.2^{C}	5.1 ± 1.2	11 ± 3.1^{D}
Fe(II) $\mu g\ (g\ dry\ soil)^{-1}$	19 ± 7.5^{C}	14 ± 3.0^{C}	4.2 ± 1.2^{D}	6.6 ± 2.6^{D}

Letters A and B indicate significant differences (*t*-test, $p < 0.05$) between the same landscape ages but different vegetation types.
Letters C and D indicate significant differences (*t*-test, $p < 0.05$) between different landscape ages and the same vegetation type.

Table 3.2. Soil water chemistry for older and younger tussock and wet sedge soil waters (average ± SE, N = 9; Figure 3.S1).

Variable	Older (Imnavait)		Younger (Toolik)	
Vegetation	Tussock	Wet Sedge	Tussock	Wet Sedge
Slope ratio	0.75 ± 0.05^{C}	0.71 ± 0.01	0.86 ± 0.00^{D}	0.77 ± 0.12
Fluorescence Index	1.56 ± 0.02	1.62 ± 0.03^{C}	1.63 ± 0.04^{A}	$1.52 \pm 0.02^{B,D}$
C/A	0.52 ± 0.02	0.55 ± 0.02	0.54 ± 0.03	0.51 ± 0.02
T/A	0.23 ± 0.08^{C}	0.45 ± 0.20	0.63 ± 0.05^{D}	1.06 ± 0.73

Letters A and B indicate significant differences (*t*-test, $p < 0.05$) between the same landscape ages but different vegetation types. Letters C and D indicate significant differences (*t*-test, $p < 0.05$) between different landscape ages and the same vegetation type.

Table 3.3. Soil water DOC chemical characteristics based on absorbance and fluorescence (CDOM and FDOM, respectively) for older and younger tussock and wet sedge soils (average ± SE, N = 9, see Figure 3.S1).

Variable	Older (Imnavait)		Younger (Toolik)		Older (Imnavait)		Younger (Toolik)	
Vegetation	Tussock	Wet sedge	Tussock	Wet sedge	Tussock	Wet sedge	Tussock	Wet sedge
Acclimation period	*First*				*Second*			
Electron donating capacity production µmol (kg soil)$^{-1}$ (day)$^{-1}$	110 ± 57	60 ± 10^{C,E}	24 ± 10	23 ± 4^{D}	160 ± 120	-1 ± 9^{F}	20 ± 8	10 ± 7
DOC production µg C (g soil)$^{-1}$ (day)$^{-1}$	18 ± 11	10 ± 1.9^{C}	7.9 ± 1.4^{A}	3.6 ± 0.4^{B,D}	26 ± 16	3.3 ± 1.0	4.7 ± 0.9^{A}	0.9 ± 1.4^{B}
$Fe_{(tot)}$ production g Fe (g soil)$^{-1}$ (day)$^{-1}$	4.5 ± 2.4	3.4 ± 0.8^{C,E}	1.0 ± 0.3	1.3 ± 0.4^{D}	11 ± 8.2	-0.3 ± 0.4^{C,F}	0.9 ± 0.3	0.6 ± 0.3^{D}
Fe(II) production µg Fe (g soil)$^{-1}$ (day)$^{-1}$	3.9 ± 2.1^{C}	1.9 ± 0.4^{C,E}	0.9 ± 0.1^{D}	0.8 ± 0.3^{D,E}	10 ± 7.8	-0.5 ± 0.4^{C,F}	0.9 ± 0.3^{A}	0.1 ± 0.0^{B,D,F}
O_2 consumption µg O_2 (g soil)$^{-1}$ (day)$^{-1}$	3.0 ± 1.1	4.2 ± 0.3^{C,E}	2.5 ± 0.5	2.8 ± 0.4^{D}	2.1 ± 1.2	2 ± 0.9^{F}	1.9 ± 0.8	2.6 ± 0.9

Letters A and B indicate significant differences (*t*-test; $p < 0.05$) between the same landscape ages but different vegetation types. Letters C and D indicate significant differences (*t*-test, $p < 0.05$) between different landscape ages and the same vegetation type. Letters E and F indicate significant differences (*t*-test, $p < 0.05$) between the first and second flushing period for the same landscape age and vegetation type (N = 3; Figure S1).

Table 3.4. EDC, DOC and iron production and O_2 consumption in the soil waters of two landscape ages and vegetation types during the first acclimation period for both experiments (N = 6) and the second acclimation period for only the first experiment (N = 3; Figure 3.S1).

Daily production rate	Precipitation events	Waterlogged soils
•OH ($\mu mol\ m^{-2}\ day^{-1}$)	200 ± 70^{A}	60 ± 20^{B}
CO_2 ($\mu mol\ m^{-2}\ day^{-1}$)	60 ± 20^{A}	20 ± 6^{B}
Summer time production		
•OH ($mmol\ m^{-2}$)	10 ± 5	4 ± 1
CO_2 ($mmol\ m^{-2}$)	4 ± 1^{A}	1 ± 0.4^{B}

Letters A and B indicate significant differences (*t*-test, $p < 0.05$) between the •OH and CO_2 production during precipitation event and under waterlogged conditions.

Table 3.5. •OH production rates during precipitation events (flushing period) and under waterlogged, low O_2 conditions (acclimation period) (average ± SE, N = 9; Figure 3.S1). •OH production rates during precipitation events were calculated using the yield of •OH per O_2 supplied with the first flush times the amount of O_2 supplied during a 4 mm per day rain event (an average precipitation event in the Arctic). •OH production rates during waterlogged, low O_2 conditions were calculated as the •OH concentration in soil water collected after the acclimation period divided by the number of days of the acclimation period. The summer time production of •OH and CO_2 from the oxidation of DOC by •OH were calculated by multiplying the daily rates by the number of days during a summer (on average) that are rainy (67 days) or characterized by static, waterlogged conditions (73 days).

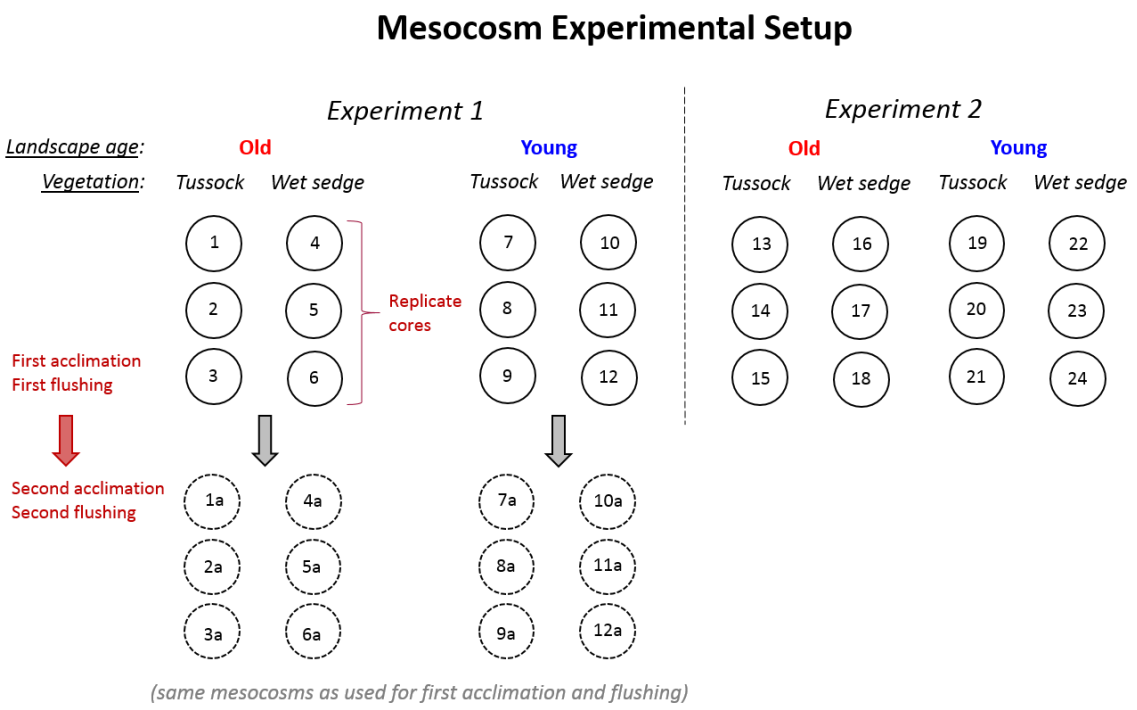

Figure 3.S1. Overview of the mesocosm experimental design. A total of 24 cores was collected (3 replicate cores x 2 landscape ages x 2 vegetation types x 2 experiments). For the first experiment, there were two acclimation periods and two flushing periods. This experiment was repeated on a second set of cores (#s 13-24), but with only one acclimation period and one flushing period (due to time constraints in the field). Averages and comparisons made in the main text used different combinations of cores. For example, in Table 1 the average values for soil properties of old-landscape tussocks (at the end of the experiments) were taken from cores 1a-3a and 13-15 (N = 6). In Table 2 the variable averages after the acclimation periods for old-landscape tussocks used cores 1-3, 1a-3a, and 13-15 (N = 9). Similarly, the averages for young-landscape wet sedge used cores 10-12, 10a-12a, and 22-24 (N = 9). In Table 4, the variable averages for old-landscape tussocks after the acclimation periods were taken from cores 1-3 and 13-15 (N=6), and averages for young-landscape wet sedge used cores 10-12 and 22-24 (N = 6). In Table 3.4, the comparison between the first and second flushing periods, for old-landscape tussocks, used cores 1-3 and 1a-3a (N = 3 comparisons of the same cores at different time points).

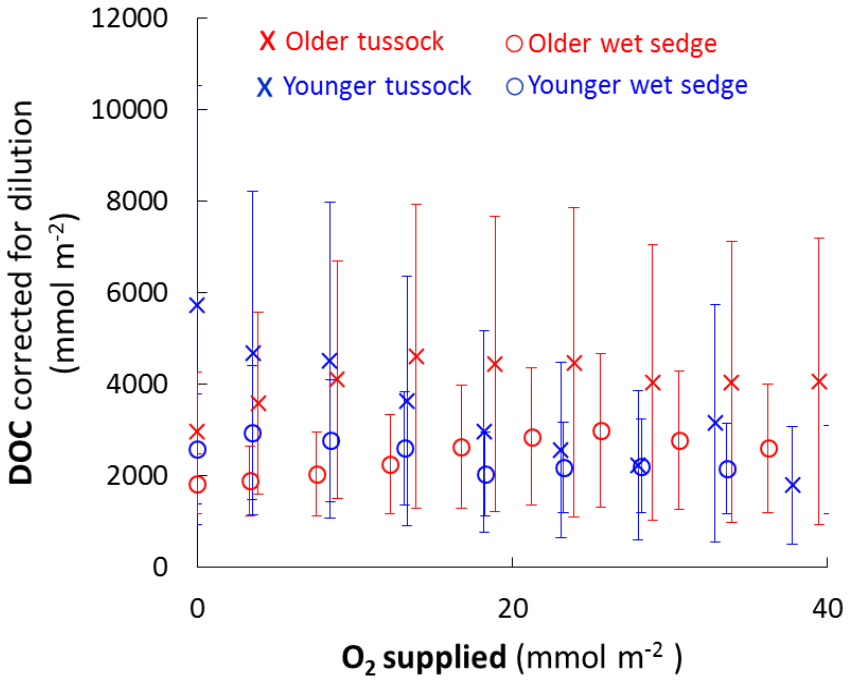

Figure 3.S2. DOC export in soil waters corrected for dilution by DI water added with flushing events, versus the O_2 supplied during flushing. DOC export was calculated from the DOC concentration measured from the soil water after each flush multiplied by the total volume of water in each of the soil mesocosms plus the volume of DI water added with each flush (i.e., concentrations were corrected for dilution by the DI water used to flush the soils). The mmol of DOC exported in the soil water was then divided by the surface area of the soil mesocosm. Values shown are average ± SE (N = 9; Figure 3.A1).

Variable	Older (Imnavait)		Younger (Toolik)		Older (Imnavait)		Younger (Toolik)	
Vegetation	Tussock	Wet sedge	Tussock	Wet sedge	Tussock	Wet sedge	Tussock	Wet sedge
Acclimation period	*First*				*Second*			
Total H_2O added (mm)	270 ± 30	300 ± 40	200 ± 10	290 ± 30	320 ± 30	300 ± 30	200 ± 10	320 ± 10

Table 3.S1. Summary of water additions and comparison to natural rainfall for each set of mesocosms. The summer rainfall amount for comparison was 271 mm, recorded between 1 June and 30 September 2017. Total H_2O added (mm) is the amount of water added during the first and second flushing periods.

3.8 Appendices

3.8.1 Calculation of •OH and CO_2 produced during a 4 mm precipitation event

We used the average precipitation events of 4 mm per day (Environmental Data Center, Toolik Field Station), the average amount of O_2 in the DI water (17 μmol O_2 per mm added), and the average •OH production yield to estimate the range in daily areal •OH production rates. Note that only one significant figure was used in the final results.

$$\boldsymbol{Average} = \frac{\mathbf{3 \pm 1\ \mu mol\ \bullet OH}}{\mathbf{\mu mol\ O_2\ m^2}}\ \boldsymbol{x}\ \frac{\mathbf{17\ \mu mol\ O_2}}{\mathbf{1\ mm\ rain}}\ \boldsymbol{x}\ \frac{\mathbf{4\ mm}}{\mathbf{1\ d}} = \frac{\mathbf{200 \pm 70\ \mu mol\ \bullet OH}}{\mathbf{m^2\ d}}$$

Assuming a yield of 1 mol CO_2 per 3 mol •OH [81], precipitation events of 4 mm per day could result in average 60 ± 20 (SE) μmol CO_2 m^{-2} d^{-1}. The amount of CO_2 that could be produced per unit area from •OH oxidation of DOC by precipitation events over the summer was calculated by assuming 67 rainy days per summer (number of days with > 0 mm precipitation, Environmental Data Center, Toolik Field Station):

$$\boldsymbol{Average} = \frac{\mathbf{200 \pm 70\ \mu mol\ \bullet OH}}{\mathbf{m^2\ day}}\ \boldsymbol{x}\ \frac{\mathbf{0.3\ \mu mol\ CO_2}}{\mathbf{1\ \mu mol\ \bullet OH}}\ \boldsymbol{x\ 67\ d} \times \frac{\mathbf{1\ mmol\ CO_2}}{\mathbf{1000\ \mu mol\ CO_2}} =$$

$$\frac{4\ \pm\ 1\ \text{mmol}\ CO_2}{m^2}$$

3.8.2 Calculation of •OH and CO_2 produced during static, waterlogged conditions

To estimate the average •OH and CO_2 production during static, waterlogged conditions (i.e., all conditions except precipitation events) we used the average •OH production and assumed that 73 of the 140 growing days during the summer (15 May—1 October) were dry (number of days with 0 mm precipitation, Environmental Data Center, Toolik Field Station). Note that only one significant figure was used in the final results.

$$\boldsymbol{Average} = \frac{\mathbf{60 \pm 20\ \mu mol\ \bullet OH}}{\mathbf{m^2\ d}}\ \times\ \mathbf{73\ d}\ \times \frac{\mathbf{1\ mmol\ \bullet OH}}{\mathbf{1000\ \mu mol\ \bullet OH}}\ =\ \frac{\mathbf{4 \pm 1\ mmol\ \bullet OH}}{\mathbf{m^2}}$$

Assuming a yield of 1 mol CO_2 per 3 mol •OH [81], waterlogged conditions during the summer would result in 1 ± 0.3 mmol CO_2 m^{-2}.

$$\boldsymbol{Average} = \frac{4 \pm 1 \text{ mmol } \bullet\text{OH}}{m^2 \text{ day}} \times \frac{0.3 \text{ mmol } CO_2}{1 \text{ mmol } \bullet\text{OH}} = \frac{1 \pm 0.3 \text{ mmol } CO_2}{m^2}$$

3.9 References

1. Page, S.E., Sander, M., Arnold, W.A., and McNeill, K. (2012) Hydroxyl radical formation upon oxidation of reduced humic acids by oxygen in the dark. *Environ. Sci. Technol.* 46, 1590–1597.

2. Page, S.E., Kling, G.W., Sander, M., Harrold, K.H., Logan, J.R., McNeill, K., and Cory, R.M. (2013) Dark formation of hydroxyl radical in arctic soil and surface waters. *Environ. Sci. Technol.* 47, 12860–12867.

3. Trusiak, A., Treibergs, L.A., Kling, G.W., and Cory, R.M. (2018) The role of iron and reactive oxygen species in the production of CO_2 in arctic soil waters. *Geochim. Cosmochim. Acta* 224, 80–95.

4. Goldstone, J.V., Pullin, M.J., Bertilsson, S., and Voelker, B.M. (2002) Reactions of hydroxyl radical with humic substances: Bleaching, mineralization and production of bioavailable carbon substrates. *Environ. Sci. Technol.* 36, 364–372.

5. Hall, S.J., and Silver, W.L. (2013) Iron oxidation stimulates organic matter decomposition in humid tropical forest soils. *Glob. Chang. Biol.* 19, 2804–2813.

6. Minella, M., De Laurentiis, E., Maurino, V., Minero, C., and Vione, D. (2015) Dark production of hydroxyl radicals by aeration of anoxic lake water. *Sci. Total Environ.* 527–528, 322–327.

7. Tong, M., Yuan, S., Ma, S., Jin, M., Liu, D., Cheng, D., and Wang, Y. (2016) Production of Abundant Hydroxyl Radicals from Oxygenation of Subsurface Sediments. *Environ. Sci. Technol.* 50, 214–221.

8. King, J.Y., Reeburgh, W.S., and Regli, S.K. (1998) Methane emission and transport by arctic sedges in Alaska: Results of a vegetation removal experiment. *J. Geophys. Res. Atmos*. 103, 29083–29092.

9. Updegraff, K., Bridgham, S.D., Pastor, J., Weishampel, P., and Harth, C. (2001) Response of CO_2 and CH4 emissions from peatlands to warming and water table manipulation. *Ecol. Appl.* 11, 311–326.

10. King, J.Y., Reeburgh, W.S., Thieler, K.K., Kling, G.W., Loya, W.M., Johnson, L.C., and Nadelhoffer, K.J. (2002) Pulse-labeling studies of carbon cycling in Arctic tundra ecosystems : The contribution of photosynthates to methane emission. *Glob. Biogeochem. Cycles* 16, 1–8.

11. Zona, D., Oechel, W.C., Kochendorfer, J., Paw, U.K.T., Salyuk, A.N., Olivas, P.C., and Lipson, D.A. (2009) Methane fluxes during the initiation of a large-scale water table manipulation experiment in the Alaskan Arctic tundra. *Glob. Biogeochem. Cycles* 23, 1–11.

12. Knorr, K.H., Glaser, B., and Blodau, C. (2008) Fluxes and ^{13}C isotopic composition of dissolved carbon and pathways of methanogenesis in a fen soil exposed to experimental drought. *Biogeosciences* 5, 1457–1473.

13. Knorr, K.H., Oosterwoud, and M.R., Blodau, C. (2008) Experimental drought alters rates of soil respiration and methanogenesis but not carbon exchange in soil of a temperate fen. *Soil Biol. Biochem.* 40, 1781–1791.

14. Lipson, D.A., Jha, M., Raab, T.K., and Oechel, W.C. (2010) Reduction of iron (III) and humic substances plays a major role in anaerobic respiration in an Arctic peat soil. *J. Geophys. Res. Biogeosci.* 115, 1–13.

15. Stumm, W., and Sulzberger, B. (1992) The cycling of iron in natural environments: Considerations based on laboratory studies of heterogeneous redox processes. *Geochim. Cosmochim. Acta* 56, 3233–3257.

16. Luther, G.W., Kostka, J.E., Church, T.M., Sulzberger, B., and Stumm, W. (1992) Seasonal iron cycling in the salt-marsh sedimentary environment: The importance of ligand complexes with Fe(II) and Fe(III) in the dissolution of Fe(III) minerals and pyrite, respectively. *Mar. Chem.* 40, 81–103.

17. Weber, K.A., Achenbach, L.A., and Coates, J.D. (2006) Microorganisms pumping iron: Anaerobic microbial iron oxidation and reduction. *Nat. Rev. Microbiol.* 4, 752–764.

18. Lipson, D.A., Zona, D., Raab, T.K., Bozzolo, F., Mauritz, M., Oechel, W.C. Water-table height and microtopography control biogeochemical cycling in an Arctic coastal tundra ecosystem. *Biogeosciences* 2012, *9*, 577–591.

19. Herndon, E.M., Yang, Z., Bargar, J., Janot, N., Regier, T.Z., Graham, D.E., and Liang, L. (2015) Geochemical drivers of organic matter decomposition in arctic tundra soils. *Biogeochemistry* 126, 397–414.

20. Roden, E.E., and Wetzel, R.G. (1996) Organic carbon oxidation and suppression of methane production by microbial Fe(III) oxide reduction in vegetated and unvegetated freshwater wetland sediments. *Limnol. Oceanogr.* 41, 1733–1748.

21. Lovley, D.R., and Phillips, E.J.P. (1988) Novel Mode of Microbial Energy Metabolism: Organic Carbon Oxidation Coupled to Dissimilatory Reduction of Iron or Manganese. *Appl. Environ. Microbiol.* 54, 1472–1480.

22. Roden, E.E., Kappler, A., Bauer, I., Jiang, J., Paul, A., and Stoesser, R. (2010) Extracellular electron transfer through microbial reduction of solid-phase humic substances. *Nat. Geosci.* 3, 417–421.

23. Lovley, D.R., and Phillips, E.J.P. (1986) Organic-Matter Mineralization with Reduction of Ferric Iron in Anaerobic Sediments. *Appl. Environ. Microbiol.* 51, 683–689.

24. Knorr, K.H. (2013) DOC-dynamics in a small headwater catchment as driven by redox fluctuations and hydrological flow paths—Are DOC exports mediated by iron reduction/oxidation cycles? *Biogeosciences* 10, 891–904.

25. Weyhenmeyer, G.A., Prairie, Y.T., and Tranvik, L.J. (2014) Browning of boreal freshwaters coupled to carbon-iron interactions along the aquatic continuum. *PLoS ONE* 9 e88104

26. Judd, K.E., and Kling, G.W. (2002) Production and export of dissolved C in arctic tundra mesocosms: The roles of vegetation and water flow. *Biogeochemistry* 60, 213–234.

27. Ward, C.P., and Cory, R.M. (2015) Chemical composition of dissolved organic matter draining permafrost soils. *Geochim. Cosmochim. Acta* 167, 63–79.

28. Hamilton, T.D. (2003) *Glacial Geology of the Toolik Lake and Upper Kuparuk River Regions*, Biological Papers of the University of Alaska, University of Alaska: Fairbanks, Alaska, pp. 1–24.

29. Kling, G.W., Kipphut, G.W., and Miller, M.C. (1991) Arctic lakes and streams as gas conduits to the atmosphere: Implications for tundra carbon budgets. *Science* 251, 298–301.

30. Johnson, L.C., Shaver, G.R., Giblin, A.E., Nadelhoffer, K.J., Rastetter, E.R., Laundre, J.A., and Murray, G.L. (1996) Effects of drainage and temperature on carbon balance of tussock tundra microcosms. *Oecologia* 108, 737–748.

31. Gebauer, R.L.E., Tenhunen, J.D.; and Reynolds, J.F. (1996) Soil aeration in relation to soil physical properties, nitrogen availability and root characteristics within an arctic watershed. *Plant Soil* 178, 37–48.

32. Hobbie, J.E., Kling, G.W. (2014) *A Changing Arctic: Ecological Consequences for Tundra, Streams and Lakes*, Oxford University Press: Oxford, UK, 31.

33. Robertson, G.P., Bledsoe, C.S., Coleman, D.C., and Sollins, P. (1999.) *Standard Soil Methods for Long-Term Ecological Research.* Oxford University Press: New York, NY.

34. Kling, G.W., Kipphut, G.W., Miller, M.M., and O'Brien, W.J. (2000) Integration of lakes and streams in a landscape perspective: The importance of material processing on spatial patterns and temporal coherence. *Freshwater Biol.* 43, 477–497.

35. Stookey, L.L. (1970) Ferrozine—A new spectrophotometric reagent for iron. *Anal. Chem.* 42, 779–781.

36. Cory, R.M., Miller, M.P., McKnight, D.M., Guerard, J.J., and Miller, P.L. (2010) Effect of instrument-specific response on the analysis of fulvic acid fluorescence spectra. *Limnol. Oceanogr. Methods* 8, 67–78.

37. Miller, W.L. (2010) Recent Advances in the Photochemistry of Natural Dissolved Organic

Matter. *Aquatic and Surface Photochemistry* 111–128.

38. Coble, P.G. (1996) Characterization of marine and terrestrial DOM in seawater using excitation-emission matrix spectroscopy. *Mar. Chem.* 51, 325–346.

39. McKnight, D.M., Boyer, E.W., Westerhoff, P.K., Doran, P.T. Kulbe, T., and Andersen, D.T. (2001) Spectrofluorometric characterization of dissolved organic matter for indication of precursor organic material and aromaticity. *Limnol. Oceanogr.* 46, 38–48.

40. Cory, R.M., Mcknight, D.M., Chin, Y., Miller, P., and Jaros, C.L. (2007) Chemical characteristics of fulvic acids from Arctic surface waters: Microbial contributions and photochemical transformations. *J. Geophys. Res. Biogeosci.* 112, 1–14.

41. Page, S.E., Arnold, W.A., and McNeill, K. (2010) Terephthalate as a probe for photochemically generated hydroxyl radical. *J. Environ. Monit. JEM* 12, 1658–1665.

42. Page, S.E., Logan, J.R., Cory, R.M., and McNeill, K. (2014) Evidence for dissolved organic matter as the primary source and sink of photochemically produced hydroxyl radical in arctic surface waters. *Environ. Sci. Process. Impacts* 16, 807–822.

43. Stumm, W., Lee, F.G. Oxygenation of ferrous iron. *Ind. Eng. Chem.* 1961, *53*, 143–146.

44. Aeschbacher, M., Graf, C., Scwarzenbach, R.P., Sander, M. (2012) Antioxidant properties of humic substances. *Environ. Sci. Technol*. 46, 4916–4925.

45. Klüpfel, L., Piepenbrock, A., Kappler, A., and Sander, M. (2014) Humic substances as fully regenerable electron acceptors in recurrently anoxic environments. *Nat. Geosci.* 7, 195–200.

46. Heitmann, T., Goldhammer, T., Beer, J., and Blodau, C. (2007) Electron transfer of dissolved organic matter and its potential significance for anaerobic respiration in a northern bog. *Glob. Chang. Biol.* 13, 1771–1785.

47. Voelker, B.M., and Sulzberger, B. (1996) Effects of fulvic acid on Fe(II) oxidation by hydrogen peroxide. *Environ. Sci. Technol.* 30, 1106–1114.

48. Yarie, J., Cleve, K. Van, Dyrness, C.T., Oliver, L., Levison, J., and Erickson, R.. (1993) Soil-solution chemistry in relation to forest succession on the Tanana River floodplain, interior Alaska. *Can. J. For. Res.* 23, 928–940.

49. Petrone, K.C., Jones, J.B., Hinzman, L.D., and Boone, R.D. (2006) Seasonal export of carbon, nitrogen and major solutes from Alaskan catchments with discontinuous permafrost. *J. Geophys. Res. Biogeosci.* 111, 1–13.

50. Vourlitis, G.L.; and Oechel, W.C. (1997) Landscape-Scale CO_2, H_2O Vapour and Energy Flux of Moist-Wet Coastal Tundra Ecosystems over Two Growing Seasons A. *Br.Ecol. Soc.* 85, 575–590.

51. Liljedahl, A.K., Hinzman, L.D., Harazono, Y., Zona, D., Tweedie, C.E., Hollister, R.D., Engstrom, R. (2011) Nonlinear controls on evapotranspiration in arctic coastal wetlands. *Biogeosciences* 8, 3375–3389.

52. Liljedahl, A.K., Boike, J., Daanen, R.P., Fedorov, A.N., Frost, G. V, Grosse, G., Hinzmanm, L.D., Iilma, Y., Jorgenson, J.C., Matveyeva, N. (2016) Pan-Arctic ice-wedge degradation in warming permafrost and its influence on tundra hydrology. *Nature Geoscience* 9, 312.

53. Armstrong, W. (1964) Oxygen Diffusion from the Roots of Some British Bog Plants. *Nature* 204, 801–802.

54. Soukup, A., Armstrong, W., Schreiber, L., Franke, R., and Votrubová, O. (2007) Apoplastic barriers to radial oxygen loss and solute penetration: A chemical and functional comparison of the exodermis of two wetland species, Phragmites australis and Glyceria maxima. *New Phytol.* 173, 264–278.

55. Jackson, R.B., Mooney, H.A., and Schulze, E.-D. (1997) A global budget for fine root biomass, surface area and nutrient contents. *Proc. Natl. Acad. Sci.* 94, 7362–7366.

56. Stuart, L., and Miller, P.C. (1981) Soil Oxygen Flux Measured Polarographically in an Alaskan Tussock Tundra A. *Proc. Natl. Acad. Sci.* 5, 139–144.

57. Huemmrich, K.F., Kinoshita, G., Gamon, J.A., Houston, S., Kwon, H., and Oechel, W.C. (2010) Tundra carbon balance under varying temperature and moisture regimes. *J. Geophys. Res.* 115, G00I02.

58. Chivers, M.R., Turetsky, M.R., Waddington, J.M., Harden, J.W., and McGuire, A.D. (2009) Effects of experimental water table and temperature manipulations on ecosystem CO2 fluxes in an Alaskan rich fen. *Ecosystems* 12, 1329–1342.

59. Gorski, C.A., Aeschbacher, M., Soltermann, D., Voegelin, A., Baeyens, B., Fernandes, M.M., and Sander, M. (2012) Redox Properties of Structural Fe in Clay Minerals. 1. Electrochemical Quantification of Electron-Donating and -Accepting Capacities of Smectites. *Environ. Sci. Technol*. 9360–9368.

60. Sander, M., Hofstetter, T.B., and Gorski, C.A. (2015) Electrochemical analyses of redox-active iron minerals: A review of nonmediated and mediated approaches. *Environ. Sci. Technol.* 49, 5862–5878.

61. Lau, M.P., Sander, M., Gelbrecht, J., and Hupfer, M. (2015) Solid phases as important electron acceptors in freshwater organic sediments. *Biogeochemistry* 123, 49–61.

62. Keller, K., Blum, J.D., and Kling, G.W. (2007) Geochemistry of Soils and Streams on Surfaces of Varying Ages in Arctic Alaska. *Arct. Antarct. Alp. Res.* 39, 84–98.

63. Chang, C.Y., Hsieh, Y.H., Cheng, K.Y., Hsieh, L.L., Cheng, T.C., and Yao, K.S. (2008) Effect of pH on Fenton process using estimation of hydroxyl radical with salicylic acid as trapping reagent. *Water Sci. Technol.* 58, 873–879.

64. Ping, C.L., Bockheim, J.G., Kimble, J.M., Michaelson, G.J., and Walker, D.A. (1998) Characteristics of cryogenic soils along a latitudinal transect in Arctic Alaska. *J. Geophys. Res.* 103, 28917–28928.

65. Stieglitz, M., Shaman, J., McNamara, J., Engel, V., Shanley, J., and Kling, G.W. (2003) An approach to understanding hydrologic connectivity on the hillslope and the implications for nutrient transport. *Glob. Biogeochem. Cycles* 17.

66. Voytek, E.B., Rushlow, C.R., Godsey, S.E., Singha, K. (2016) Identifying hydrologic flowpaths on arctic hillslopes using electrical resistivity and self-potential. *Geophysics* 81, WA225–WA232.

67. Neilson, B.T., Cardenas, M.B., O'Connor, M.T., Rasmussen, M.T., King, T.V., and Kling, G.W. (2018) Groundwater flow and exchange across the land surface explain carbon export patterns in continuous permafrost watersheds. *Geophys. Res. Lett.* 45, 7596–7605.

68. Weyhenmeyer, G.A., Müller, R.A., Norman, M., and Tranvik, L.J. (2016) Sensitivity of freshwaters to browning in response to future climate change. *Clim. Chang.* 134, 225–239.

69. Sarkkola, S., Nieminen, M., Koivusalo, H., Laurén, A., Kortelainen, P., Mattsson, T., and Finér, L. (2013) Science of the Total Environment Iron concentrations are increasing in surface waters from forested headwater catchments in eastern Finland. *Sci. Total Environ.* 463–464, 683–689.

70. Ekström, S.M., Regnell, O., Reader, H.E., Nilsson, P.A., Löfgren, S., and Kritzberg, E.S. (2016) Increasing concentrations of iron in surface waters as a consequence of reducing conditions in the catchment area. *J. Geophys. Res. Biogeosci*. 121, 479–493.

71. Koenigk, T., Brodeau, L., Graversen, R.G., Karlsson, J., Svensson, G., Tjernstrom, M., and Wille, U. (2013) Arctic climate change in 21st century CMIP5 simulations with EC-Earth. *Clin. Dyn.* 40, 2719–2743.

72. Nilsson, J., Sørensen, L.S., Barletta, V.R., and Forsberg, R. (2015) Mass changes in Arctic ice caps and glaciers: Implications of regionalizing elevation changes. *Cryosphere* 9, 139–150.

73. Liljedahl, A.K., Hinzman, L.D., Kane, D.L., Oechel, W.C., Tweedie, C.E., and Zona, D. (2017) Tundra water budget and implications of precipitation underestimation. *Water Resour. Res.* 53, 6472–6486.

74. Barber, V.A., Juday, G.P., Finney, B.P. (2000) Reduced growth of Alaskan white spruce in the twentieth century from temperature-induced drought stress. *Lett. Nat.* 405, 668.

75. Al, D.E.T., Inje, T.V., Lekseev, G.A., and Aslowski, W.M. (2000) The Arctic Ocean Response to the North Atlantic Oscillation. *Am. Meteorol. Soc.* 95, 2671–2696.

76. Olivas, P.C., Oberbauer, S.F., Tweedie, C.E., Oechel, W.C., and Kuchy, A. (2010) Responses of CO_2 flux components of Alaskan Coastal Plain tundra to shifts in water table. *J. Geophys. Res.* 115, 1–13.

77. Hultman, J., Waldrop, M.P., Mackelprang, R., David, M.M., Mcfarland, J., Blazewicz, S.J., and Jansson, J.K. (2015) Multi-omics of permafrost, active layer and thermokarst bog soil microbiomes. *Nature* 521, 208.

78. Cole, J.J., Caraco, N.F., Kling, G.W., Kratz, T.K. (1994) Carbon Dioxide Supersaturation in the Surface Waters of Lakes. *Science* 265, 1568–1570.

79. Raymond, P.A., Hartmann, J., Lauerwald, R., Sobek, S., McDonald, C., Hoover, M., Butman, D., Striegl, R., Mayorga, E., Humborg, C., et al. (2013) Global carbon dioxide emissions from inland waters. *Nature* 503, 355.

80. Kritzberg, E.S., Ekstrom, S.M. Increasing iron concentrations in surface waters—a factor behind brownification? (2012) *Biogeosciences* 9, 1465–1478.

81. Goldstone, J.V., Pullin, M.J., Bertilsson, S., and Voelker, B.M. (2002) Reactions of hydroxyl radical with humic substances: Bleaching, mineralization, and production of bioavailable carbon substrates. *Environ. Sci. Technol.* 36, 364–372.

Chapter 4
Hydroxyl Radical (•OH) Oxidizes Dissolved Organic Matter (DOM) to Carbon Dioxide (CO_2)

4.1 Abstract

Hydroxyl radical (•OH), produced from the abiotic oxidation of ferrous iron, is a highly reactive oxidant of dissolved organic matter (DOM) in the environment. •OH production and subsequent oxidation of DOM by •OH to carbon dioxide (CO_2) was measured in soil waters in the Alaskan Arctic, and the production yield of CO_2 per •OH ranged from 2 to 30 mol CO_2 per mol •OH across arctic soil waters. Controls on the production yield of CO_2 per •OH across soil waters were determined in controlled laboratory experiments where CO_2 production from oxidation of DOM by •OH was measured as a function of pH (5, 7) and DOM chemical composition. While pH did not impact the production yield of CO_2 to •OH, DOM composition may explain some variability in the production yield of CO_2 per •OH. DOM with high antioxidant content had a lower production yield of CO_2 per •OH than did DOM with low antioxidant content. Given that antioxidants within DOM can react with •OH to produce low energy radicals instead of CO_2, these findings suggest that the presence of antioxidants within DOM lowers the production yield of CO_2 per •OH. Furthermore, our findings show that the antioxidant content of DOM accounts for the variability in the production yield of CO_2 per •OH across arctic soil waters. Thus, the antioxidant content of DOM should be considered when estimating the amount of CO_2 produced from the DOM oxidation by •OH across the landscape.

4.2 Introduction

Hydroxyl radical (•OH) is a highly reactive and unselective oxidant of dissolved organic matter (DOM) [1,2]. •OH oxidizes DOM by adding aromatic compounds, hydrogen atom abstraction, and electron transfer reactions [1,3-5]. Direct addition of •OH results in hydroxylation and cleavage of side chain groups, resulting in low molecular weight acid production after the oxidation of DOM with •OH [1,3]. •OH oxidation can also initiate electron transfer reactions leading to the production of organic radical cation species, which can then oxidize DOM to partially oxidized or degraded aromatic or aliphatic compounds, low molecular weight acids, or carbon dioxide (CO_2) [1,3,6].

Prior work has shown that CO_2 production from the oxidation of DOM by •OH in arctic soil waters is comparable to the microbial respiration of DOM in arctic surface waters [2,7,8]. However, estimates of the importance of the CO_2 production from the oxidation of DOM by •OH are based on the production yield of CO_2 per •OH from a controlled laboratory study where •OH was produced electrochemically in simple solutions of fulvic and humic acids [1]. The production yield of CO_2 per •OH in this controlled laboratory study varied from less than 0.1 up to 0.5 mol CO_2 per 1 mol •OH [1]. The production yield of CO_2 per •OH in the controlled laboratory study was within the theoretical production yield of 0.3 mol CO_2 per 1 mol •OH [1]. In arctic soil waters, the production yield of CO_2 per •OH was higher than in the laboratory study and ranged from 2 to 30 mol CO_2 per 1 mol •OH [2]. This higher yield measured in the soil waters suggests that the estimate of CO_2 production from this abiotic process might be underestimated if the production yield of CO_2 per •OH is higher than the yield applied from the controlled laboratory study [1]. Currently, controls on the variability in the production yield of

CO_2 per •OH remain too poorly understood to quantify CO_2 production from oxidation of DOM by •OH across different environments.

The production yield of CO_2 per •OH is expected to decrease with increasing pH (pH 4 - 9) due to changes in the antioxidant capacity of DOM [9]. The electron donating capacity (EDC) of DOM increases with increasing pH, resulting in higher antioxidant capacity of DOM at higher than at a lower pH [9]. Antioxidants within DOM react with •OH to produce low energy radicals instead of CO_2, resulting in a low production yield of CO_2 per •OH [9]. Thus, at pH 7 •OH is more likely to be quenched by antioxidants than at pH 5, resulting in the lower production yield of CO_2 per •OH at a high than at a low pH [9]. Although CO_2 production from oxidation of DOM by •OH was shown to be independent of pH in a controlled laboratory study (pH 4 and 10) [1], no study has compared the production yield of CO_2 per •OH over the pH range of natural waters (pH ~ 5-7).

In addition to pH, DOM chemical composition may affect the production yield of CO_2 per •OH. For example, •OH is more likely to partially oxidize aromatic carbon (C) within DOM to produce low molecular weight compounds than to completely oxidize aromatic C within DOM to CO_2 [6]. Thus, soil waters with a higher aromatic C content of DOM are expected to have a lower production yield of CO_2 per •OH when compared to soil waters with a low aromatic C content of DOM [9]. In addition, phenolic C, a subset of the aromatic fraction of DOM, may act as an antioxidant by quenching reactive oxygen species, including •OH [9]. Thus, phenolic C may decrease the production yield of CO_2 per •OH because it reacts with •OH to produce low energy radicals instead of CO_2 [9]. Although a higher aromatic or phenolic C content within the aromatic fraction of DOM may impact the production yield of CO_2 per •OH, no study has measured the production yield of CO_2 per •OH as a function of DOM composition.

The objectives of this study were to determine the controls of (1) pH and (2) DOM composition on the production yield of CO_2 per •OH. We studied •OH and CO_2 production in fulvic acid solutions amended with Fe(II) at two different pH values and with four different fulvic acid isolates. We compared the measurements of •OH and CO_2 production in the laboratory solutions of fulvic acids amended with Fe(II) with previously published data on the •OH and CO_2 production in arctic soil waters [2] to determine whether pH or DOM composition could explain the variability in the production yield of CO_2 per •OH measured in soil waters.

4.3 Materials and Methods

4.3.1 Preparing fulvic acid isolates

Four terrestrially-derived fulvic acids (FA) were used in this study: (1) Suwannee River FA, (2) Imnavait Creek FA (called Imnavait River in Cory et al. [10]), (3) Toolik Lake FA, and (4) Tussock Watershed Lower Creek FA (called Toolik Watershed Lower Creek in Cory et al. [10]). Suwannee River FA was obtained from the International Humic Substances Society and the other three FAs were collected from the Alaskan Arctic as previously described in Cory et al. [10]. FA stock solutions were prepared at 2.8 ± 0.01 mM C by dissolving freeze-dried, solid FAs in air-equilibrated MilliQ water (Millipore Simplicity ultraviolet system) and stirring for 24 hours at room temperature in the dark [2]. The FA stock solutions were stored in the dark at 4 ºC for less than one month prior to use in experiments described below.

4.3.2 Experimental design

The FA stock solutions were amended with reduced ferrous iron (Fe(II), referred to as FA+Fe(II) solutions, and were pH adjusted in two different ways to achieve study objectives on the roles of (1) pH and (2) DOM composition in the production yield of CO_2 per •OH. First, to

study the effect of pH on the production yield of CO_2 per •OH, an air-equilibrated Suwannee River FA stock solution was amended with ~50 µM of ferrous ammonium sulfate (FAS, $(NH_4)_2Fe(SO_4)_2$, Puriss p.a., Sigma-Aldrich) and then adjusted to a pH of 5 or 7 with sodium hydroxide (Puriss p.a., Fisher Scientific; Figure 4.1). Second, to study the effect of DOM composition on the production yield of CO_2 per •OH, air-equilibrated FA solutions (Suwannee River FA, Imnavait Creek FA, Toolik Lake FA, and Tussock Watershed Lower Creek FA) were amended with a range of ferrous chloride concentrations ($FeCl_2$, Puriss p.a., Sigma-Aldrich) including 50, 100, 250, 500 µM of Fe(II)) and adjusted to a pH of 5 with sodium hydroxide (Figure 4.1). After pH adjustment, FA+Fe(II) solutions were stirred in the dark for 12 hours to equilibrate the FA with Fe(II) (Figure 4.1). After 12 hours, total and reduced iron were measured in triplicate in each FA+Fe(II) solution (Figure 4.1, Tables 4.1 and 4.2; details *below*).

Immediately after iron measurements, FA+Fe(II) solutions were used to measure •OH and CO_2 production from Fe(II) oxidation by H_2O_2 (Figure 4.1). Suwannee River FA+FAS solutions (pH 5 and 7) were amended with a range of H_2O_2 concentrations (final concentrations of 5, 10, 20, 50, and 100 µM), whereas FA+$FeCl_2$ solutions were amended with 20 µM H_2O_2 (Figure 4.1). •OH and CO_2 production were quantified after 24 hours with added H_2O_2 (treatment) relative to controls amended the same volume of MilliQ water (Figure 4.1; details *below*). The production yield of CO_2 per •OH was quantified as the molar ratio of CO_2 production (µM) to •OH production (µM). All values are reported as the mean ± standard error (SE) from triplicate measurements of each analyte (e.g., Fe(II), •OH, CO_2), unless otherwise stated.

4.3.3 DOM composition

All FA stock solutions were analyzed for chromophoric and fluorescent dissolved organic matter (CDOM and FDOM, respectively), organic carbon composition, and electron donating capacity (EDC). CDOM and FDOM were analyzed in a 1-cm pathlength quartz cuvette using a spectrofluorometer (Aqualog, Horiba) as previously described [e.g., 11,12]. The FAs were diluted 5- to 10- fold with MilliQ water to achieve an absorbance unit (A) at 254 nm less than 0.6 prior to the analysis [13]. The fluorescence index (FI) was calculated as the ratio of emission intensity at 470 nm to emission intensity at 520 nm at an excitation wavelength of 370 nm [10,14]. All FAs used in this study have been previously characterized for their organic carbon composition using ^{13}C nuclear magnetic resonance (NMR), including aromatic C content [10,15,16]. In FAs, the EDC of DOM was measured colorimetrically using 2, 2-azino-bis (3-ethylbenzothiazoline-6-sulfonic acid; ABTS+•) at 734 nm in 1-cm pathlength methacrylate cuvettes as previously described [7]. In this study, EDC was a measure of electrons donated only by the DOM because it was the only reduced species in the FA stock solutions (i.e., prior to amending with Fe(II)).

4.3.4 Dissolved iron

Total and reduced iron concentrations were analyzed in triplicate in each FA+Fe(II) solution by the ferrozine method [17] immediately after a 12-hour air equilibration (Figure 4.1). FA+Fe(II) solutions amended with Fe(II) > 50 µM were diluted 2- to 5- fold in air-equilibrated MilliQ water prior to analysis. Absorbance for iron measurements was measured on a Horiba Aqualog spectrofluorometer in 1-cm pathlength methacrylate cuvettes [2].

4.3.5 •OH production

•OH production from Fe(II) oxidation was quantified using terephthalate (TPA) [18] as a probe for •OH as previously described [2,7]. Briefly, •OH production was quantified upon addition of 1 mL of H_2O_2 solution (treatment) or 1 mL of MilliQ water (control) to 0.7 mL of FA+Fe(II) solution and 10.3 mL of a TPA solution (Figure 4.1) [2]. TPA was allowed to react with the •OH produced in the FA+Fe(II) solution for 24 hours at room temperature in the dark prior to analysis of 2-hydroxyterephthalic acid (hTPA), the product of the TPA reaction with •OH [18]. •OH concentrations in the treatment (H_2O_2 added) and control (MilliQ water) FA+Fe(II) solutions were determined using standard additions of 0, 25, and 50 nM hTPA to account for matrix effects [18]. hTPA was quantified on an Acquity Ultra High Performance H-Class LC (uPLC; Waters, Inc.) with UV-visible and fluorescence detection on an Acquity uPLC BEH C_{18} column (2.1 x 50 mm; 1.7 µm sieve size). The yield for hTPA formation from •OH reaction with TPA was assumed to be 35% [18]. •OH production was calculated as the difference in •OH concentrations between the treatment and control FA+Fe(II) solutions. •OH production was reported as the concentration of •OH produced in each vial divided by the Fe(II) concentration in the •OH measurement vial (see *Section 4.3.7.*).

4.3.6 CO_2 production

CO_2 production during DOC oxidation by •OH was quantified by adding 1 mL of H_2O_2 (treatment) or 1 mL of MilliQ water (control) to 11 mL of FA+Fe(II) solution (Figure 4.1). After a 24-hour reaction time at room temperature in the dark, the treatment (added H_2O_2) and control (no added H_2O_2) FA+Fe(II) solutions were analyzed for dissolved inorganic carbon (DIC) concentrations using a DIC analyzer (Apollo, Inc.). CO_2 production was calculated as the difference in DIC concentrations between the treatment and control FA+Fe(II) solutions (Figure

4.1). CO_2 production was reported as the concentration of CO_2 produced divided by the Fe(II) concentration in the CO_2 measurement vial (see *Section 4.3.7.*).

4.3.7 Methodological constraints in comparing •OH and CO_2 production

The concentration of Fe(II) differed between the experimental vials used to quantify •OH and CO_2 production because of the methodological constraints between •OH and CO_2 analyses. In the vials used to quantify •OH production, the H_2O_2 (treatment) or MilliQ water (control) were added to an FA+Fe(II) solution that was diluted ~17-fold with the TPA solution to ensure that TPA was present in excess to trap all the •OH produced (Figure 4.1) [2,18]. Thus, Fe(II) concentrations in the vials used to quantify •OH concentrations were ~17-fold lower than Fe(II) concentrations in the vials used to quantify CO_2 production. To account for dilution in the vial for •OH production, •OH was multiplied by the dilution factor of ~17-fold.

To compare only the effect of pH or DOM composition and not the effect of Fe(II) concentration on the production yield of CO_2 per •OH, •OH and CO_2 production were divided by the Fe(II) concentration in their corresponding vials. There was a range of Fe(II) concentrations that FA were amended with and the Fe(II) concentrations did vary a little between different experiments (Table 4.S1, 4.S2). To eliminate the Fe(II) concentration as the influence the production yield of CO_2 per •OH (Figure 4.3), the •OH and CO_2 production were divided by Fe(II) present in the vial initially when the experiments were set up."

4.3.8 The EDC of DOM in soil waters

Previously reported production yields of CO_2 per •OH for arctic soil waters with low Fe(II) concentrations (< 5 μM) were analyzed to evaluate the relationship between the production yield of CO_2 per •OH and the EDC of DOM [2]. The ABTS+• method measures the EDC of all reduced species present in the solution, which is predominantly DOM and Fe(II) in

arctic soil waters [2]. Prior work concluded that in arctic soil waters with high DOM concentrations (1,000 – 10,000 μM-C) and Fe(II) < 5 μM, the EDC was primarily measuring electrons donated by DOM [2]. When Fe(II) < 5 μM, Fe(II) could not account for the electrons donated in these soil waters.

4.4 Results

4.4.1 Chemical composition of the fulvic acids

The fulvic acids (FAs) in this study had similar fluorescence index values (a proxy for the aromatic C content of DOM). However, the FAs differed in their aromatic C content previously quantified by ^{13}C-NMR [10] and their electron donating capacity (EDC) (Table 4.1). Suwannee River FA and Imnavait Creek FA had significantly higher aromatic C content and EDC than Toolik Lake FA and Tussock Watershed Lower Creek FA ($p < 0.05$; Table 4.1) [10]. The EDC of DOM was generally higher in the FAs with high aromatic C content, although the relationship was only significant at the $p = 0.07$ level for this dataset of FAs (n = 4; Figure 4.2).

4.4.2 CO_2 was produced under conditions conducive to •OH production

CO_2 production from all FA+Fe(II) solutions used to study the effect of pH and DOM composition (Figure 4.1, Table S4.1., 4.S2) was positively, linearly correlated with •OH production (Figure 4.3). There were no significant differences between the slopes of the relationship between CO_2 and •OH production for each FA+Fe(II) solution in this study based on the least-square regression fit (Figure 4.3; $p > 0.05$). In all FA+Fe(II) solutions, the production yield of CO_2 per •OH ranged from 0.3 to 5.8 μM of CO_2 per 1.0 μM of •OH (n = 31; Table 4.3). The difference in Fe(II) salts used for SRFA+Fe(II) and FA+Fe(II) experiments could have had

an impact on the •OH and CO_2 production, and thus, the production yield of CO_2 per •OH, however it is impossible to determine the influence of the two different salts (see *Methods*).

4.4.3 Effects of pH and DOM composition on the production yield of CO_2 per •OH

The production yield of CO_2 per •OH did not vary with the pH but varied with the chemical composition of DOM in FA+Fe(II) solutions (Figure 4.4, Table 4.2). For Suwanee River FA samples there were no significant differences in the production yield of CO_2 per •OH between pH 5 and pH 7 ($p > 0.05$; Table 4.2). The production yield of CO_2 per •OH decreased with the increasing EDC of DOM in FA+Fe(II) solutions. However, the relationship between the production yield of CO_2 per •OH and the EDC of DOM was marginally significant ($p = 0.07$; Figure 4.5).

4.4.4 Comparison of the production yield of CO_2 per •OH between laboratory solutions and soil waters

The average production yield of CO_2 per •OH in soil waters (Table 4.3) [2] was higher than the average production yield in FA+Fe(II) solutions ($p < 0.05$; Figure 4.3, Table 4.3), but there was a similar range of production yields between the two groups. Similar to FA+Fe(II) solutions, pH had no effect on the production yield of CO_2 per •OH in soil waters (Figure 4.4) [2]. The production yield of CO_2 per •OH decreased with the estimated EDC of DOM in both soil waters and FA+ Fe(II) solutions ($p < 0.05$; Figure 4.5).

4.5 Discussion

4.5.1 CO_2 produced from oxidation of DOM by •OH

Oxidation of DOM by •OH to CO_2 was evident from the increasing CO_2 production with increasing •OH production in FA+Fe(II) solutions (Figure 4.2), consistent with the previous

work [1,2]. This positive, linear relationship between •OH and CO_2 was expected for two reasons. First, it was expected that CO_2 would be produced in proportion to •OH if DOM oxidation by •OH was the only process producing CO_2 during the experiment. There was no other known process that could produce CO_2 in FA+ Fe(II) solutions. For example, microbial respiration of DOM of CO_2 was unlikely to take place in FA+Fe(II) solutions prepared in the laboratory from fulvic acid isolates that had no microbes present. FA+Fe(II) solutions were kept in the dark to prevent photochemical oxidation of DOM to CO_2. Second, DOM was likely the main sink to react with •OH in the FA+Fe(II) solutions given the high DOM concentrations [2,7,19]. Chloride, ammonium, and sulfate concentrations in these FA+Fe(II) from the added Fe(II) salts were 10- to 100- times lower than the DOM concentrations (Table 4.S1, 4.S2), indicating their concentrations were too low to quench or react with •OH [1,20,21,22]. Even in some arctic surface waters with higher carbonate and lower DOM compared to this study, DOM was the main sink for •OH [19]. Therefore, in the laboratory FA+Fe(II) solutions, DOM was likely the main sink for •OH resulting in the production of CO_2 (Figure 4.2).

4.5.2 CO_2 production independent of pH but dependent on antioxidants in DOM

The pH did not impact the production yield of CO_2 per •OH in FA+Fe(II) solutions across the pH range of arctic soils waters (pH from 5 to 7; Figure 4.4). This finding suggests that the variability in the production yield of CO_2 per •OH in soil waters that span pH 5 to pH 7 cannot be explained by the differences in pH. This result is consistent with previous findings that suggested the production yield of CO_2 per •OH was independent of pH [2]. In contrast to pH, DOM composition may have affected the production yield of CO_2 per •OH in FA+Fe(II) solutions and in soil waters.

The significant, linear decrease in the production yield of CO_2 per •OH with the increasing EDC of DOM suggests that antioxidants in DOM might be quenching •OH in FA+Fe(II) solutions and in soil waters (Figure 4.5) [9]. The reaction of •OH with antioxidants in DOM is thought to result in the production of lower energy DOM radicals instead of CO_2 [9]. Production of lower energy radicals instead of CO_2 would lower the production yield of CO_2 per •OH (Figure 4.4) [9]. Therefore, some of the large variability in the production yield of CO_2 per •OH may be explained by differences in the antioxidant content of the DOM in FA+Fe(II) solutions and in soil waters.

4.5.3 Explanations for the greater range in the production yield of CO_2 per •OH in soil waters than in laboratory solutions

The greater range in the production yield in CO_2 per •OH in soil waters than in FA+ Fe(II) solutions prepared in the laboratory (Table 4.3, Figure 4.4) might be due to the underestimation of •OH production or overestimation of CO_2 production in soil waters. First, soil waters are heterogeneous solutions with more complex chemistry [2,7] than the laboratory solutions made with only fulvic acids isolates and iron salts (see *Methods*). Those differences in the water chemistry of soil waters and laboratory solutions might lower the yield of hTPA produced from reaction of •OH with the TPA probe in soil waters compared with the laboratory solutions [2]. While it is not possible to determine the controls on the yield of hTPA from •OH reaction with TPA, the yield of 0.35 mol hTPA per 1 mol •OH applied in this study is the upper limit [20]. The yield of hTPA may be four times lower, resulting in four times greater •OH production than reported [2,23]. If the yield of hTPA is lower in soil waters than in FA+Fe(II) solutions, then •OH is underestimated . Underestimation of •OH productions results in overestimation of the production yield of CO_2 per •OH in soil waters.

Second, the production yield of CO_2 per •OH could be overestimated if there are processes other than oxidation of DOM by •OH to produce CO_2, such as microbial respiration in soil waters. There was likely no CO_2 from respiration in the FA+Fe(II) solutions given that these were prepared with freeze-dried fulvic acids in laboratory grade MilliQ water (treated by UV), and amended with iron salts. However, in soil waters, microbes could have passed through the 0.2 µm filters. The upper limit on CO_2 produced from microbial respiration based on previous experiments in arctic waters done with microbes added at 20% by volume and accounting for higher DOM concentration in soil waters than in surface waters would be 18 µM day^{-1} CO_2 [24]. If there was any CO_2 produced from microbial respiration during the incubation of soil waters that could result in the higher production yield of CO_2 per •OH in in soil waters than in the FA+Fe(II) solutions. Thus, microbial respiration could result in the greater range in the production yield of CO_2 per •OH in soil waters than in FA+Fe(II) solutions.

Third, the greater range in the production yield of CO_2 per •OH in soil waters than in FA+Fe(II) solutions might be due to the differences in DOM antioxidant content in FA+Fe(II) solutions and soil waters. FA+Fe(II) solutions were prepared using fulvic acids isolated from arctic surface waters [10]. The isolation of fulvic acids from whole water DOM by solid-phase extraction changes the composition of DOM composition compared to the whole water DOM [16,25,26]. For example, there is a preferential isolation of aromatic DOM compounds with higher antioxidant content during solid-phase extraction than present initially in the whole water [16,25,26]. Consistent with that observation, FA+Fe(II) solutions prepared in the laboratory had higher EDC, a proxy for antioxidant DOM content, than did the soil waters (Figure 4.5, Table 4.1). Although the EDC of DOM was estimated only for a subset of soil waters were Fe(II) was < 5 uM, the range of the production yield of CO_2 per •OH in these soil waters encompassed the

range of the production yield of CO_2 per •OH measured from all soil waters studied (Trusiak et al. 2018). Therefore, it is possible that the greater range of the EDC of DOM in soil waters compared to the FA+Fe(II) could account for the greater range in the production yield of CO_2 per •OH measured in soil waters than in Fe(II)+DOM solutions. The differences in the EDC of DOM between FA+Fe(II) solutions and soil waters could account for the greater range of the production yield of CO_2 per •OH in soil waters than in FA+Fe(II) solutions.

4.6 Conclusions

Findings from this study demonstrate that CO_2 is produced from the oxidation of DOM by •OH in the dark, consistent with prior work [1,2]. In this study, the yield of CO_2 per •OH was lower in the laboratory FA+Fe(II) solutions than in natural soil waters [2], likely due to the difference in the DOM chemical composition between fulvic acid isolates used in the laboratory studies and DOM in the soil waters. Higher antioxidant content of DOM, as estimated by electron donating capacity, was correlated with a lower production yield of CO_2 per •OH possibly due to the quenching of •OH by antioxidants. The differences in the antioxidant content between FA+Fe(II) solutions and soil waters could explain some of the variability in the production yield of CO_2 per •OH. The production yield of CO_2 per •OH in FA+ Fe(II) solutions did not vary across the pH range of the natural soil waters studied, suggesting that the variability in the production yield of CO_2 per •OH in soil waters cannot be explained by pH differences.

In the Arctic soil waters, there is a wide range in DOM chemical composition, including antioxidant content, across landscape surface age and vegetation type [2,7,8,16]. These differences in DOM composition between soil waters might alter the production yield of CO_2 per •OH as the permafrost soils in the Arctic are thawing. DOM from permafrost soils has lower aromatic C content than DOM from the active layer, and thus less antioxidants than DOM from

the active layer of arctic soils [16]. As the DOM from permafrost soils is released, the production yield of CO_2 per •OH might increase, resulting in up to 10 % more CO_2 produced from this abiotic oxidation of DOM by •OH in the future.

4.7 Acknowledgments

Research was supported by NSF CAREER-1351745, DEB-1026843, 1637459, and 1753731, PLR-1504006, and NSF GRFP.

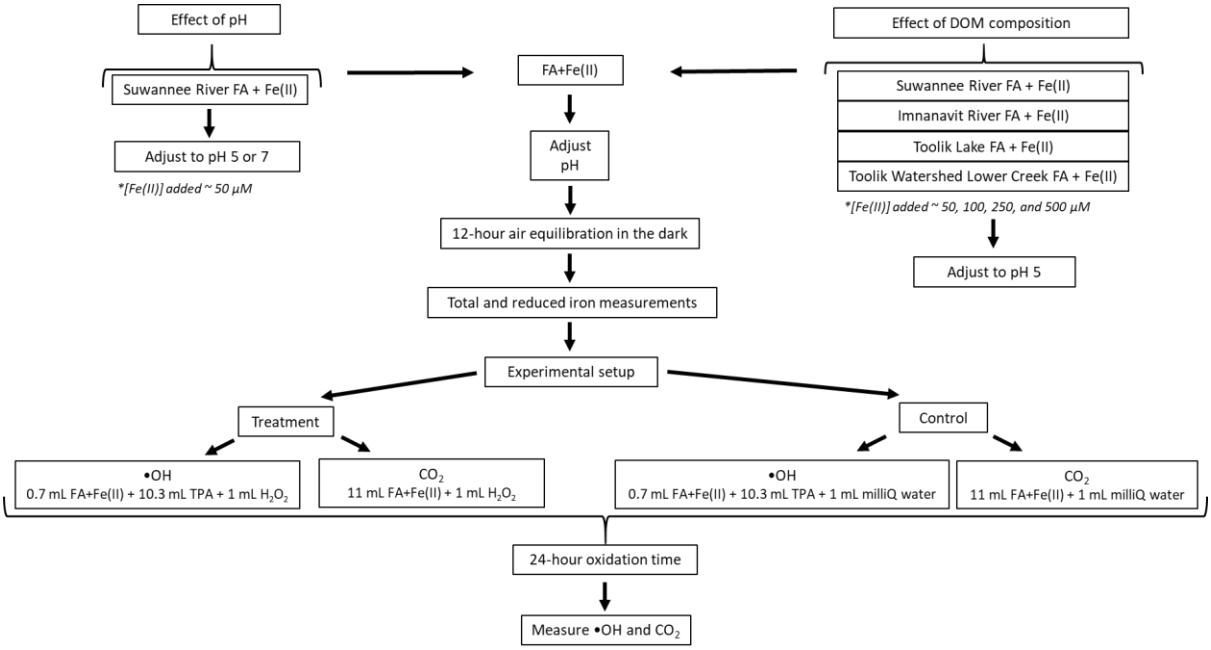

Figure 4.1. Experimental design to study the effect of pH and DOM composition on the production yield of CO_2 per •OH. Fe(II) was added as ferrous ammonium sulfate (FAS, $(NH_4)_2Fe(SO_4)_2$) to study the effect of pH on the production yield of CO_2 per •OH, whereas Fe(II) was added as iron chloride ($FeCl_2$) to study the effect of DOM composition on the production yield of CO_2 per •OH. All FA+Fe(II) solutions were amended with 20 µM H_2O_2, except Suwannee River FA+ Fe(II) solutions (pH 5 and 7), which were amended with a range of H_2O_2 concentrations (5, 10, 20, 50, and 100 µM).

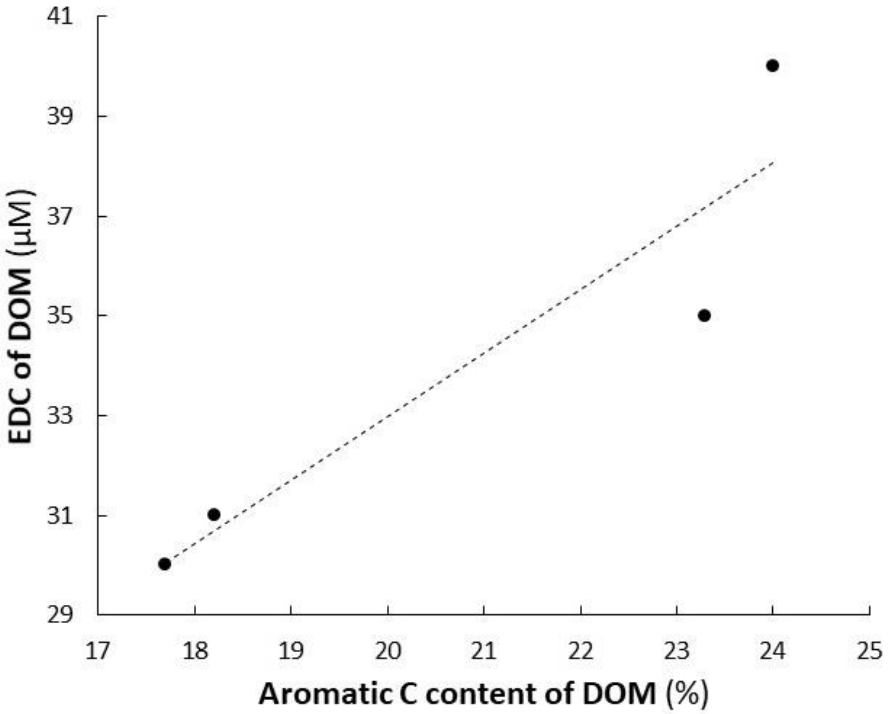

Figure 4.2. Electron donating capacity (EDC) of DOM (µM) versus aromatic carbon content of DOM (%) in the four fulvic acids used in the study. DOM data were fit using a least-squares regression, where EDC of DOM (µM) = [1.3 ± 0.4] x aromatic C content of DOM (%) + [7.5 ± 7.6], p = 0.07, (mean ± SE).

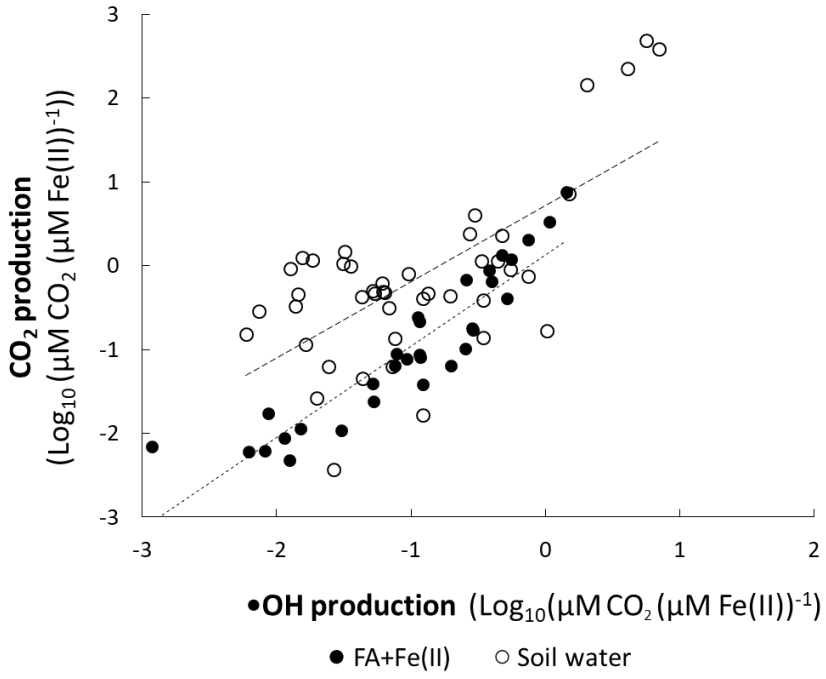

Figure 4.3. CO_2 production versus •OH production (both divided by Fe(II) concentrations) upon introduction of H_2O_2 in FA+Fe(II) solutions (black filled) and in soil waters (black outline). Both CO_2 and •OH production were measured after a 24-hour oxidation by H_2O_2 (treatment) relative to controls (MilliQ water added instead of H_2O_2). Values plotted are log values of measured concentrations. Data for soil waters was previously reported in Trusiak et al. (2018). FA+Fe(II) solutions were fit using a least-squares regression (black line), where CO_2 production ($\mu M\ CO_2\ (\mu M\ Fe(II))^{-1}$) = [1.1± 0.1] x •OH production (μM •OH $(\mu M\ Fe(II))^{-1}$) + [0.1 ± 0.1], $p < 0.05$. Soil water data were fit using a least-squares regression (grey line), where CO_2 production ($\mu M\ CO_2\ (\mu M\ Fe(II))^{-1}$) = [0.9 ± 0.2] x •OH production (μM •OH $(\mu M\ Fe(II))^{-1}$) + [0.7 ± 0.2], $p < 0.05$.

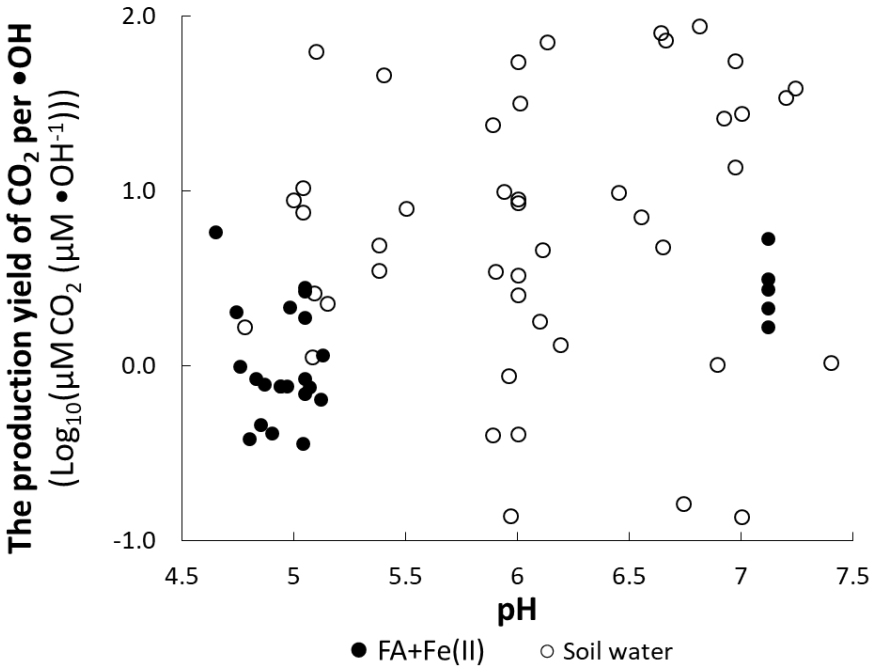

Figure 4.4. The production yield of CO_2 per •OH versus pH of FA+Fe(II) solutions (black filled) and soil waters (black outline). The production yields are plotted as log_{10} values of molar ratios between the CO_2 production (μM) and •OH production (μM). Soil water data were previously reported in Trusiak et al. (2018).

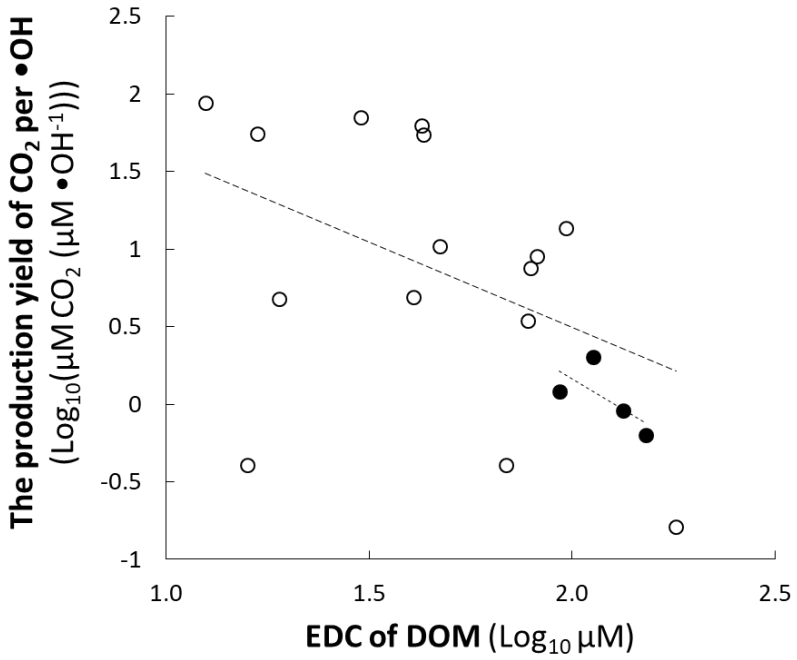

Figure 4.5. The production yield of CO_2 per •OH versus electron donating capacity (EDC) of DOM in FA+Fe(II) solutions (black filled) and in soil waters (black outline). The values are plotted as log values of measured concentrations and of molar ratios between CO_2 production (µM) and •OH production (µM). For soil waters, the data was selected from Trusiak et al. (2018) (details in Methods). The estimated EDC of DOM in arctic soil waters spanned a larger range (71 ± 11 µM) than the EDC of DOM in the FA+Fe(II) solutions (34 ± 2 µM) (Figure 4.5, Table 4.1).For FA+Fe(II) solutions, data were fit using a least-squares regression, where the production yield of CO_2 (µM CO_2 (µM •$OH)^{-1}$) = [-1.6 ± 1.2] x EDC of DOM (µM) + [3.3 ± 2.5], $p = 0.4$. Soil water data were fit using a least-squares regression, where the production yield of CO_2 (µM CO_2 (µM •$OH)^{-1}$) = [-1.1 ± 0.7] x EDC of DOM (µM) + [2.7 ± 1.1], $p < 0.05$.

Fulvic acid	FI[a]	Electron donating capacity (μM)	% Aromatic
Suwannee River	1.39 ± 0.01	40 ± 1	24.0[b]
Imnavait River	1.40 ± 0.01	35 ± 1	23.3[c]
Toolik Lake	1.39 ± 0.01	30 ± 1	17.7[c]
Toolik Watershed Lower Creek	1.40 ± 0.01	31 ± 1	18.2[c]

[a] FI denotes fluorescence index.
[b] Percent aromatic carbon for Suwanee River fulvic acid previously reported in Weishaar et al. (2003)
[c] Percent aromatic carbon calculated from ^{13}C-NMR spectra following Weishaar et al. (2003) for the arctic fulvic acids from Cory et al. (2007)

Table 4.1. Optical spectroscopy and ^{13}C nuclear magnetic resonance (NMR) characteristics of the fulvic acids used in the study. Values are reported as the average ± standard error of replicate vials (n = 2).

Solution	pH	The production yield of CO_2 per •OH (μM CO_2 per 1.0 μM •OH)
SRFA+FAS	5	1.8 ± 0.4
SRFA+FAS	7	3.0 ± 0.6

Table 4.2. The average production yield of CO_2 per •OH in SRFA+Fe(II) solutions at pH 3, 5, and 7, where iron was added as ferrous ammonium sulfate (FAS). Data are reported as the average ± standard error of replicate vials (n = 5 for each pH level).

Solution	**The average production yield of CO_2 per •OH** (μM CO_2 per 1.0 μM •OH)	**The minimum production yield of CO_2 per •OH** (μM CO_2 per 1.0 μM •OH)	**The maximum production yield of CO_2 per •OH** (μM CO_2 per 1.0 μM •OH)
DOM+Fe(II)	1.5 ± 0.3^{A}	0.3	5.8
Soil water	19 ± 4^{B}	0.1	88

Letters A and B indicate significant differences ($p < 0.05$) between the average production yields.
Soil water data were previously reported in Trusiak et al. (2018).

Table 4.3. The average production yield of CO_2 per •OH in FA+Fe(II) solutions and in soil waters. Data are reported as the average ± standard error of water samples (n = 31 for FA+Fe(II); n = 44 for soil waters).

Solution	pH	Fe_{tot} *(μM)*	Fe(II) *(μM)*	DOM *(μM-C)*
SRFA+FAS	5.05	36 ± 0	25 ± 5	2100
SRFA+FAS	7.12	10 ± 0	2 ± 1	2100

Table 4.S1. Measured pH, total and reduced iron, and DOM concentrations in Suwannee River Fulvic Acid (SRFA) solutions amended with ~50 μM of ferrous ammonium sulfate (FAS) after adjusting the pH to ~5 and 7. The measurements were done before the amendment with H_2O_2 (treatment) or MilliQ water (control). Data are reported as the average ± standard of replicate vials (n = 5).

Solution	pH	Fe_{tot} (μM)	Fe(II) (μM)	DOM (μM-C)
SRFA+$FeCl_2$	5.1	35 ± 0	23 ± 1	2100
	5.1	77 ± 0	61 ± 9	2100
	5.0	153 ± 4	122 ± 1	2100
	4.9	281 ± 1	239 ± 8	2100
Imnavait River FA+$FeCl_2$	4.9	33 ± 1	22 ± 2	3100
	4.9	63 ± 1	47 ± 2	3100
	4.8	178 ± 2	142 ± 7	3100
	4.8	340 ± 3	318 ± 5	3100
Toolik Lake FA+$FeCl_2$	5.0	25 ± 1	13 ± 2	2700
	5.1	36 ± 0	21 ± 1	2700
	4.9	272 ± 4	239 ± 1	2700
	5.0	277 ± 10	240 ± 9	2700
Toolik Watershed Lower Creek FA+$FeCl_2$	4.9	37 ± 0	25 ± 4	2700
	4.9	65 ± 1	40 ±1	2700
	4.8	154 ± 3	125 ± 15	2700
	4.8	282 ± 11	250 ± 9	2700

Table 4.S2. Measured pH, total and reduced iron, and DOM concentrations in Suwannee River fulvic acid (SRFA) and the arctic fulvic acid solutions amended with ~ 50, 100, 250, and 500 µM ferrous chloride ($FeCl_2$). The measurements were done before the amendment with H_2O_2 (treatment) or MilliQ water (control). Data are reported as the average ± standard error of replicate vials (n = 3).

4.8 References

1. Goldstone, J. V., Pullin, M. J., Bertilsson, S. and Voelker, B. M. (2002) Reactions of hydroxyl radical with humic substances: bleaching, mineralization, and production of bioavailable carbon substrates. *Environ. Sci. Technol.* 36, 364–372.

2. Trusiak, A.; Treibergs, L.A.; Kling, G.W.; Cory, R.M. (2018) The role of iron and reactive oxygen species in the production of CO_2 in arctic soil waters. *Geochim. Cosmochim. Acta* 224, 80–95.

3. Walling, C. (1974) Fenton's reagents revisited. *Accounts of Chemical Research* 8, 125-131

4. Sulzberger, B., and Durisch-Kaiser, E. (2009). Chemical characterization of dissolved organic matter (DOM): A prerequisite for understanding UV-induced changes of DOM absorption properties and bioavailability. *Aquatic Sciences* 71, 104–126.

5. Wenk, J., von Gunten, U., and Canonica, S. (2011) Effect of dissolved organic matter on the transformation of contaminants induced by excited triplet states and the hydroxyl radical. *Environ. Sci. Technol.* 45, 1334-1340

6. Westerhoff, P., Aiken, G., Amy, G., and Debroux, J. (1999). Relationships between the structure of natural organic matter and its reactivity towards molecular ozone and hydroxyl radicals. *Water Research* 33, 2265–2276.

7. Page, S. E., Kling, G. W., Sander, M., Harrold, K. H., Logan, J. R., McNeill, K. and Cory, R. M. (2013) Dark formation of hydroxyl radical in arctic soil and surface waters. *Environ. Sci. Technol.* 47, 12860–12867.

8. Trusiak, A.; Treibergs, L.A.; Kling, G.W.; Cory, R.M. (2019) The controls of rion and oxygen on hydroxyl radical production in soils. *Soil systems* 3,1.

9. Aeschbacher, M., Graf, C., Schwarzenbach, R. P. and Sander, M. (2012) Antioxidant properties of humic substances. *Environ. Sci. Technol.* 46, 4916–4925.

10. Cory, R.M., McKnight, D.M., Chin, Y.P., Miller, P., and Jaros, C.L. (2007) Chemical characteristics of fulvic acids from Arctic surface waters: microbial contributions and photochemical transformations. *J. Geophys. Res.* 112, 1–14.

11. Cory, R.M., McNeill, K., Cotner, J.P., Amado, A., Purcell, J.M., and Marshall, A.G. (2010) Singlet oxygen in the coupled photochemical and biochemical oxidation of dissolved organic matter. *Environ. Sci. Technol.* 44, 3683–9.

12. Cory, R.M., and Kaplan, L.A. (2012) Biological lability of streamwater fluorescent dissolved organic matter. *Limnol. Oceanogr.* 57, 1347–1360.

13. Miller, M.P., Simone, B.E., McKnight, D.M., Cory, R.M., Williams, M.W., and Boyer,

E.W. (2010) New light on a dark subject: Comment. *Aquat. Sci.* 72, 269–275.

14. McKnight, D.M., Boyer, E.W., Westerhoff, P.K., Doran, P.T., Kulbe, T., and Andersen, D.T. (2001) Spectrofluorometric characterization of dissolved organic matter for indication of precursor organic matter and aromaticity. *Limnol. Oceanogr.* 46, 38–48.

15. Weishaar, J.L., Aiken, G.R., Bergamaschi, B.A., Fram, M.S., Fujii, R., and Mopper, K. (2003) Evaluation of specific ultraviolet absorbance as an indicator of the chemical composition and reactivity of dissolved organic carbon. *Environ. Sci. Technol.* 37, 4702–8.

16. Ward C. P., and Cory R. M. (2015) Chemical composition of dissolved organic matter draining permafrost soils. *Geochimica et Cosmochimica Acta* 167, 63–79.

17. Stookey, L. L. (1970). Ferrozine a new spectrophotometric reagent for iron. *Analytical Chemistry* 42, 779–781.

18. Page, S. E., Arnold, W. A., and McNeill, K. (2010). Terephthalate as a probe for photochemically generated hydroxyl radical. *Journal of Environmental Monitoring* 12, 1658–1665.

19. Page, S. E., Logan, J. R., Cory, R. M., and McNeill, K. (2014). Evidence for dissolved organic matter as the primary source and sink of photochemically produced hydroxyl radical in arctic surface waters. *Environ. Sci. Processes & Impacts* 16, 807–822.

20. Brezonik, P.L., and Fulkerson-Brekken, J. (1988) Nitrate-Induced Photolysis in Natural Waters: Controls on Concentrations of Hydroxyl Radical Photo-Intermediates by Natural Scavenging Agents, *Environ. Sci. Technol.* 32, 3004.

21. Buxton, G.V., Greenstock, C. L., Helman, W. P., and Ross, A. B. (1988) Critical review of rate constants for reactions of hydrated electrons, hydrogen atoms and hydroxyl radicals in aqueous solution, *J. Phys. Chem. Ref. Data* 17, 513.

22. Qian, J., Mopper, K., and Kieber, D.J. (2001) Photochemical Production of the Hydroxyl Radical in Antarctic Waters. *Deep-Sea Res.* 48, 741.

23. Charbouillot, T., Brigante, M., Mailhot, G., Maddigapu, P. R., Minero, C., and Vione, D. (2011). Performance and selectivity of the terephthalic acid probe for hydroxyl radical as a function of temperature, pH and composition of atmospherically relevant aqueous media. *Journal of Photochemistry and Photobiology A: Chemistry* 222, 70–76.

24. Cory, R.M, Crump, B.B, Dobkowski, J.A., Kling, G.W. (2013) Surface exposure to sunlight simulates CO_2 release from permafrost soil carbon in the Arctic. *PNAS* 9 (110), 3429-3434.

25. Dittmar, T., Koch, B., Hertknorn, N., and Kattner, G. (2008). A simple and efficient

method for the solid-phase extraction of dissolved organic matter (SPE-DOM) from seawater. *Limnol. Oceanogr. Methods* 6, 230-235.

26. Sleighter, R.L., and Hatcher, P.G. (2008). Molecular characterization of dissolved organic matter (DOM) along a river to ocean transect of the lower Chesapeake Bay by ultrahigh resolution electrospray ionization Fourier transform ion cyclotron resonance mass spectrometry. *Marine Chemistry* 110(3–4), 140–152.

Chapter 5
Conclusions

5.1 Controls on •OH and CO_2 Production from Abiotic Fe(II) Oxidation in Soils

This dissertation investigated hydroxyl radical (•OH) and carbon dioxide (CO_2) production from abiotic redox reactions involving reduced ferrous iron (Fe(II)) and dissolved organic carbon (DOC) in soils. My results improve our understanding of natural processes leading to the production of CO_2 by identifying a novel pathway for abiotic CO_2 production in soils. Specifically, I showed that •OH, produced mainly from Fe(II) oxidation by dissolved oxygen in soils, can oxidize DOC to CO_2. However, there is a large variability among different soil waters in the amount of •OH and CO_2 produced from this abiotic Fe(II) oxidation. I identified controls on the amount of •OH and CO_2 produced to predict how these processes impact carbon cycling now and in the future. By investigating •OH and CO_2 production in soils, I demonstrated that (1) •OH is produced primarily from Fe(II) oxidation in arctic soils with hydrogen peroxide being produced as the intermediate, (2) hydrological connectivity across the arctic landscape results in higher •OH production in wet sedge than in tussock dominated landscapes, (3) dissolved oxygen availability limits *in situ* •OH production in arctic soils, and (4) that the yield of CO_2 produced from the oxidation of DOC by •OH is related to the electron donating capacity and antioxidant content of soil waters.

My results showed that •OH is produced during Fe(II) and DOC oxidation in arctic soil waters because hydrogen peroxide (H_2O_2), the intermediate expected to be produced from Fe(II) and reduced DOC oxidation by dissolved oxygen, was measured upon the oxidation of arctic soil

waters (**Chapter 1**, **Chapter 2**). H_2O_2 produced from the oxidation of Fe(II) or reduced DOC subsequently oxidized the remaining Fe(II) and reduced DOC in arctic soil waters to produce •OH (**Chapter 1**). My study also identified whether oxidation of Fe(II) or reduced DOC was the primary electron donor to produce •OH in arctic soils [1], and thus, the primary control on the •OH production. The oxidation of Fe(II) accounted for the majority (> 70%) of •OH produced during oxidation of arctic soil waters (**Chapter 2**). These results improve previous work by showing that Fe(II) oxidation alone controlled up to 80% of •OH production in Fe(II)-rich soil waters.

I found that downhill transport of Fe(II) from the upland tussock dominated landscapes to the lowland wet sedge dominated landscapes at my Arctic study site provides an important source of Fe(II) for •OH production in the lowlands where wet sedge vegetation dominates (**Chapter 3)**. My results showed different concentrations of Fe(II) between the two vegetation types depending on whether Fe(II) was measured *in situ* from soil waters collected in the field or from soil waters collected from soil core mesocosms. *In situ* Fe(II) concentrations were higher in wet sedge than tussock soils, whereas in the mesocosm study Fe(II) concentrations were lower in wet sedge than tussock soils. These differences in Fe(II) concentrations between the two vegetation types were likely due to the lack of hydrological connectivity between the tussock and wet sedge soils in the mesocosm studies, i.e., there was no transport of Fe(II) with water downhill from tussock to wet sedge soils. Tussock soils had an iron-rich mineral layer within 10-30 cm of the soil surface that was not present in wet sedge soils, and that was likely the source of Fe(II) produced in the tussock soils in the mesocosm study. However, *in situ,* Fe(II) produced in the tussock soils was likely transported with water downhill to lowland wet sedge soils, resulting in higher *in situ* Fe(II) concentrations in wet sedge than tussock soils. I refined

the model for Fe(II) and •OH production across the arctic landscape by showing that *in situ* Fe(II) concentrations are higher on the lowland wet sedge landscapes than on the upland tussock landscapes due to the hydrological connectivity between the two vegetation types (**Chapter 3**) [1].

The magnitude of •OH production in soils was controlled by the balance between the Fe(II) production rate and the dissolved oxygen supply rate to oxidize Fe(II) (**Chapter 3**). Fe(II) production rate was higher on the older and on the tussock dominated landscapes than on the younger and on the wet sedge dominated landscapes. Under static waterlogged conditions, dissolved oxygen supplied by diffusion from the atmosphere and by plant aerenchyma was not sufficient to oxidize all of the Fe(II) produced in any of the arctic soils studied, resulting in low •OH production under those oxygen-limiting conditions. During experimental, simulated rainfall events when dissolved oxygen was supplied to the soils with oxygenated rain water, •OH production was up to three times higher than under waterlogged conditions. Throughout both waterlogged conditions and rainfall events, there was always detectable Fe(II) present. This result suggests that the dissolved oxygen supply rate did not exceed the Fe(II) production rate. If it did, there would be no detectable Fe(II) present as it would all be consumed by oxidation. Thus, the dissolved oxygen supply rate was limiting •OH production even during rainfall events. Given that the majority of the soils in the Alaskan Arctic are waterlogged with high Fe(II) and low dissolved oxygen concentrations [1-3], it is likely that dissolved oxygen supply rate limits •OH production in all arctic soils (**Chapter 3**).

By showing that •OH oxidizes DOC to CO_2, my results improve our understanding of CO_2 production in soils by including an abiotic pathway for CO_2 production from Fe(II) oxidation (**Chapters 2, 4**) [4]. My findings demonstrate that CO_2 was produced from DOC

oxidation by •OH because •OH and CO_2 were significantly, positively correlated. Additionally, CO_2 was produced under conditions conducive to the oxidation of DOC by •OH in the controlled laboratory experiments and in the majority of the soil waters tested. Both in the controlled experiments and in arctic soil waters, waters were filtered to remove any microbes and kept in the dark to prevent photochemical reactions, thus there was no pathway for CO_2 production other than DOC oxidation by •OH (**Chapter 2**). My work demonstrated for the first time that abiotic DOC oxidation by •OH to CO_2 happens in soils in the Arctic and likely in any other soils rich in Fe(II) and DOC that could be conducive to •OH production. However, the production yield of CO_2 per •OH varied 2- to 50-fold in the controlled experiments and in soil waters (**Chapter 2, Chapter 4**), indicating that the variability in the soil water DOC chemical composition may control the production yield of CO_2 per •OH.

I found that DOC chemical composition may control the production yield of CO_2 per •OH (**Chapter 4**). Specifically, DOC with a higher electron donating capacity had a lower production yield of CO_2 per •OH than DOC with a lower electron donating capacity. The electron donating capacity of DOC is positively correlated with its antioxidant capacity, or its capacity to quench reactive oxygen species, including •OH [5]. Thus, antioxidants within the DOC pool can quench •OH, leading to production of low energy radicals instead of CO_2 [5], and thus, lower the production yield of CO_2 per •OH (**Chapter 2, Chapter 4**). The electron donating capacity of DOC may explain the variability in the amount of CO_2 produced in arctic soil waters and should be taken into consideration when estimating CO_2 production from oxidation of DOC by •OH.

My results establish a novel pathway for production of CO_2 from oxidation of DOC by •OH in Fe(II)- and DOC-rich environments. The current view is that the majority of CO_2 in soils

and soil waters is produced through biological pathways where microbes respire DOC and produce CO_2. However, my research showed that abiotic Fe(II) oxidation leads to CO_2 production from oxidation of DOC by •OH in soils, and that the amount of CO_2 produced through this process may be comparable to the microbial production of CO_2 in surface waters (**Chapter 2, Chapter 3**) [1]. My findings improve future prediction of how much •OH and CO_2 might be produced through this process because I identified environmental controls on the magnitude of •OH and CO_2 production in soils.

As thawing arctic permafrost soils release organic C and Fe(II), CO_2 production from abiotic Fe(II) oxidation may increase in importance due to the higher DOC and Fe(II) concentrations [6,7], and thus •OH production in soils. CO_2 production from DOC oxidation by •OH may be also higher in the future because DOC draining thawing permafrost soils has lower aromaticity and thus lower antioxidant content than DOC produced in the upper, thawed soil layers [8]. Thus, based on my findings, oxidation of permafrost DOC by •OH could lead to more CO_2 produced per amount of DOC than is currently measured today. However, with climate warming the hydrological regime in the Arctic is expected to change as well. For example, frequency of heavy rainfall might increase or the water table height might decrease, resulting in changes in the Fe(II) production rates and the dissolved oxygen supply rates to the soils [9,10]. Depending on how the changes in rainfall alter the balance between the dissolved oxygen supply rate to oxidize Fe(II) and the Fe(II) production rate, the magnitude of •OH and CO_2 production in soils might change in the future.

5.2 Future Work: •OH's Role in the Soil C Cycling

The findings from this dissertation generated a number of new questions that could improve understanding of the controls on carbon cycling in soils:

(1) Is •OH produced from oxidation of particulate Fe(II) and, if so, how does that change the estimates of CO_2 production from abiotic oxidation of Fe(II)?

(2) Is there partially oxidized DOC produced from •OH oxidation of DOC and, if so, does it impact microbial respiration?

(3) Does •OH produced in soil water oxidize methane to CO_2?

Given that the majority of Fe(II) may be in the particulate form in soils [11], my work to date examining •OH production only from dissolved Fe(II) may be substantially under-estimating **CO_2** that could be produced by redox reactions of iron in arctic soil waters. Recent work showed that particulate Fe(II) in sediments can be oxidized to yield •OH [12]. •OH production from oxidation of anoxic sediments was positively correlated with reactive particulate Fe(II) [12]. In the Arctic, low oxygen waterlogged soils create reducing condition that can lead to accumulation of particulate Fe(II) [3]. My preliminary results showed that 70% of arctic soils tested had significantly higher •OH production from oxidation of particulate and dissolved Fe(II) than from the oxidation of just dissolved Fe(II) (Figure 5.1.). Because both solutions contained dissolved Fe(II), this finding suggests that particulate Fe(II) in arctic soils produced •OH. However, controls on the production of •OH from particulate Fe(II) oxidation are not well understood.

•OH production likely is higher in soils with higher reactive particulate Fe(II) that is redox active and thus readily available to be oxidized to CO_2. Mackinawite, pyrite, or iron phyllosilicates were shown to be the most redox active iron minerals that produced •OH upon oxidation [12,13]. The yield of •OH per mole of particulate Fe(II) will likely increase with increasing fractions of Fe(II) in forms of mackinawite, pyrite, or iron phyllosilicates relative to total Fe(II) in the solid phase [12,13]. Determining the potential of particulate Fe(II) in arctic

soils to produce •OH is important to estimate the effect of oxidation of DOC by •OH on the arctic C cycling because the particulate Fe(II) concentrations are an order of magnitude larger than the dissolved Fe(II) concentrations [3,11]. If particulate Fe(II) produced as much or more •OH as the dissolved Fe(II), the current predictions of CO_2 produced from oxidation of DOC by •OH are underestimates.

Once produced, •OH may partially oxidize DOC [4], impacting the C cycle more than already estimated by providing labile compounds for microbes to respire to CO_2 [1]. While the partial oxidation of DOC by •OH was shown previously only in a controlled laboratory experiment [4], it is likely that it happens in natural soil waters just like the complete oxidation of DOC by •OH to CO_2 production shown in my results (**Chapter 2, Chapter 4**). •OH is an unselective oxidant that can oxidize large DOC compounds to small partially oxidized DOC compounds like low molecular weight acids such as acetate, formate, malonate, and oxalate [4]. For example, it has been shown that •OH can oxidize lignin, a large, less labile compound, to smaller, more biolabile compounds [14]. While studying the DOC composition before and after oxidation by •OH using FT-ICR MS was unsuccessful (*see Appendix)*, low molecular weight DOC compounds, such as acetate can be quantified using ion chromatography without interferences from Fe(II) [3]. Thus, comparing low molecular weight compound concentrations before and after oxidation by •OH could quantify the amount of labile DOC produced from oxidation of DOC by •OH in arctic soil waters. Given the importance of understanding of the fate of soil C in the Arctic, understanding processes that might impact microbial respiration of DOC to CO_2 is crucial for better estimates of future CO_2 emissions from arctic soils.

Another way in which •OH might impact the arctic C cycle is by oxidizing methane produced and stored in arctic soils. It is well known that •OH can oxidize methane to carbon

monoxide and carbon dioxide, as shown in the atmosphere [e.g., 15]. In arctic soils rich in methane, •OH might be oxidizing methane to CO_2. Because methane is ~30-times more potent as a greenhouse gas than is CO_2 [16], its oxidation by •OH to CO_2 in soils would reduce the magnitude of warming caused by the greenhouse gas emissions [17]. The kinetics and the mechanism of the reactions between methane and •OH in soils are currently unknown. Studying this process to determine how much methane could be oxidized by •OH is necessary for estimating rates of methane oxidation and CO_2 emissions from arctic soils.

5.3 Appendices

5.3.1 Limitations in Understanding Effects of Fe(II) Complexation on •OH Production

Fe(II) oxidation, and thus, •OH production might be influenced by the form of Fe(II) present in soil waters (i.e., Fe(II) complexation). While Fe(II) was identified as the primary electron donor to produce •OH, the amount of •OH produced was not strongly correlated to the moles of Fe(II) oxidized to ferric iron (Fe(III)) (**Chapter 2**). For example, per mol of Fe(II) oxidized in soil waters, the amount of •OH produced varied by 10- to 100- fold, limiting the ability to predict •OH production in soil waters based on the amount of Fe(II) oxidized alone (**Chapter 2**). In natural systems, the rate and extent of Fe(II) oxidation might be controlled by the complexation of iron by DOC [18-21].

In the acidic, organic carbon rich soils in the Arctic, a close molecular association between iron and DOC is likely a key control on iron complexation, and Fe(II)'s reactivity and ability to produce •OH [18-21]. This is because arctic soil waters contain high DOC concentrations and low concentrations of other potential ligands for iron (e.g., low sulfide, carbonate, chloride, bromide) [1]. DOC in arctic soil waters is enriched in carboxylic acids from the degradation of plant and soil matter [8]. Over the pH range of soil waters in the Arctic (pH 5

– 7) [22], deprotonated carboxylic acids may be the most abundant ligand that complexes with both Fe(II) and Fe(III). Previous controlled laboratory studies suggested that DOC affects the rates of Fe(II) oxidation and Fe(III) reduction due to complexation of iron with carboxylic acids [3,22,23]. However, few studies have directly investigated complexation of iron with DOC, and no study has directly tested whether this complexation alters the rates of iron redox cycling and production of •OH in natural systems.

To test this idea, I measured iron redox state and complexation in arctic soil waters using X-ray Absorption Fine Structure spectroscopy (XAFS) [24-27]. XAFS has been previously applied to study the form of iron in sediments and soils [24-27]. XAFS studies of iron redox state and complexation in liquid samples are less common because of the need for high concentrations of iron. However, due to the high iron concentrations in arctic soil waters, XAFS could be used to analyze the chemistry of dissolved iron in arctic soil waters. Using XAFS, I found that dissolved iron was mainly present as Fe(II) in the arctic soil waters studied, consistent with previous field measurements (**Chapter 2**, **Chapter 3**) [22]. The XAFS spectra for Fe(II) complexed with reference DOC overlapped with the spectra for arctic soil waters, suggesting that Fe(II) in the soil waters was complexed with DOC (Figure 5.2). The result was consistent with previous work that measured Fe(II) complexation in soil waters using XAFS and found that spectra of Fe(II) in soil waters were comparable to the spectra of Fe(II) complexed with DOC [28-30]. However, none of the previous work compared soil water spectra to free Fe(II) in a solution to quantify how much Fe(II) was complexed to DOC versus how much Fe(II) was free. While trying to quantify Fe(II) complexed to DOC versus free Fe(II), I found methodological constraints to identifying what Fe(II) was complexed using XAFS.

My XAFS results showed that there were no differences in the reference spectra of Fe(II) bound to DOC and free Fe(II) (data not shown). The lack of difference between Fe(II) complexed with DOC and free Fe(II) suggested either that (1) the atomic environment around the Fe(II) was not affected by DOC and so XAFS is not an appropriate method to study Fe(II) complexation in liquid samples, or that (2) there were issues with the Fe(II) complexed with DOC or free Fe(II) references used in the study. First, there is no way to identify whether the atomic environment around Fe(II) is affected by the complexation with DOC in aqueous solution, because XAFS has been previously mostly applied to sediments and soils with crystalline structure that is not present in aqueous solutions.

Second, to analyze XAFS results, the soil water spectra need to be a compared to reference spectra that represent forms of iron expected to be present in soil waters. For example, in arctic soil waters rich in Fe(II) and DOC, the two main forms of iron expected would be free Fe(II) and Fe(II) complexed with DOC. The database for references of Fe(II) complexes in aqueous solutions that soil waters could be compared to was very limited because very little XAFS analysis of aqueous solution has been done and an extensive database has not been developed. Thus, to identify Fe(II) complexation in soil waters by XAFS and determine the percentage of free Fe(II) versus that complexed to DOC, references for each expected Fe(II) complex present, including free Fe(II), were needed. Due to the complex nature of DOC, selecting the right organic compound was difficult as not much is known about the interactions of Fe(II) with DOC. For example, currently there is no understanding of how the complexation between Fe(II) and citric acid versus salicylic acid, two simple organic compounds commonly used in Fe(II) oxidation studies, might differ and whether those differences could impact XAFS results. Once an organic compound was selected, the only way to add Fe(II) to the reference

DOC solution was to use an iron salt. Adding an iron salt to the reference DOC solution could alter Fe(II) complexation because the salts could complex with Fe(II) in addition to DOC and reduce or eliminate the free Fe(II) in the solution. For example, my results showed that ferrous ammonium sulfate cannot be used as the source of Fe(II) in reference solutions because Fe(II) complexed with sulfate, forming Fe(II) sulfate complexes instead of Fe(II)-DOC complexes or instead of staying in a solution as free Fe(II). To use a compound representative of arctic DOC and to minimize the formation of additional Fe(II) complexes not expected to form in arctic soil waters, citric acid was used as the DOC reference compound and ferrous iron chloride was used as the reference Fe(II). However, there was no way to measure if these references appropriately represented the Fe(II)-DOC complex and free Fe(II), and whether the Fe(II)-citric acid complex and free Fe(II) were the primary species in the reference solutions. In addition to problems with representative references, XAFS can alter the composition of aqueous solutions during the analysis.

During the XAFS analysis of the aqueous solutions including Fe(II) references and soil waters, the high beam energy needed for XAFS caused photochemical reactions that changed the iron redox state. For example, a solution of Fe(II) complexed with Suwannee River Fulvic Acid, a terrestrial DOC representative, was oxidized by the XAFS beam to Fe(III) over the course of the analysis (Figure 5.3). The oxidation resulted in the solution having a different final iron redox state than initially, and thus changed the forms of iron present in the solution. The changes to iron redox state during XAFS did not happen in all of the reference solutions and soil waters studied, and it was unclear what about the composition of the reference solutions and soil waters prompted the oxidation or reduction of iron present.

The study on the effect of Fe(II) complexation on Fe(II) oxidation, and thus, •OH production, was not completed. The lack of reliable reference solutions of Fe(II) complexed with DOC and free Fe(II), as well as changes in iron redox state during the XAFS analysis, made the collected XAFS data unusable to determine how Fe(II) complexation affects •OH production. Nonetheless, new knowledge on the problems and limitations of the XAFS analysis was gained, and those new findings will be used in a manuscript in preparation on studying interactions between iron and DOM in arctic soil and surface waters [21].

5.3.2 Limitation in Studying Partial Oxidation of DOC by •OH

In addition to CO_2 being the product of DOC oxidation by •OH, •OH can partially oxidize DOC to produce low molecular weight acids [31]. The partial oxidation of DOC by •OH has been shown in a controlled laboratory setting where •OH was produced electrochemically [31], but never in a natural environment. •OH oxidizes DOC through hydroxylation, where oxygen is incorporated into DOC [31]. Thus, it is expected that oxidation of DOC by •OH results in DOC compounds with higher oxygen content (i.e., more oxidized).

To test this, I studied changes in DOC composition using ultra-high resolution Fourier transform-ion cyclotron resonance mass spectrometry (FT-ICR MS) at the Environmental Molecular Science Laboratory (EMSL, a DOE national laboratory user facility) in Richland, WA. FT-ICR MS measures the elemental composition of the molecules within the DOC pool, i.e., the amount of carbon, hydrogen, and oxygen in each DOC molecule [8,32]. A range of reference solutions of Fe(II) and DOC and arctic soil waters were analyzed by FT-ICR MS before and after the oxidation by •OH to identify whether there were any changes in the DOC composition as expected if •OH was partially oxidizing DOC. Preliminary results from references solution of Fe(II) and DOC showed an increase in oxygen-containing compounds in

DOC after oxidation by •OH, consistent with hydroxylation of DOC by •OH and thus, partial oxidation of DOC by •OH (Figure 5.4). However, FT-ICR MS detection of organic compounds within DOC depends on the efficiency of the ionization. Fe(II) itself can ionize and interfere with the ionization of DOC compounds by limiting the efficiency of their ionization. Thus, the presence of Fe(II) can lower the number of DOC compounds that become ionized (and thus detected). Consistent with this expectation, in reference solutions of Fe(II) and DOC and in arctic soil waters, 50% less DOC compounds were detected by FT-ICR MS than in a solution with no Fe(II) present, making the collected data unreliable as we do not know what DOC compounds were not ionized and thus, not detected (Figure 5.4). Currently, there are no methods of removing Fe(II) from the reference solutions or arctic soil waters oxidized with •OH before FT-ICR MS analysis without impacting DOC composition. Thus, partial oxidation of DOC by •OH in solutions with Fe(II) cannot be studied by FT-ICR MS without artificially affecting DOC composition. Major new efforts to develop methods to examine the interactions between iron and DOC without affecting the DOC composition have been undertaken, however, as of now there is no successful method for identifying those interactions.

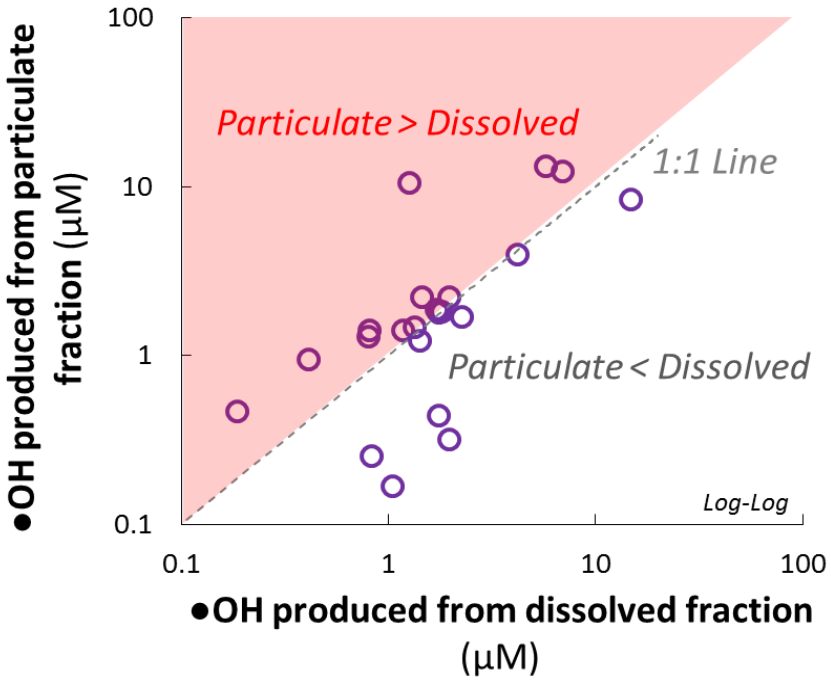

Figure 5.1. The amount of •OH produced from particulate and dissolved Fe(II) fraction versus •OH produced from only dissolved Fe(II) fraction in arctic soils and soil waters. In soils and soil waters plotting above 1:1 line, •OH was produced from the particulate fraction, suggesting that particulate Fe(II) in arctic soils could be oxidized by dissolved oxygen to produce •OH.

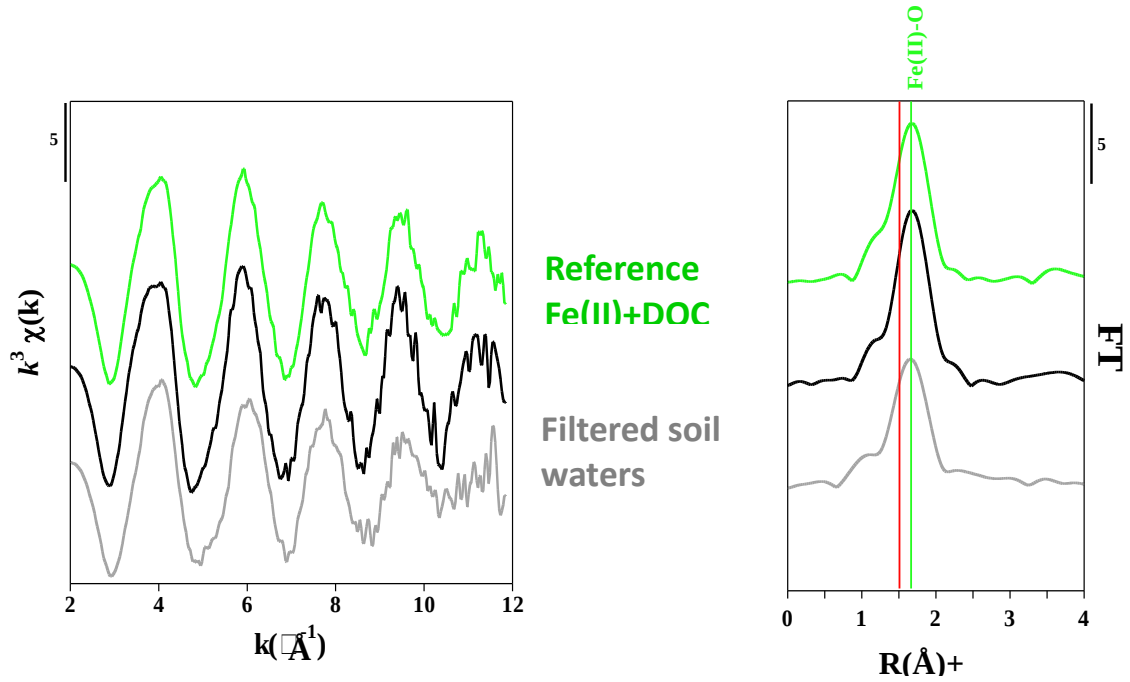

Figure 5.2. XAFS spectra of the reference Fe(II) complexed with DOC (Fe(II)+DOC, green) and the arctic soil waters (grey and black). Comparison of the spectra shows strong overlap between the reference Fe(II)+DOC solution and the soil waters, suggesting that the Fe(II) is soil waters is complexed with DOC.

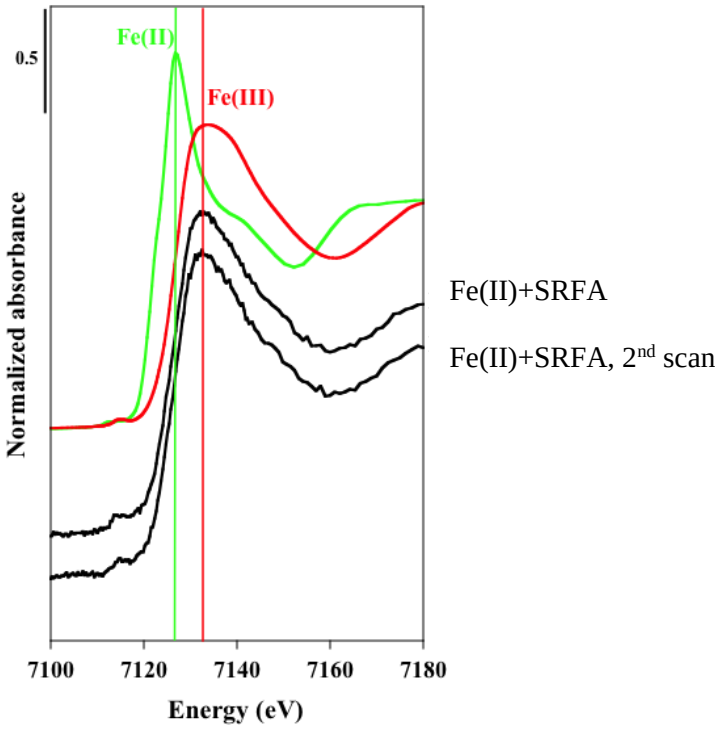

Figure 5.3. XAFS spectra of a solution of Fe(II) complexed with Suwannee River Fulvic Acid (Fe(II)+SRFA, black) and the Fe(II) and Fe(III) reference (green and red, correspondingly). Fe(II) in the solution of Fe(II)+SRFA was oxidized to Fe(III) during the XAFS measurements as the peaks for the Fe(II)+SRFA correspond to the Fe(III) reference instead of Fe(II) reference.

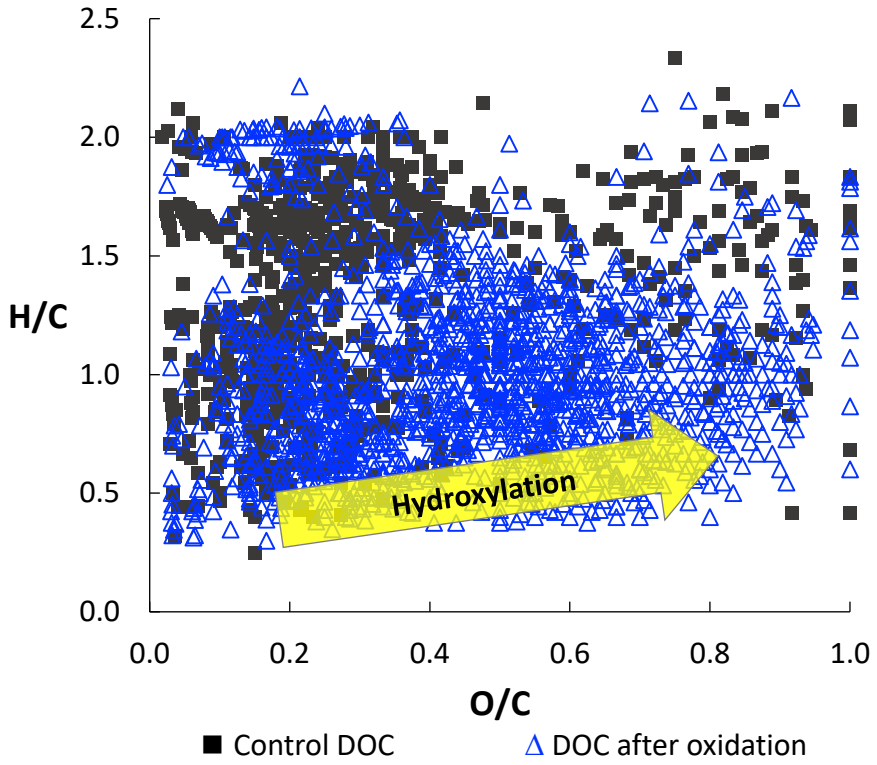

Figure 5.4. Van Krevelen diagram showing all individual DOC compounds detected by FT-ICR plotted as hydrogen to carbon (H/C) and oxygen to carbon (O/C) ratios. Each symbol corresponds to one individual DOC compound. Plotted are compounds unique to control DOC and DOC after oxidation. DOC before oxidation by •OH (Control DOC, black squares) plots at lower O/C values while DOC after oxidation by •OH (DOC after oxidation, blue triangles) plots at higher O/C. The increase in O/C is consistent with hydroxylation of DOC by •OH.

5.4 References

1. Page, S. E., Kling, G. W., Sander, M., Harrold, K. H., Logan, J. R., McNeill, K. and Cory, R. M. (2013) Dark formation of hydroxyl radical in arctic soil and surface waters. *Environ. Sci. Technol.* 47, 12860–12867.

2. Lipson, D., Jha, M., Raab, T. K. and Oechel, W. C. (2010) Reduction of iron (III) and humic substances plays a major role in anaerobic respiration in an Arctic peat soil. *J. Geophys. Res. Biogeosci.* 115, 1–13.

3. Herndon, E. M., Yang, Z., Bargar, J., Jano,t N., Regier, T. Z., Graham, D. E. and Liang, L. (2015) Geochemical drivers of organic matter decomposition in arctic tundra soils. *Biogeochemistry* 126, 397–414.

4. Goldstone, J. V., Pullin, M. J., Bertilsson, S. and Voelker, B. M. (2002) Reactions of hydroxyl radical with humic substances: bleaching, mineralization, and production of bioavailable carbon substrates. *Environ. Sci. Technol.* 36, 364–372.

5. Aeschbacher, M., Graf, C., Scwarzenbach, R. P. and Sander, M. (2012) Antioxidant properties of humic substances. *Environ. Sci. Technol.* 46, 4916–4925.

6. Ping, C.L., Bockheim, J.G., Kimble, J.M., Michaelson, G.J., Walker, D.A. (1998) Characteristics of cryogenic soils along a latitudinal transect in Arctic Alaska. *J. Geophys. Res.* 103, 28917–28928.

7. Liljedahl, A.K., Hinzman, L.D., Kane, D.L., Oechel, W.C., Tweedie, C.E., Zona, D. (2017) Tundra water budget and implications of precipitation underestimation. *Water Resour. Res.* 53, 6472–6486.

8. Ward C. P. and Cory R. M. (2015) Chemical composition of dissolved organic matter draining permafrost soils. *Geochimica et Cosmochimica Acta* 167, 63–79.

9. Ekström, S.M., Regnell, O., Reader, H.E., Nilsson, P.A., Löfgren, S., Kritzberg, E.S. (2016) Increasing concentrations ofiron in surface waters as a consequence of reducing conditions in the catchment area. *J. Geophys. Res. Biogeosci.* 121, 479–493.

10. Koenigk, T., Brodeau, L., Graversen, R.G., Karlsson, J., Svensson, G., Tjernstrom, M., Wille, U. (2013) Arctic climate change in 21st century CMIP5 simulations with EC-Earth. *Climate Dynamics* 40, 2719–2743.

11. Lindsay, W.L., and Schwab, A.P. (1982). The chemistry of iron in soils and its availability to plants. *Journal of Plant Nutrition* 5(4–7), 821–840.

12. Tong, M., Yuan, S., Ma, S., Jin, M., Liu, D., Cheng, D., and Wang, Y. (2016). Production of Abundant Hydroxyl Radicals from Oxygenation of Subsurface Sediments. *Environ. Sci. Technol.* 50, 214–221.

13. Zhang, P., Huang, W., Ji, Z., Zhou, C., Yuan, S. (2018). Mechanism of hydroxyl radical production from pyrite oxation by hydrogen peroxide: Surface versus aqueous reactions. *Geochimica et Cosmochimica Acta* 238, 394–410.

14. Waggoner D.C., Chen H., Willoughby A.S. and Hatcher P.G. (2015) Formation of black carbon-like and alicyclic aliphatic compounds by hydroxyl radical initiated degradation of lignin. *Org. Geochem.* 82, 69–76.

15. Rigby, M., Montzka, S. A., Prinn, R.G., White, J.W.C., Young, D., O'Doherty, S., and Park, S. (2017). Role of atmospheric oxidation in recent methane growth. *Proceedings of the National Academy of Sciences* 114(21), 5373–5377.

16. Yvon-Durocher, G., Allen, A.P., Bastviken, D., Conrad, R., Gudasz, C., St-Pierre, A., Thanh-Duc, N., and del Giorgio, P.A. (2014) Methane fluxes show consistent temperature dependence across microbial to ecosystem scales. *Nature* 507 (7493)

17. IPCC, 2014: Climate Change 2014: Synthesis Report. Contribution of Working Groups I, II and III to the Fifth Assessment Report of the Intergovernmental Panel on Climate Change

18. Voelker B.M. and Sulzberger B. (1996) Effects of fulvic acid on Fe(II) oxidation by hydrogen peroxide. *Environ. Sci. Technol.* 30, 1106–1114.

19. Chang, C.Y., Hsieh, Y.H., Cheng, K.Y., Hsieh, L.L., Cheng, T.C., and Yao, K.S. (2008). Effect of pH on Fenton process using estimation of hydroxyl radical with salicylic acid as trapping reagent. *Water Science and Technology* 58, 873–879.

20. Burns, J.M., Craig, P.S., Shaw, T.J., and Ferry, J.L. (2010). Multivariate examination of Fe(II) / Fe(III) cycling and consequent hydroxyl radical generation. *Environ. Sci. Technol.* 44, 7226–7231.

21. Fujii, M., Rose, A.L., Waite, T.D., and Omura, T. (2010). Oxygen and superoxide-mediated redox kinetics of iron complexed by humic substances in coastal seawater. *Environ. Sci. Technol.* 44, 9337–9342.

22. Vermilyea, A.W., and Voelker, B.M. (2009). Photo-fenton reaction at near neutral pH. *Environ. Sci. Technol.* 43, 6927–6933.

23. Miller, C.J., Rose, A.L., and Waite, T.D. (2009). Impact of natural organic matter on H_2O_2-mediated oxidation of Fe(II) in a simulated freshwater system. *Geochimica et Cosmochimica Acta* 73, 2758–2768.

24. Bianconi, A. (1980). Surface X-RAY absorption spectroscopy : surface EXAFS and surface XANES. *Application of Surface Science 6*, 392–418.

25. Karlsson, T., Persson, P., Skyllberg, U., Mörth, C.M., and Giesler, R. (2008). Characterization of Iron(III) in Organic Soils Using Extended X-ray Absorption Fine Structure Spectroscopy. *Environ. Sci. Technol. 42*(15), 5449–5454.

26. Karlsson, T., and Persson, P. (2012). Complexes with aquatic organic matter suppress hydrolysis and precipitation of Fe(III). *Chemical Geology 322–323*, 19–27.

27. Herndon, E., AlBashaireh, A., Singer, D., Roy Chowdhury, T., Gu, B., and Graham, D. (2017). Influence of iron redox cycling on organo-mineral associations in Arctic tundra soil. *Geochimica et Cosmochimica Acta* 207, 210–231.

28. Sundman, A., Karlsson, T., Laudon, H., and Persson, P. (2013). XAS study of iron speciation in soils and waters from a boreal catchment. *Chemical Geology* 364, 93–102.

29. Daugherty, E.E., Gilbert, B., Nico, P.S., and Borch, T. (2017). Complexation and Redox Buffering of Iron(II) by Dissolved Organic Matter. *Environ. Sci. Technol.* 51(19), 11096–11104.

30. Cory, R.M. (*In prep*) Iron mediates oxidation of DOM.

31. Sleighter, R.L., and Hatcher, P.G. (2008) Molecular characterization of dissolved organic matter (DOM) along a river to ocean transect of the lower Chesapeake Bay by ultrahigh resolution electrospray ionization Fourier transform ion cyclotron resonance mass spectrometry. *Marine Chemistry* 110(3–4), 140–152.

32. Ward, C.P., and Cory, R.M. (2016). Complete and Partial Photo-oxidation of Dissolved Organic Matter Draining Permafrost Soils. *Environ. Sci. Technol.* 50(7), 3545–3553.